ANALYSIS OF INTESTINAL SPLANCHNOPLEURE DEVELOPMENT

By

Nichelle I. Winters

Dissertation

Submitted to the Faculty of the

Graduate School of Vanderbilt University

In partial fulfillment of the requirements

for the degree of

DOCTOR OF PHILOSOPHY

in

Cell and Developmental Biology

August, 2012

Nashville, Tennessee

Approved:

Professor Chin Chiang

Associate Professor Ambra Pozzi

Professor Agnes B. Fogo

Professor Robert J. Coffey

Professor David M. Bader

ACKNOWLEDGEMENTS

This work would not have been possible without the support of many. I gratefully acknowledge the financial support of the Vanderbilt Medical Scientist Training Program, the American Heart Association, the Vanderbilt Digestive Disease Research Center, and the National Institutes of Health. I have been fortunate to work with many individuals who have generously offered training, intellectual input, and provided essential reagents. In particular, Dr. Michael Stark (BYU) and Dr. Jeanette Hyer (UCSF) hosted me in their laboratories and provided invaluable training in electroporation and lineage tracing techniques. I would like to thank my committee members, Dr. Chin Chiang, Dr. Agnes Fogo, Dr. Ambra Pozzi and Dr. Robert Coffey for their insight and thought provoking conversation. I have greatly valued their career guidance and instruction on how to become a better scientist. The Vanderbilt MSTP has provided an essential network of friends and training. I have benefited greatly from a supportive laboratory environment led by Dr. David Bader who has been a mentor and a friend. I have learned a lot about how to do good science, how to do effective science and how to have fun while working hard from David. I am very grateful to my colleagues and friends in the Bader Lab who have kept things interesting the past few years—Rebecca Thomason, Emily Cross, Hillary Carter, Kt Gray, Michelle Robertson, Elise Pfaltzgraff, Paul Miller, Sam Reddy, Cheryl Seneff, Pierre Hunt, Ryan Roberts, and Adam Greer. Finally, I would like to thank my family—my parents, Cody, Ben, Kate, Desmond and Conner—who I can always count on.

TABLE OF CONTENTS

Page

LIST OF TABLES

LIST OF FIGURES

CHAPTER I

INTRODUCTION

The following chapter provides an overview of the state of the field in coelomic vasculogenesis and mesothelial development prior to the completion of the research presented herein. Though the research presented in this volume focuses on the intestine, the foundational concepts of these studies are based in cardiac research which will be reviewed in detail.

Adult Mesothelium: Structure and Function

In the adult, mesothelium is a simple squamous epithelium that forms the surface layer of all coelomic organs. Typically, mesothelia are found in conjunction with an underlying thin connective tissue layer in a serosal membrane. Serosal membranes are named regionally based on the organ or body cavity they line: epicardium (heart), parietal pericardium (pericardial cavity), visceral pleura (lungs), parietal pleura (pleural cavities), visceral peritoneum (abdominal viscera), and parietal peritoneum (abdominal cavity). Despite the varied organs and compartments that mesothelium envelops, its structure remains consistent throughout the body (Di Paolo et al., 2007; Herrick and Mutsaers, 2004; Michailova and Usunoff, 2006).

The major structural features of mesothelium reflect its epithelial nature. Mesothelial cells are polarized with apical surface modifications including microvilli and cilia (Bird, 2004) and have an underlying basement membrane (Margetts et al., 2005; Michailova and Usunoff, 2006). Tight junctions, evidenced by the localization of ZO-1 (Foley-Comer et al., 2002), create a diffusion barrier between the coelomic space and the submesothelial connective tissue. E-cadherin (Lopez-Cabrera et al., 2006; Margetts

et al., 2005) and cytokeratin [mostly subtypes 8, 18, and 19] (Connell and Rheinwald, 1983; Mackay et al., 1990) confer further cell-cell adhesion and structural support. Interestingly, mesothelial cells also express N-cadherin (Davidson et al., 2001; Han et al., 1997; Pelin et al., 1994) and vimentin (Connell and Rheinwald, 1983; Mackay et al., 1990) proteins classically considered to be mesenchymal markers though the significance of this is not known.

The primary function of mesothelium in the adult is to form a non-adhesive surface for the movement of coelomic organs against each other and the body wall. Mesothelial cells in all body cavities secrete an apical coating composed of glycosamineglycans [primarily hyaluronan] (Yung et al.), proteoglycans (Yung and Chan, 2007c; Yung et al., 1995) and phospholipids including phosphatidylcholine (Beavis et al., 1994), the major component of pulmonary surfactant (Yung and Chan, 2007a). This layer provides a non-adhesive surface for organ movement. Other functions include regulation of the ionic and cellular components of coelomic fluid and regulation of inflammation and fibrinolysis (Cheong et al., 2001; Yung and Chan, 2007b).

In the developing embryo, mesothelia are essential for organogenesis. Mesothelial layers serve as important signaling centers and as a cellular progenitor population for coelomic organs. Mesothelial derivatives include vascular mural cells and fibroblasts. The origins and development of mesothelial layers are discussed in detail below.

Coelomic Organogenesis

Prior to gastrulation, the early avian embryo is composed of two layers of cells, the dorsal epiblast and ventral hypoblast, joined only at the margin lying on top of a large yolk sac (Figure 1.1 A). The embryo proper will be formed entirely by cells of the epiblast while the hypoblast gives rise to extraembryonic tissues. Gastrulation begins with a

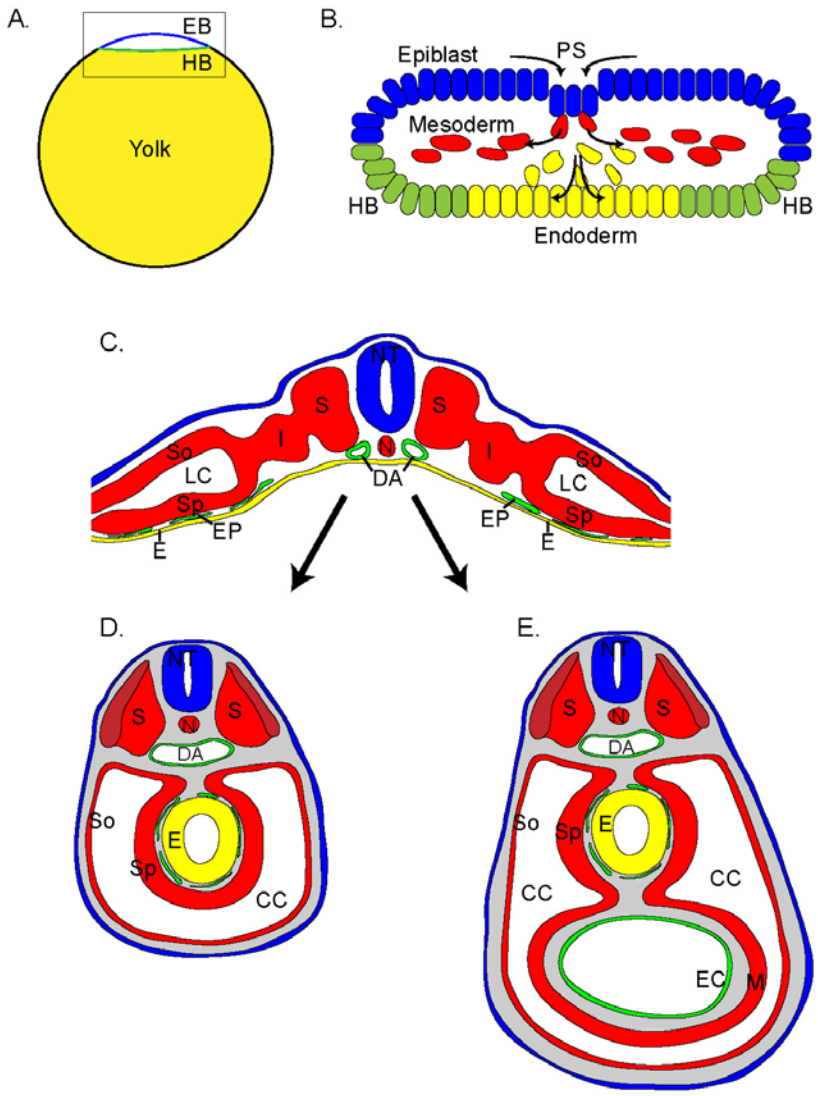

Figure 1.1 Avian gastrulation and organogenesis. A) The avian blastoderm composed of epiblast (EB) and hypoblast (HB) sits on top of the large yolk sac. **B)** During gastrulation, single epiblast cells migrate in through the primitive streak (PS). Endodermal cells move downward and outward to replace the hypoblast. Mesodermal cells populate the cavity. **C)** The mesoderm forms the midline notochord (N), paraxial mesoderm which generates somites (S), intermediate mesoderm (I) and lateral plate mesoderm which divides into somatic (So) and splanchnic (Sp) mesoderm. The lateral cavities (LC) are located between the lateral plate mesoderm layers. An endothelial plexus (EP) lies between the splanchnic mesoderm and endoderm. **D)** In the majority of the coelomic cavity, the endoderm is enveloped by splanchnic mesoderm to generate the gut tube. **E)** The heart is generated by bringing the two sides of cardiogenic splanchnic mesoderm together at the midline to form the myocardium (M). The endoderm is displaced dorsally. The endothelial plexus forms the endocardium (EC). CC, coelomic cavity; DA, dorsal aorta, E, endoderm; EB, epiblast; EC, endocardium; EP, endothelial plexus; HB, hypoblast; I, intermediate mesoderm; LC, lateral cavity; M, myocardium; N, notochord; NT, neural tube; PS, primitive streak; S, somite; So, somatic mesoderm; Sp, splanchnic mesoderm.

thickening in the epiblast called the primitive streak that initially forms at the posterior region of the future embryo. The primitive streak gradually elongates from posterior to anterior led by Hensen's node, a structure analogous to the amphibian blastopore. Single cells from the epiblast migrate in through the primitive streak and Hensen's node to generate the endoderm and mesoderm (Figure 1.1 B). The endoderm migrates first and takes the place of the hypoblast cells. The mesoderm follows and populates the space between the epiblast and endoderm. Once the primitive streak has reached its most anterior location, it regresses back along the same axis, anterior to posterior. Gastrulation is complete once Hensen's node has reached the tail portion of the embryo. The embryo now consists of three germ layers: dorsal ectoderm, middle mesoderm, and ventral endoderm.

In the area of the future coelomic cavity, the mesoderm is divided into regions along the medial-lateral axis. At the midline is the notochord, an important signaling center in the embryo. The paraxial, intermediate, and lateral plate mesoderm segments extend from the midline on both the right and left sides of the embryo (Figure 1.1 C). The paraxial mesoderm will generate the somites. The intermediate mesoderm contributes to the kidneys and gonads. The lateral plate mesoderm forms the body wall musculature and the mesodermal components of all the coelomic organs.

Organogenesis begins with division of the lateral plate mesoderm into two layers. The dorsal layer, termed somatic mesoderm, associates with the overlying ectoderm. The ventral layer, called splanchnic mesoderm, is closely associated with the underlying endoderm. The space between the two layers of lateral plate mesoderm generates the future coelomic cavity bounded by mesoderm. Lateral folding of the embryo brings the right and left lateral plates and the underlying endoderm together in the midline generating a tube. Loss of the ventral mesentery unites the right and left coelomic cavities into a common coelom. Throughout the majority of the coelomic cavity, the

splanchnic mesoderm envelops the endoderm (Figure 1.1 D). However, the heart tube forms by displacing the endoderm dorsally as the lateral splanchnic mesoderm layers are brought together (Figure 1.1 E).

The tube formed of endoderm and splanchnic mesoderm generates the gut tube including the esophagus, crop, proventriculus, ventriculus, small and large intestine and cloaca of the adult bird. The lungs, liver, and pancreas are formed by endodermal buds from the gut tube that associate with the surrounding splanchnic mesoderm. The spleen is a mesodermal only outgrowth that forms within the dorsal mesentery of the gut tube. Thus, the majority of coelomic organs are formed from a combination of endoderm and mesoderm. The heart and spleen are the only exceptions.

Coelomic Vasculogenesis

The vasculature has long been a focus of developmental biology studies. In 1980, Meier performed a scanning electron microscopy study of the early avian embryo and demonstrated that as early as Hamburger and Hamilton stage (HH) 10, an extensive vascular plexus resides between the splanchnic mesoderm and endoderm (Meier, 1980). Since then, antibodies have been developed that recognize endothelial antigens. In 1996, Sugi and Markwald utilized the antibody QH1, which recognizes a cell surface antigen that appears early in endothelial differentiation of the quail, to trace the development of the vascular system. They found that an endothelial plexus is first observed in development within the region of the cardiogenic splanchnic mesoderm prior to fusion of the bilateral heart fields. Endothelial cells were later noted within the extracardiac region in communication with the cardiac plexus. The endothelial cells were positioned uniformly between the splanchnic mesoderm and endoderm in the same location as Meier observed (Meier, 1980; Sugi and Markwald, 1996). A similar

developmental pattern was observed in the mouse with the endothelial plexus first observed in the cardiogenic regions (Drake and Fleming, 2000).

Endocardium

The heart has two distinct endothelial populations: the endocardium lining the lumen of the heart and the endothelium of the coronary vasculature. The coronary vasculature will be described in depth below. The initial vascular plexus described above observed in the cardiogenic region forms the endocardium. As the bilateral heart fields unite, the endocardial cells are brought together at the midline to form the luminal lining of the heart tube (DeRuiter et al., 1993).

The origin of the endocardial progenitor cells, however, remains controversial. Genetic lineage tracing studies in the mouse have suggested that the endocardium and myocardium arise from a multipotent progenitor within the cardiogenic splanchnic mesoderm (Laugwitz et al., 2008; Misfeldt et al., 2009). In the avian embryo, cell lineage tracing studies have long suggested an alternative possibility. Single cells within the epiblast of chick embryos were tagged with a retrovirus prior to ingression through the primitive streak. The embryos were then incubated until after heart tube formation. Labeled myocardial or endocardial clonal cell clusters were identified but an individual clone never contained both cell types (Cohen-Gould and Mikawa, 1996; Wei and Mikawa, 2000). These studies indicated the endocardial and myocardial lineages diverged prior to gastrulation and that the cardiogenic splanchnic mesoderm housed two separate progenitor populations. Recently Milgrom-Hoffman *et al*. demonstrated by live imaging in avian embryos that cardiac endocardium was derived from ingrowth of endothelial cells of the extracardiac plexus into the cardiac crescent. The cardiac and extracardiac endothelial plexuses remained in communication throughout this process. Endothelial cells transplanted into the cardiogenic region gave rise to endocardial but not

myocardial progeny. Furthermore, through murine lineage tracing studies, the authors demonstrated heterogeneity among endocardial populations and suggested at least a subset of endocardial cells in the mouse were derived from endothelial cells (Milgrom-Hoffman et al., 2011). Thus, in the avian embryo it appears the endocardial and myocardial lineages diverge prior to ingression of cells through the primitive streak. The endocardium is then derived from the endothelial plexus that resides between the splanchnic mesoderm and endoderm of the embryo. Further research is needed to clarify the origin of endocardium in the mouse. Currently, a multipotent cardiogenic progenitor and/or a distinct endothelial progenitor are possible.

Other coelomic organs

Though the endothelial plexus of the embryo is first observed between the mesoderm and endoderm near or within the cardiogenic region, this plexus is later distributed throughout much of the embryo as demonstrated by Meier (Meier, 1980). Through generation of chick-quail chimeras, Pardanaud et al. determined that the splanchnopleure (combination of splanchnic mesoderm and endoderm) had extensive vasculogenic potential while the somatopleure (combination of somatic mesoderm and ectoderm) was exceedingly limited in its ability to generate endothelial cells. Early quail organ rudiments of the gut tube, pancreas, lung, and spleen were transplanted into the coelomic cavity of chick embryos. All the transplanted fragments generated extensive vascular networks within the grafted tissue and established a connection with the host. In contrast, transplanted limb buds (derived from the somatopleure) were unable to generate a vasculature; instead, host vessels invaded and populated the grafts. At the time of tissue isolation for transplantation, an endothelial plexus was already present between the endoderm and mesoderm while limited endothelial cells were present within the somatopleure (Pardanaud et al., 1989). Later studies by the same group

demonstrated the endoderm promoted endothelial formation and invasion of the host while the ectoderm was inhibitory accounting for the variable vasculogenic potential (Pardanaud and Dieterlen-Lievre, 1999). Thus, the endothelial plexus associated with the splanchnic mesoderm and endoderm that gives rise to the endocardium has extensive vasculogenic potential in multiple coelomic organs.

In-depth studies of vascular formation and remodeling in specific organs offer further detail on the origins of endothelial cells to coelomic organs. A study of avian development revealed that in the lungs, endothelial cells surrounded the endodermal bud as it first formed. This plexus was then remodeled to generate the entirety of both the pulmonary and bronchial vasculatures. The investigators in the study did not observe sprouting from the dorsal aorta, atria, or cardinal veins throughout this process (DeRuiter et al., 1993). Expansion of the pulmonary plexus in the avian embryo has been demonstrated to occur through both sprouting angiogenesis and vasculogenesis from the surrounding mesenchyme (Anderson-Berry et al., 2005; Makanya et al., 2007). To clarify terminology, angiogenesis is defined as growth from pre-existing endothelial vessels while vasculogenesis is the *de novo* differentiation of endothelial cells (Patel-Hett and D'Amore, 2011). Angiogenesis from the primary endothelial plexus and vasculogenesis from the periphery have also been demonstrated to be a major mechanism of pulmonary vascular formation in the mouse (deMello et al., 1997; Schwarz et al., 2009). Interestingly, the primary pulmonary endothelial plexus of the mouse lacked arterial-venous fate specification suggesting extensive plasticity exists in the early plexus (Schwarz et al., 2009).

The murine liver bud forms in a similar fashion as the lung bud. Matsumoto and colleagues demonstrated that endothelial cells formed a plexus around the endodermal cells that will generate the liver bud and loss of endothelium resulted in abnormal liver morphogenesis (Matsumoto et al., 2001). In the human, it was observed that the

vasculature of the liver was derived from remodeling of this primitive vascular plexus. The initial endothelial plexus expanded via angiogenesis to reach the outer periphery of the liver with some additional vasculogenesis from the surrounding mesenchyme contributing after the initial remodeling (Gouysse et al., 2002).

The intestinal splanchnopleure is continuous with the yolk sac which is the site of an extensive vasculature. Bilateral vitelline arteries and veins supply both the forming gut tube and the yolk sac. The initial vascular plexus present between the endoderm and splanchnic mesoderm extends from the embryo proper into the yolk sac. Noble, *et al*. demonstrated that this plexus lacked venous or arterial specification. Through live imaging in avian embryos, they observed that capillaries of the primitive endothelial plexus fused to generate first the vitelline arteries and then the vitelline veins. Interestingly, the venous circulation was subsequently enlarged by addition of arterial sprouts that broke off from the circulation creating small pockets of blood before reconnecting to the venous side. Blood flow was essential for both arterial and venous patterning and specification (le Noble et al., 2004). Thus, remodeling of the primitive endothelial plexus appears to be the major mechanism of vascular formation in the intestine.

Taken together, these studies demonstrate that the early endothelial plexus present between the splanchnic mesoderm and endoderm is remodeled within each coelomic organ individually to generate the majority of the vasculature of that organ. There is significant plasticity throughout the process of remodeling and the initial plexus lacks arterial and venous specification. Avian lineage tracing studies suggest these endothelial cells may be specified even prior to gastrulation (Cohen-Gould and Mikawa, 1996; Wei and Mikawa, 2000). A potential and notable exception to the above method of coelomic vasculogenesis is found within the coronary circulation. The primary endothelial plexus within the heart tube generates the endocardium but is not thought to

contribute to the coronary circulation in any significant way. Instead, the coronary vasculature is formed through *de novo* vasculogenesis requiring the presence of the cardiac mesothelium (Katz et al., 2012; Riley and Smart, 2011).

Cardiac Mesothelial Development

Discovery of the proepicardium

Development of mesothelium has been studied almost exclusively in the heart. In 1969, Francis Manasek performed one of the first studies that led to our current understanding of cardiac mesothelial development. Through examination of the early heart tube with light and transmission electron microscopy, Manasek concluded that epicardial cells originated outside of the initial myocardial layer though did not identify a source. This observation contradicted the prevailing dogma of the day that stated that the splanchnic mesoderm of the heart tube, termed the “epi-myocardium”, contained both mesothelial progenitors and myoblasts (Manasek, 1969). Manasek also noted that coronary blood vessels were absent from the early myocardium and suggested epicardium may play a role in their development (Manasek, 1969; Manasek, 1970). Nine years later, with the use of scanning electron microscopy, Ho and Shimada identified villi projecting from the region of the sinus venosus and concluded these cells were the origin of the epicardium (Ho and Shimada, 1978). These villous projections, that would later be termed the proepicardium (PE), contacted the heart and migrated as a sheet to envelop the myocardium [Figure 1.2 A-B]; (Ho and Shimada, 1978). In 1992, Mikawa and Fischman demonstrated that coronary blood vessels form by *in situ* vasculogenesis and not by angiogenic sprouts from the aorta. A few years later, Mikawa and Gourdie definitively identified the PE as an origin of vascular smooth muscle cells and endothelium of the coronary blood vessels as well as fibroblasts of the heart (Mikawa

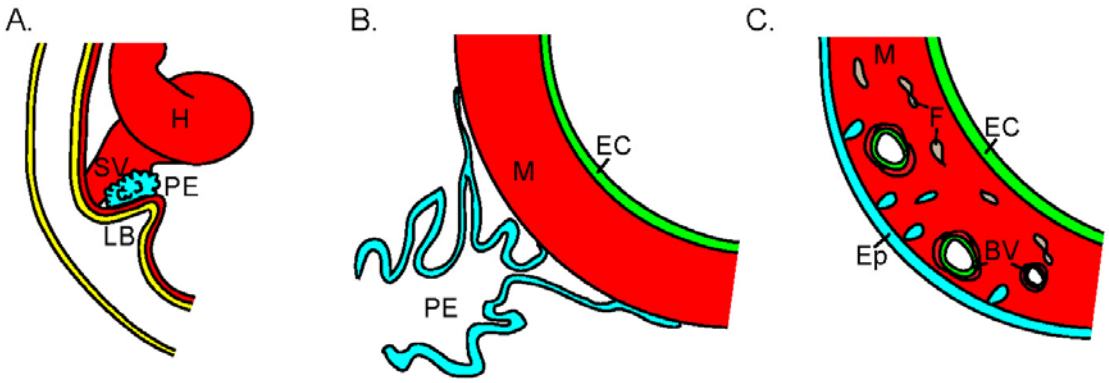

Figure 1.2 Development of the proepicardium. A) The PE forms near the liver bud (LB) and sinus venosus (SV) of the heart (H) on the dorsal body wall of the embryo. **B)** Proepicardial villi cross the pericardial cavity to contact the myocardium (M) and migrate out over the myocardium to establish the epicardium (Ep). **C)** Epicardial cells delaminate and migrate into the myocardium to give rise to fibroblasts (F) and blood vessels (BV). BV, blood vessel; EC, endocardium; F, fibroblast; H, heart tube; LB, liver bud; M, myocardium; PE, proepicardium; SV, sinus venosus.

and Gourdie, 1996). However, as mesenchymal cells were present within the PE when it first formed, it was unclear whether the mesenchymal cells migrated with the epithelial PE to give rise to the fibroblasts and blood vessels or if mesothelial cells directly contributed to the stroma of the heart. It was subsequently discovered that epicardial cells underwent epithelial-to-mesenchymal transition (EMT) after reaching the heart to generate the cellular derivatives observed by Mikawa and Gourdie [Figure 1.2] (Dettman et al., 1998).

These studies established the fundamental concepts of epicardial development including an exogenous origin of mesothelial progenitors, migration as an epithelial sheet, delamination and invasion into the myocardium, and differentiation into vascular cells and fibroblasts (Figure 1.2). Since that time, epicardial research has expanded enormously. Topics of particular relevance to the following studies include vasculogenic potential, origin and induction of the PE, and molecular cross-talk with the myocardium.

Origin of coronary endothelium

As described above, it has been clearly demonstrated that the coronary arteries do not sprout from the aorta. Rather, an endothelial plexus forms just below the epicardium and coalesces to form the coronary arteries. These vessels then pierce the aorta to establish blood flow (Eralp et al., 2005). While the proepicardial origin of vascular smooth muscle cells and cardiac fibroblasts is well accepted, there is some controversy over whether mesothelial cells contribute cells to the coronary endothelium. Other proposed origins for coronary endothelial cells include the hepatic endothelium (Lie-Venema et al., 2005; Poelmann et al., 1993; Viragh et al., 1993), sinus venosus (Red-Horse et al., 2010; Vrancken Peeters et al., 1997), and endocardium (Katz et al., 2012; Red-Horse et al., 2010).

Isolated quail proepicardia transplanted into the pericardial cavities of host chick embryos have been documented to give rise to coronary endothelial cells in multiple studies (Guadix et al., 2006; Perez-Pomares et al., 2002). However, both mesothelium and mesenchymal cells of the PE are transplanted in these experiments. Static images of sections through the region of the avian PE appear to demonstrate sprouting of endothelial cells from both the sinus venosus and hepatic endothelium into the proepicardial mesenchyme (Viragh et al., 1993; Vrancken Peeters et al., 1997). Poelmann et al found that the vasculogenic potential of transplanted PE was entirely dependent on co-transplantation with a piece of the hepatic primordium. Thus, the authors concluded mesothelial cells of the PE did not give rise to endothelial cells but rather the PE served as a conduit for endothelial cells of the hepatic sinusoids to reach the heart (Poelmann et al., 1993). The variation observed in PE transplantation experiments could be due to stage dependent changes if, for example, proepicardial mesothelial cells become progressively specialized. Additionally, endothelial progenitors have not been reported to localize to the PE until HH17 (Vrancken Peeters et al., 1997).

Other studies have suggested that mesothelium gives rise directly to endothelial cells. A vital dye labeled applied to the quail epicardium revealed labeled coronary endothelial cells within the myocardium after 48 hours of development suggesting a direct mesothelial contribution to coronary endothelium (Perez-Pomares et al., 2002). Additionally, the mesothelial marker Wt1 and the endothelial marker QH1 have been shown to be co-expressed in a subset of proepicardial cells indicating endothelial cells arise from mesothelial progenitors (Ishii et al., 2009).

The consensus in the field appears to be that the avian PE delivers at least a subpopulation if not the major population of coronary endothelial cells to the developing heart (Ishii et al., 2009; Riley and Smart, 2011). The relative contribution to endothelial cells from mesenchymal versus mesothelial cells of the PE is not known. The origin of

the mesenchymal endothelial progenitors within the PE is also not clear though they potentially arise from multiple sources including the sinus venosus, hepatic sinusoids, and proepicardial mesothelial cells.

Murine genetic lineage tracing studies of the PE have offered additional conflicting data on the origin of coronary endothelium. *Tbx18* and *Wt1* encode transcription factors expressed in the PE from the earliest stages of proepicardial development. However, both the *Tbx18* and *Wt1* genetic lineages do not include cardiac endothelial cells (Cai et al., 2008; Zhou et al., 2008a). Thus, murine PE has been thought to have a very limited vasculogenic potential.

The lack of an apparent proepicardial origin of endothelium in the mouse led researchers to examine other potential sources. The PE attaches to the atrioventricular region of the heart in close proximity to the sinus venosus and then migrates outward over the myocardium. The appearance of endothelial cells within the myocardium follows a similar pattern thought to be due to arrival and endothelial progenitors with the PE. Red-horse and colleagues hypothesized this pattern could alternatively be due to angiogenic outgrowth from the sinus venosus. On close examination, they identified angiogenic sprouts from the sinus venosus and through organ culture experiments concluded the sinus venosus was indeed a potential origin of coronary endothelium. They next utilized a tamoxifen inducible *VE-cadherin-cre* mouse line crossed with a *Rosa26R*^{lacZ} reporter strain to trace the potential origin of endothelial cells. Tamoxifen was administered in low doses to induce single cell recombination between E7.5 and E9.5, a time when VE-cadherin was not detected in the PE but was present in the sinus venosus. They later identified labeled clones extending from the sinus venosus endothelium into the coronary endothelium. They also identified a minor potential contribution to coronary endothelium from the endocardium. The authors concluded the sinus venosus endothelium was the major source of both arterial and venous coronary

endothelial cells and the PE was not the origin of coronary endothelium (Red-Horse et al., 2010).

Subsequent studies have added additional insights regarding the role of the PE in coronary development. Cossette et al. examined markers of endothelium, including Pecam, FLK1, and VE-cadherin, in mice through early stages of PE development. Notably, VE-Cadherin was identified within the PE at E9.5 (Cossette and Misra, 2011) suggesting the previous single cell lineage tracing studies reported by Red-Horse *et al*. could have labeled proepicardial mesenchymal cells in addition to sinus venosus endothelium (Red-Horse et al., 2010). Cossette and colleagues identified three different populations of endothelial cells within the mesenchyme of the PE: those appearing to sprout from the sinus venosus, those appearing to sprout from the hepatic sinusoids and those associated with neither the sinus venosus nor the liver and thought to be derived from mesothelial contributions to the mesenchyme (Cossette and Misra, 2011). In this regard, the murine PE actually closely resembled the avian PE with apparent contributions of mesenchymal endothelial cells from all three neighboring tissues (Ishii et al., 2009; Viragh et al., 1993; Vrancken Peeters et al., 1997). It was, however, unclear if these endothelial cells with the proepicardial mesenchyme subsequently migrated to the heart with the PE (Cossette and Misra, 2011).

Recently, two additional markers have been identified that label the PE, *Scleraxis,* (*Scx*) and *Semaphorin3D* (*Sema3D*). Interestingly, these markers identify a proepicardial subpopulation largely unmarked by *Wt1* or *Tbx18*. Descendants of *Scx* or *Sema3d* expressing cells include epicardial cells, fibroblasts, sinus venosus endothelium, a minor endocardial population and importantly, coronary endothelium (Katz et al., 2012). Thus, similar to the avian PE, a picture has emerged in the mouse of a mixed population of endothelial progenitors within the PE. Endothelial cells appear to

migrate to and from the PE, sinus venosus, and hepatic endothelium and potentially mix with a minor population of the endocardium.

Origin of the proepicardium

Similar to the endothelial cells of the PE, the exact origin of the proepicardial mesothelial cells is still debated. The PE develops in close proximity to the liver bud and sinus venosus of the heart tube (Figure 1.2 A). Both hepatic mesothelium and sinus venous mesoderm have been described as potential origins of the PE in avian embryos (Dettman et al.; Ishii et al., 2007; Manner, 1992; van Wijk et al., 2009). Each of these proposed origins describes the same morphological location. The 3-dimensional morphology of the region is complex due to the looping of the heart, the presence of the anterior intestinal portal, the liver bud, and the continuous mesodermal lining over the surface of all of the structures in the area. A slight variation in the plane, level of section, or developmental timing demonstrates different anatomical relationships so that the PE locationally encompasses the region over both the sinus venosus and liver bud (Viragh et al., 1993). However, the proposed tissue origins also imply different potential lineages for the PE: either originating from coelomic mesothelium (entirely extracardiac) or diverging from the cardiac lineage. The lineal relationship of epicardial and myocardial cells is of interest in the field due to the ongoing search for a source of multipotent progenitor cells that may have a regenerative capacity in the adult mammalian heart (Laugwitz et al., 2008).

Ishii *et al*. demonstrated that the avian liver bud was capable of inducing expression of the PE marker genes *Wt1, Tbx18* and *Cfc1* in competent regions of the lateral plate mesoderm posterior to the heart (Ishii et al., 2007). However, the molecular basis for the inductive capability of the liver has not yet been identified and since these studies relied on heterotopic transplantation, it is not known if the liver bud is necessary

for induction of the PE in situ. These data suggest coelomic mesothelium and the PE may share a molecular regulatory network. However, it is not known what normally regulates mesothelial differentiation throughout the remainder of the coelom (see below). For example, the great arteries of the heart do not derive their mesothelial lining from the PE. When outgrowth of the PE is inhibited, this additional mesothelial population can partially compensate for the lack of epicardium by forming a mesothelial layer over the outflow tract myocardium. However, the origin of this mesothelial progenitor population and the signaling mechanisms regulating its development are unknown (Gittenberger-de Groot et al., 2000). Until we understand mesothelial differentiation in organs other than the heart, it will be difficult to place epicardial development into the context of other mesothelial lineages.

Other studies have suggested the avian PE arises from a common myocardial/epicardial progenitor residing in or near the inflow region of the heart (Kruithof et al., 2006; van Wijk et al., 2009). This was initially suggested by the observation that avian proepicardia removed from the embryo and placed in culture spontaneously differentiated into cardiomyocytes (Kruithof et al., 2006). Though notably, propepicardia transplanted *in vivo* into the pericardial cavity of a host embryo have not been observed to differentiate into cardiomyocytes (Manner, 1999; Perez-Pomares et al., 1997). A second study in avian embryos in support of a common epicardial/myocardial progenitor demonstrated that a vital dye label placed on the mesoderm just caudal to the cardiac inflow tract prior to PE differentiation led to labeled cells within both the PE and inflow tract myocardium. The region at the time of labeling uniformly expressed *Tbx18*, a proepicardially enriched gene. However, as numerous cells were targeted with the initial vital dye label, the authors acknowledge this technique could not distinguish between a single population of multipotent progenitors or a mixed pool of already specified epicardial and myocardial progenitors (van Wijk et al., 2009).

Genetic lineage tracing studies of murine cardiac development indicate major lineages of the heart including atrial and ventricular cardiomyocytes and the conduction system arise from an Islet1+ common precursor cell (Laugwitz et al., 2008). However, there is conflicting data as to whether the PE is derived from this Islet1+ progenitor population (Sun et al., 2007; Zhou et al., 2008b). Taken together, these studies indicate the PE may share a developmental origin with myocardium and/or coelomic mesothelium. Further research including single cell lineage tracing will help determine when these lineages diverge.

Induction of the proepicardium

The molecular signals inducing localized formation of the PE are also not yet clear though both bone morphogenetic protein (BMP) and fibroblast growth factor (FGF) signaling are involved. *BMP2* expressed by the myocardium was identified as a crucial regulator of epicardial villi protrusion in avian embryos. Inhibition of BMP signaling through induced expression of *Noggin* (a gene encoding a protein that binds to BMP ligands preventing their interaction with their receptor) in the myocardium led to decreased villi formation from the PE and, in 30% of cases, failure to attach to the myocardium. In contrast, overexpression of BMP2 by the myocardium led to increased villi protrusion and attachment to the heart (Ishii et al., 2010). Thus, in this study, *BMP2* promoted epicardial development. However, data from another laboratory demonstrated that *BMP2*-expressing cells transplanted within the right sinus horn of the heart inhibited PE differentiation. Interestingly, this effect was also seen with transplanted Noggin-loaded beads. Epicardial differentiation of PE explants was also inhibited with treatment with either BMP2 or Noggin (Schlueter et al., 2006). These data suggest that the level of BMP2 signaling is essential and that epicardial differentiation can be inhibited by either excessive or reduced BMP2. In an additional study, Kruithof et al. examined expression

patterns of *BMP* and *FGF* ligands in the region of the PE. They identified, among others, *BMP2* in the myocardium and base of the PE and *FGF2* throughout the PE. They then conducted *in vitro* PE differentiation assays. From these experiments, they concluded *BMP2* expression at the base of the PE promoted myocardial differentiation at the expense of epicardial development. *FGF2* induced epicardial differentiation and prevented myocardial formation (Kruithof et al., 2006). The same group perturbed BMP2 and FGF signaling *in vivo* though injections of ligands or inhibitors into the yolk sac of chick embryos. They found that combined BMP2 stimulation and FGF inhibition led to failure of PE development. However, BMP2 stimulation alone had no effect on PE differentiation (van Wijk et al., 2009). The variable effects of BMP2 reported throughout these studies could be due simply to the concentration or location of the BMP2 signal. A signal from within the sinus horn or yolk sac presumably reaches the base of the PE while a myocardial signal reaches the apical surface. A single injection of a protein or inhibitor will also lead to a very different concentration profile than that observed with continuous production from either transplanted cells or transduction of resident cells. Additionally, it is clear the presence or absence of other signaling factors can modulate the observed effect. These data do demonstrate that both BMP and FGF signaling are likely involved in the specification and development of the PE and potentially balanced against one another.

Signaling functions of the epicardium

Inhibition of epicardial development either mechanically or molecularly leads to a spectrum of defects ranging from a thin, disorganized myocardium to necrosis, pericardial hemorrhaging and death of the embryo (Gittenberger-de Groot et al., 2000; Kwee et al., 1995; Mellgren et al., 2008; Moore et al., 1999; Tevosian et al., 2000; Yang et al., 1995). One of the primary functions of epicardium is to give rise to cardiac

fibroblasts and cells of the coronary vasculature. Thus, defects in the myocardium observed in epicardial deficient animals can at least partially be attributed to the lack of a coronary blood supply and absence of cardiac fibroblasts contributing to the expansion of the heart wall (Snider et al., 2009).

Beyond a cellular contribution, molecular crosstalk between the epicardium and myocardium is well documented. Stuckmann, et al demonstrated the epicardium promoted *in vitro* proliferation of the myocardium. This capability was dependent on erythropoietin (EPO) and retinoic acid (RA) signaling through an unidentified molecular mediator (Stuckmann et al., 2003). In 2005, Lavine et al. identified FGF9 as a potential downstream mediator of the mitogenic effect of RA. Treatment of epicardial cells or explanted hearts with RA induced *FGF9* expression in the epicardium and inhibition of FGF9 signaling in murine hearts led to decreased myocardial proliferation. However, *FGF9* was expressed transiently in the epicardium encompassing only a brief period of myocardial proliferation and was also expressed in the endocardium (Lavine et al., 2005). Thus, epicardial *FGF9* was clearly not continuously required for myocardial proliferation as much of myocardial expansion occurred after *FGF9* expression was maintained only in the endocardium. In a subsequent study, the same group determined FGF signaling induced sonic hedgehog (Shh) expression within the epicardium. Shh then signaled to the myocardium and induced expression of vascular endothelial growth factor (VEGF) ligands and angiopoietin-2 (Ang-2). These factors then regulated development of the coronary vasculature (Lavine et al., 2008; Lavine et al., 2006). An additional study of FGF signaling in avian embryos demonstrated *FGFR1* expressed in the epicardium was involved in regulating epicardial EMT, myocardial invasion by epicardially derived cells, and the lineage decision between coronary endothelium and vascular smooth muscle (Pennisi and Mikawa, 2009). These studies pointed to a role for FGF signaling in regulating coronary vascular development and thus, indirectly

supporting myocardial proliferation. Another FGF ligand, FGF10, expressed in the myocardium promoted development of the cardiac fibroblast lineage (Vega-Hernandez et al., 2011). Importantly, cardiac fibroblasts have been demonstrated to signal directly to the myocardium to regulate proliferation (Ieda et al., 2009). Thus, the pro-mitotic influence of FGF signaling on cardiomyocytes may not be through direct paracrine signaling but rather related to promotion of coronary vessel and cardiac fibroblast development.

Insulin like growth factor-2 (IGF2) expressed by the epicardium has also been identified as a mediator of cardiomyocyte proliferation. Disruption of *IGF2* or its receptors led to decreased myocardial proliferation in the mouse (Li et al., 2011). Brade et al. proposed a molecular cascade in which RA signaling induced production of EPO by the liver. Secreted EPO then crossed the pericardial cavity to bind to epicardial surface receptors and induce *IGF2* expression within the epicardium (Brade et al., 2011). Thus, these studies present *IGF2* as a molecular mediator for the mitogenic influence of the epicardium.

Hepatic Mesothelium Development

In contrast to the well studied PE and epicardium, relatively little is known about the development of mesothelia of other coelomic organs. The liver develops in close proximity to the PE as described above. The septum transversum mesenchyme is described as the origin of hepatic mesothelium though this has not been examined directly (Asahina et al., 2011).

The descendants of hepatic mesothelium have been investigated in both the avian and murine embryo. The developing hepatic mesothelium of the quail directly labeled with a vital dye was observed to give rise to liver sinusoid endothelium and hepatic stellate cells, a specialized fibroblast population (Perez-Pomares et al., 2004).

Wt1 has also been identified in hepatic mesothelial and submesothelial cells. Genetic lineage tracing of *Wt1*-expressing cells within the murine liver identified hepatic stellate cell and perivascular mesenchymal cell descendants including vascular smooth muscle. However, hepatic endothelial cells were not derived from the *Wt1*-lineage (Asahina et al., 2011). Taken together, these studies indicate the hepatic mesothelium shares a similar potential with the PE in giving rise to fibroblasts, vascular smooth muscle and potentially endothelium. Notably, the discrepancy in the mesothelial origin of hepatic endothelium again arises between data derived from direct labeling of cells for lineage tracing studies in the avian embryo versus murine genetic lineage tracing experiments.

There have been a few studies of the embryonic signaling function of hepatic mesothelium. Similar to the epicardium, hepatic mesothelium has been implicated in regulating hepatoblast proliferation during development. Increased proliferation of murine embryonic hepatoblasts was observed when co-cultured with hepatic mesothelium. *Wt1*-deficient mesothelial cells lacked this pro-mitotic influence (Onitsuka et al., 2010). Decreased proliferation of hepatoblasts has also been observed *in vivo* in *Wt1*-deficient mice. These mice also exhibited precocious differentiation of hepatic stellate cells. Knockout of *Wt1* resulted in loss of hepatic mesothelial expression of the retinoic acid (RA) synthesizing enzyme, RALDH2. Molecular inhibition of RA synthesis *in vivo* in chicken embryos also led to decreased liver size and treatment of hepatic explants with RA increased proliferation. Thus, synthesis of RA by hepatic mesothelium was proposed as the mechanism by which mesothelial cells promote hepatoblast proliferation (Ijpenberg et al., 2007). Hepatic mesothelium was also demonstrated to be FGF9-positive (Colvin et al., 1999) and isolated mesothelial cells expressed other potential mediators of hepatoblast proliferation including pleiotrophin and hepatocyte growth factor (Onitsuka et al., 2010). The specific function of mesothelial expression of these proteins in liver morphogenesis is currently unknown. These studies demonstrate

parallel features of epicardium and hepatic mesothelium in regulating proliferation of underlying parenchymal cells.

Pulmonary Mesothelium Development

The origin and lineage of pleural mesothelium has not been studied in avian embryos. In mouse studies, it has been found that similar to the heart and liver, the *Wt1*-positive mesothelial lineage of the lungs gives rise to perivascular cells through delamination from the epithelium and migration (Morimoto et al., 2010; Que et al., 2008). However, only 25% of all pulmonary vascular smooth muscle cells were derived from mesothelium with the remaining 75% of unknown origin. Additionally, mesenchymal cells, and potentially a limited population of endothelial cells were derived from the mesothelium (Que et al., 2008).

Signaling functions of mesothelium also have been studied only in the mouse. The mesothelium and the endodermal epithelium of the lungs both express *FGF9.* *FGF9*-deficient mice develop hypoplastic lungs due to reduced airway branching and a decrease in mesenchymal cells (Colvin et al., 2001). Recently, Yin *et al*. determined that pulmonary mesothelial- and endodermal-derived FGF9 have distinct functions in pulmonary development and regulate mesenchymal proliferation and airway branching, respectively (Yin et al., 2011). Weaver *et al*. additionally reported that *FGF9* inhibited visceral smooth muscle cell differentiation in the lungs and postulated secretion of FGF9 from the mesothelium maintains the outer mesenchymal cells in an undifferentiated state (Weaver et al., 2003). *RALDH2* and *IGF1* have been demonstrated to be expressed by early postnatal pleural mesothelium and adult pleural cell lines, respectively, but the developmental expression or function of these genes is not known (Hind et al., 2002; Lee et al., 1993). Thus, the *Wt1*-lineage and the potential signaling function of mesothelium in the lungs are similar to other coelomic organs.

Pancreatic Mesothelium

The development of pancreatic mesothelium has not been investigated. However, induced deficiency of *Wt1* in adult mice led to rapid onset organ failure and death. These mice exhibited an array of defects including atrophy of the exocrine pancreas. Interestingly, the liver, lungs, and intestine did not have any apparent deficiencies. The rapid progression to death of the animals was likely due to advanced glomerulosclerosis and failure of erythropoiesis. The only cells detected in the wild type adult pancreas to express *Wt1* were mesothelium and pancreatic stellate cells. The investigators postulated the loss of *Wt1* in the adult pancreas led to activation of cytokine expression by pancreatic stellate cells which then promoted atrophy. Furthermore, they hypothesized based on the *Wt1* expression pattern that pancreatic stellate cells may be derived from mesothelium during development (Chau et al., 2011). Additional research is needed to determine the function of pancreatic mesothelium in the embryo and adult.

Intestinal Mesothelium Development

Finally, a small number of studies in the mouse have provided insight into intestinal mesothelial development. A study from our laboratory demonstrated that *Wt1*-positive intestinal mesothelial cells delaminated from the epithelium and migrated into the mesenchyme. The *Wt1*-lineage gave rise to over 75% of intestinal vascular smooth muscle cells but less than 10% of endothelial cells. Additionally, expression of *Wt1* in the embryonic mouse intestine was observed to start within the dorsal mesentery and then progressively encompass the gut tube. This observation suggested *Wt1*-positive mesothelial progenitors may migrate onto the surface of the gut tube as seen in the heart. However, sections through the gut tube did not clearly demonstrate a migratory cellular population (Wilm et al., 2005). Thus, the origin of intestinal mesothelium

remained unclear though the mesothelial lineage again encompassed vascular smooth muscle.

Little is known regarding the paracrine functions of intestinal mesothelium. The intestinal *FGF9* expression pattern resembles that of the lungs with both the endoderm and mesothelium expressing *FGF9* sandwiching non-expressing mesenchyme (Colvin et al., 1999; Lavine et al., 2005). *FGF9*-deficient mice have been reported to develop a shortened small intestine due to decreased mesenchymal proliferation and premature differentiation (Geske et al., 2008). However, the relative function of endodermal versus mesothelial *FGF9* in the intestine is not known.

Summary

The heart diverges from the basic pattern of other coelomic organs in two ways: first, the heart does not include endodermally derived tissues and second, the early endothelial plexus of the embryo does not remodel to form the vasculature supplying the parenchyma of the heart. Mesothelium is intimately tied to vascular formation in all coelomic organs investigated to date. In the heart, cardiac mesothelium is derived from an external, migratory population. It is not known if this mechanism of mesothelial formation is also unique to the heart or if other coelomic organs employ a similar developmental mechanism.

The intestinal vasculature resides near the surface of the parenchyma below the serosal membrane similar to the location of the coronary blood vessels. Additionally, the gut tube is the parent structure of the majority of coelomic organs. Thus, we sought to determine the origin of the mesothelium and vasculature of the developing intestine.

Dissertation Hypothesis and Summary of Aims

Mesothelium lines the surface of all coelomic organs and the internal body wall and is an essential tissue for embryogenesis. However, mesothelial development has only been extensively investigated in a single organ—the heart. The research presented herein will address the following question: is the mechanism of mesothelial formation observed in the heart also utilized by other coelomic organs? The lungs, liver, and pancreas all develop as buds from the gut tube and the intestine is structurally similar to the heart. Thus, the gut tube is an ideal organ for investigations of mesothelial development. My central hypothesis is that the intestinal mesothelium arises from an extrinsic, migratory precursor population similar to the epicardium.

Importantly, in the adult organism, mesothelial cells are thought to give rise to invasive fibrotic cells in several pathological conditions including idiopathic pulmonary fibrosis, peritoneal sclerosis and peritoneal adhesions. The involvement of mesothelium in these diseases reflects the embryonic potential of mesothelial cells to undergo an epithelial to mesenchymal transition and generate fibroblasts. However, mesothelia in the embryo can also give rise to vascular cells, a potentially supportive cell type for repairing injured adult tissues. Identifying the normal mechanisms that govern mesothelial formation and differentiation in diverse organs is essential to understand and potentially modulate the behavior of these cells in the injured adult toward healing and away from fibrosis. Determining the origin of mesothelia throughout the coelom is a critical first step for studies of mesothelial developmental biology to progress. Three aims were designed to test the central hypothesis that the cardiac model of mesothelial and vascular formation can be applied to diverse coelomic organs including the intestine.

Aim 1. Description of mesodermal development in the intestine. Before detailed investigations of mesothelial and vascular development could proceed, a basic description of mesodermal development within the intestine was necessary.

Immunohistochemistry and transgenic quail were utilized to examine development of the intestine from the first establishment of the organ primordium through generation of the definitive structure. Mesothelium was first present in the intestine at day six of development. An obvious migratory source of progenitor cells was not observed contrary to the cardiac model of mesothelial formation. Additionally, the major surface blood vessels of the intestine were first present within the mesentery and then later observed over the intestine. This aim is detailed in Chapter II.

Aim 2. Determine the origin of intestinal mesothelial cells. To determine if mesothelial cells of the intestine were indeed derived from resident progenitor cells, the splanchnic mesoderm was labeled by delivery of a reporter plasmid to surface cells via electroporation or by infection with a replication incompetent retrovirus. Additionally, chimeric intestines were generated by transplanting quail intestinal primordia into the coelomic cavity of chick embryos. These assays demonstrated the major mechanism of mesothelial formation in the intestine was through differentiation of resident progenitors cells distributed along the anterior-posterior axis of the intestinal primordium. This aim is detailed in Chapter III.

Aim 3. Determine the origin of intestinal vascular cells. To determine the origin of vascular smooth muscle and endothelial cells of the intestine, chimeras were again generated utilizing donor splanchnopleure derived from transgenic quail that expressed a fluorescent protein localized to the nuclei of endothelial cells. These experiments demonstrated that endothelial cells at all levels of the intestinal vasculature including the large surface blood vessels were derived from remodeling of a primitive vascular plexus resident to the splanchnopleure. Additionally, vascular smooth muscle cells of the intestine were derived from resident cells. This aim is detailed in Chapter IV.

Taken together, these studies demonstrate that the intestinal primordium contains resident mesothelial, vascular, and endothelial progenitors. This is in direct

contrast to the heart in which these lineages must be recruited from an extrinsic source. My hypothesis that there was a common mechanism of mesothelial formation utilized throughout the coelom was therefore rejected as at least two mechanisms of mesothelial generation exist within the coelomic cavity. These studies demonstrate mesothelial populations may be more heterogeneous than previously suspected despite their common structural appearance. Further research will elucidate whether additional mechanisms can be identified for generation of this essential cell type..

References

Anderson-Berry, A., O'Brien, E. A., Bleyl, S. B., Lawson, A., Gundersen, N., Ryssman, D., Sweeley, J., Dahl, M. J., Drake, C. J., Schoenwolf, G. C. et al. (2005). Vasculogenesis drives pulmonary vascular growth in the developing chick embryo. *Dev Dyn* **233**, 145-53.

Asahina, K., Zhou, B., Pu, W. T. and Tsukamoto, H. (2011). Septum transversum-derived mesothelium gives rise to hepatic stellate cells and perivascular mesenchymal cells in developing mouse liver. *Hepatology* **53**, 983-95.

Beavis, J., Harwood, J. L., Coles, G. A. and Williams, J. D. (1994). Synthesis of phospholipids by human peritoneal mesothelial cells. *Perit Dial Int* **14**, 348-55.

Bird, S. D. (2004). Mesothelial primary cilia of peritoneal and other serosal surfaces. *Cell Biol Int* **28**, 151-9.

Brade, T., Kumar, S., Cunningham, T. J., Chatzi, C., Zhao, X., Cavallero, S., Li, P., Sucov, H. M., Ruiz-Lozano, P. and Duester, G. (2011). Retinoic acid stimulates myocardial expansion by induction of hepatic erythropoietin which activates epicardial Igf2. *Development* **138**, 139-48.

Cai, C. L., Martin, J. C., Sun, Y., Cui, L., Wang, L., Ouyang, K., Yang, L., Bu, L., Liang, X., Zhang, X. et al. (2008). A myocardial lineage derives from Tbx18 epicardial cells. *Nature* **454**, 104-8.

Chau, Y. Y., Brownstein, D., Mjoseng, H., Lee, W. C., Buza-Vidas, N., Nerlov, C., Jacobsen, S. E., Perry, P., Berry, R., Thornburn, A. et al. (2011). Acute multiple organ failure in adult mice deleted for the developmental regulator Wt1. *PLoS Genet* **7**, e1002404.

Cheong, Y. C., Laird, S. M., Li, T. C., Shelton, J. B., Ledger, W. L. and Cooke, I. D. (2001). Peritoneal healing and adhesion formation/reformation. *Hum Reprod Update* **7**, 556-66.

Cohen-Gould, L. and Mikawa, T. (1996). The fate diversity of mesodermal cells within the heart field during chicken early embryogenesis. *Dev Biol* **177**, 265-73.

Colvin, J. S., Feldman, B., Nadeau, J. H., Goldfarb, M. and Ornitz, D. M. (1999). Genomic organization and embryonic expression of the mouse fibroblast growth factor 9 gene. *Dev Dyn* **216**, 72-88.

Colvin, J. S., White, A. C., Pratt, S. J. and Ornitz, D. M. (2001). Lung hypoplasia and neonatal death in Fgf9-null mice identify this gene as an essential regulator of lung mesenchyme. *Development* **128**, 2095-106.

Connell, N. D. and Rheinwald, J. G. (1983). Regulation of the cytoskeleton in mesothelial cells: reversible loss of keratin and increase in vimentin during rapid growth in culture. *Cell* **34**, 245-53.

Cossette, S. and Misra, R. (2011). The identification of different endothelial cell populations within the mouse proepicardium. *Dev Dyn* **240**, 2344-53.

Davidson, B., Nielsen, S., Christensen, J., Asschenfeldt, P., Berner, A., Risberg, B. and Johansen, P. (2001). The role of desmin and N-cadherin in effusion cytology: a comparative study using established markers of mesothelial and epithelial cells. *Am J Surg Pathol* **25**, 1405-12.

deMello, D. E., Sawyer, D., Galvin, N. and Reid, L. M. (1997). Early fetal development of lung vasculature. *Am J Respir Cell Mol Biol* **16**, 568-81.

DeRuiter, M. C., Gittenberger-de Groot, A. C., Poelmann, R. E., VanIperen, L. and Mentink, M. M. (1993). Development of the pharyngeal arch system related to the pulmonary and bronchial vessels in the avian embryo. With a concept on systemic-pulmonary collateral artery formation. *Circulation* **87**, 1306-19.

Dettman, R. W., Denetclaw, W., Jr., Ordahl, C. P. and Bristow, J. (1998). Common epicardial origin of coronary vascular smooth muscle, perivascular fibroblasts, and intermyocardial fibroblasts in the avian heart. *Dev Biol* **193**, 169-81.

Di Paolo, N., Sacchi, G., Del Vecchio, M. T., Nicolai, G. A., Brardi, S. and Garosi, G. (2007). State of the art on autologous mesothelial transplant in animals and humans. *Int J Artif Organs* **30**, 456-76.

Drake, C. J. and Fleming, P. A. (2000). Vasculogenesis in the day 6.5 to 9.5 mouse embryo. *Blood* **95**, 1671-9.

Eralp, I., Lie-Venema, H., DeRuiter, M. C., van den Akker, N. M., Bogers, A. J., Mentink, M. M., Poelmann, R. E. and Gittenberger-de Groot, A. C. (2005). Coronary artery and orifice development is associated with proper timing of epicardial outgrowth and correlated Fas-ligand-associated apoptosis patterns. *Circ Res* **96**, 526-34.

Foley-Comer, A. J., Herrick, S. E., Al-Mishlab, T., Prele, C. M., Laurent, G. J. and Mutsaers, S. E. (2002). Evidence for incorporation of free-floating mesothelial cells as a mechanism of serosal healing. *J Cell Sci* **115**, 1383-9.

Geske, M. J., Zhang, X., Patel, K. K., Ornitz, D. M. and Stappenbeck, T. S. (2008). Fgf9 signaling regulates small intestinal elongation and mesenchymal development. *Development* **135**, 2959-68.

Gittenberger-de Groot, A. C., Vrancken Peeters, M. P., Bergwerff, M., Mentink, M. M. and Poelmann, R. E. (2000). Epicardial outgrowth inhibition leads to compensatory mesothelial outflow tract collar and abnormal cardiac septation and coronary formation. *Circ Res* **87**, 969-71.

Gouysse, G., Couvelard, A., Frachon, S., Bouvier, R., Nejjari, M., Dauge, M. C., Feldmann, G., Henin, D. and Scoazec, J. Y. (2002). Relationship between vascular development and vascular differentiation during liver organogenesis in humans. *J Hepatol* **37**, 730-40.

Guadix, J. A., Carmona, R., Munoz-Chapuli, R. and Perez-Pomares, J. M. (2006). In vivo and in vitro analysis of the vasculogenic potential of avian proepicardial and epicardial cells. *Dev Dyn* **235**, 1014-26.

Han, A. C., Peralta-Soler, A., Knudsen, K. A., Wheelock, M. J., Johnson, K. R. and Salazar, H. (1997). Differential expression of N-cadherin in pleural mesotheliomas and E-cadherin in lung adenocarcinomas in formalin-fixed, paraffin-embedded tissues. *Hum Pathol* **28**, 641-5.

Herrick, S. E. and Mutsaers, S. E. (2004). Mesothelial progenitor cells and their potential in tissue engineering. *Int J Biochem Cell Biol* **36**, 621-42.

Hind, M., Corcoran, J. and Maden, M. (2002). Alveolar proliferation, retinoid synthesizing enzymes, and endogenous retinoids in the postnatal mouse lung. Different roles for Aldh-1 and Raldh-2. *Am J Respir Cell Mol Biol* **26**, 67-73.

Ho, E. and Shimada, Y. (1978). Formation of the epicardium studied with the scanning electron microscope. *Dev Biol* **66**, 579-85.

Ieda, M., Tsuchihashi, T., Ivey, K. N., Ross, R. S., Hong, T. T., Shaw, R. M. and Srivastava, D. (2009). Cardiac fibroblasts regulate myocardial proliferation through beta1 integrin signaling. *Dev Cell* **16**, 233-44.

Ijpenberg, A., Perez-Pomares, J. M., Guadix, J. A., Carmona, R., Portillo-Sanchez, V., Macias, D., Hohenstein, P., Miles, C. M., Hastie, N. D. and Munoz-Chapuli, R. (2007). Wt1 and retinoic acid signaling are essential for stellate cell development and liver morphogenesis. *Dev Biol* **312**, 157-70.

Ishii, Y., Garriock, R. J., Navetta, A. M., Coughlin, L. E. and Mikawa, T. (2010). BMP signals promote proepicardial protrusion necessary for recruitment of coronary vessel and epicardial progenitors to the heart. *Dev Cell* **19**, 307-16.

Ishii, Y., Langberg, J., Rosborough, K. and Mikawa, T. (2009). Endothelial cell lineages of the heart. *Cell Tissue Res* **335**, 67-73.

Ishii, Y., Langberg, J. D., Hurtado, R., Lee, S. and Mikawa, T. (2007). Induction of proepicardial marker gene expression by the liver bud. *Development* **134**, 3627-37.

Katz, T. C., Singh, M. K., Degenhardt, K., Rivera-Feliciano, J., Johnson, R. L., Epstein, J. A. and Tabin, C. J. (2012). Distinct compartments of the proepicardial organ give rise to coronary vascular endothelial cells. *Dev Cell* **22**, 639-50.

Kruithof, B. P., van Wijk, B., Somi, S., Kruithof-de Julio, M., Perez Pomares, J. M., Weesie, F., Wessels, A., Moorman, A. F. and van den Hoff, M. J. (2006). BMP and FGF regulate the differentiation of multipotential pericardial mesoderm into the myocardial or epicardial lineage. *Dev Biol* **295**, 507-22.

Kwee, L., Baldwin, H. S., Shen, H. M., Stewart, C. L., Buck, C., Buck, C. A. and Labow, M. A. (1995). Defective development of the embryonic and extraembryonic circulatory systems in vascular cell adhesion molecule (VCAM-1) deficient mice. *Development* **121**, 489-503.

Laugwitz, K. L., Moretti, A., Caron, L., Nakano, A. and Chien, K. R. (2008). Islet1 cardiovascular progenitors: a single source for heart lineages? *Development* **135**, 193-205.

Lavine, K. J., Long, F., Choi, K., Smith, C. and Ornitz, D. M. (2008). Hedgehog signaling to distinct cell types differentially regulates coronary artery and vein development. *Development* **135**, 3161-71.

Lavine, K. J., White, A. C., Park, C., Smith, C. S., Choi, K., Long, F., Hui, C. C. and Ornitz, D. M. (2006). Fibroblast growth factor signals regulate a wave of Hedgehog activation that is essential for coronary vascular development. *Genes Dev* **20**, 1651-66.

Lavine, K. J., Yu, K., White, A. C., Zhang, X., Smith, C., Partanen, J. and Ornitz, D. M. (2005). Endocardial and epicardial derived FGF signals regulate myocardial proliferation and differentiation in vivo. *Dev Cell* **8**, 85-95.

le Noble, F., Moyon, D., Pardanaud, L., Yuan, L., Djonov, V., Matthijsen, R., Breant, C., Fleury, V. and Eichmann, A. (2004). Flow regulates arterial-venous differentiation in the chick embryo yolk sac. *Development* **131**, 361-75.

Lee, T. C., Zhang, Y., Aston, C., Hintz, R., Jagirdar, J., Perle, M. A., Burt, M. and Rom, W. N. (1993). Normal human mesothelial cells and mesothelioma cell lines express insulin-like growth factor I and associated molecules. *Cancer Res* **53**, 2858-64.

Li, P., Cavallero, S., Gu, Y., Chen, T. H., Hughes, J., Hassan, A. B., Bruning, J. C., Pashmforoush, M. and Sucov, H. M. (2011). IGF signaling directs ventricular cardiomyocyte proliferation during embryonic heart development. *Development* **138**, 1795-805.

Lie-Venema, H., Eralp, I., Maas, S., Gittenberger-De Groot, A. C., Poelmann, R. E. and DeRuiter, M. C. (2005). Myocardial heterogeneity in permissiveness for epicardium-derived cells and endothelial precursor cells along the developing heart tube at the onset of coronary vascularization. *Anat Rec A Discov Mol Cell Evol Biol* **282**, 120-9.

Lopez-Cabrera, M., Aguilera, A., Aroeira, L. S., Ramirez-Huesca, M., Perez-Lozano, M. L., Jimenez-Heffernan, J. A., Bajo, M. A., del Peso, G., Sanchez-Tomero, J. A. and Selgas, R. (2006). Ex vivo analysis of dialysis effluent-derived mesothelial cells as an approach to unveiling the mechanism of peritoneal membrane failure. *Perit Dial Int* **26**, 26-34.

Mackay, A. M., Tracy, R. P. and Craighead, J. E. (1990). Cytokeratin expression in rat mesothelial cells in vitro is controlled by the extracellular matrix. *J Cell Sci* **95 (Pt 1)**, 97-107.

Makanya, A. N., Hlushchuk, R., Baum, O., Velinov, N., Ochs, M. and Djonov, V. (2007). Microvascular endowment in the developing chicken embryo lung. *Am J Physiol Lung Cell Mol Physiol* **292**, L1136-46.

Manasek, F. J. (1969). Embryonic development of the heart. II. Formation of the epicardium. *J Embryol Exp Morphol* **22**, 333-48.

Manasek, F. J. (1970). Histogenesis of the embryonic myocardium. *Am J Cardiol* **25**, 149-68.

Manner, J. (1992). The development of pericardial villi in the chick embryo. *Anat Embryol (Berl)* **186**, 379-85.

Manner, J. (1999). Does the subepicardial mesenchyme contribute myocardioblasts to the myocardium of the chick embryo heart? A quail-chick chimera study tracing the fate of the epicardial primordium. *Anat Rec* **255**, 212-26.

Margetts, P. J., Bonniaud, P., Liu, L., Hoff, C. M., Holmes, C. J., West-Mays, J. A. and Kelly, M. M. (2005). Transient overexpression of TGF-{beta}1 induces epithelial mesenchymal transition in the rodent peritoneum. *J Am Soc Nephrol* **16**, 425-36.

Matsumoto, K., Yoshitomi, H., Rossant, J. and Zaret, K. S. (2001). Liver organogenesis promoted by endothelial cells prior to vascular function. *Science* **294**, 559-63.

Meier, S. (1980). Development of the chick embryo mesoblast: pronephros, lateral plate, and early vasculature. *J Embryol Exp Morphol* **55**, 291-306.

Mellgren, A. M., Smith, C. L., Olsen, G. S., Eskiocak, B., Zhou, B., Kazi, M. N., Ruiz, F. R., Pu, W. T. and Tallquist, M. D. (2008). Platelet-derived growth factor receptor beta signaling is required for efficient epicardial cell migration and development of two distinct coronary vascular smooth muscle cell populations. *Circ Res* **103**, 1393-401.

Michailova, K. N. and Usunoff, K. G. (2006). Serosal membranes (pleura, pericardium, peritoneum). Normal structure, development and experimental pathology. *Adv Anat Embryol Cell Biol* **183**, i-vii, 1-144, back cover.

Mikawa, T. and Gourdie, R. G. (1996). Pericardial mesoderm generates a population of coronary smooth muscle cells migrating into the heart along with ingrowth of the epicardial organ. *Dev Biol* **174**, 221-32.

Milgrom-Hoffman, M., Harrelson, Z., Ferrara, N., Zelzer, E., Evans, S. M. and Tzahor, E. (2011). The heart endocardium is derived from vascular endothelial progenitors. *Development* **138**, 4777-87.

Misfeldt, A. M., Boyle, S. C., Tompkins, K. L., Bautch, V. L., Labosky, P. A. and Baldwin, H. S. (2009). Endocardial cells are a distinct endothelial lineage derived from Flk1+ multipotent cardiovascular progenitors. *Dev Biol* **333**, 78-89.

Moore, A. W., McInnes, L., Kreidberg, J., Hastie, N. D. and Schedl, A. (1999). YAC complementation shows a requirement for Wt1 in the development of epicardium, adrenal gland and throughout nephrogenesis. *Development* **126**, 1845-57.

Morimoto, M., Liu, Z., Cheng, H. T., Winters, N., Bader, D. and Kopan, R. (2010). Canonical Notch signaling in the developing lung is required for determination of arterial smooth muscle cells and selection of Clara versus ciliated cell fate. *J Cell Sci* **123**, 213-24.

Onitsuka, I., Tanaka, M. and Miyajima, A. (2010). Characterization and functional analyses of hepatic mesothelial cells in mouse liver development. *Gastroenterology* **138**, 1525-35, 1535 e1-6.

Pardanaud, L. and Dieterlen-Lievre, F. (1999). Manipulation of the angiopoietic/hemangiopoietic commitment in the avian embryo. *Development* **126**, 617-27.

Pardanaud, L., Yassine, F. and Dieterlen-Lievre, F. (1989). Relationship between vasculogenesis, angiogenesis and haemopoiesis during avian ontogeny. *Development* **105**, 473-85.

Patel-Hett, S. and D'Amore, P. A. (2011). Signal transduction in vasculogenesis and developmental angiogenesis. *Int J Dev Biol* **55**, 353-63.

Pelin, K., Hirvonen, A. and Linnainmaa, K. (1994). Expression of cell adhesion molecules and connexins in gap junctional intercellular communication deficient human mesothelioma tumour cell lines and communication competent primary mesothelial cells. *Carcinogenesis* **15**, 2673-5.

Pennisi, D. J. and Mikawa, T. (2009). FGFR-1 is required by epicardium-derived cells for myocardial invasion and correct coronary vascular lineage differentiation. *Dev Biol* **328**, 148-59.

Perez-Pomares, J. M., Carmona, R., Gonzalez-Iriarte, M., Atencia, G., Wessels, A. and Munoz-Chapuli, R. (2002). Origin of coronary endothelial cells from epicardial mesothelium in avian embryos. *Int J Dev Biol* **46**, 1005-13.

Perez-Pomares, J. M., Carmona, R., Gonzalez-Iriarte, M., Macias, D., Guadix, J. A. and Munoz-Chapuli, R. (2004). Contribution of mesothelium-derived cells to liver sinusoids in avian embryos. *Dev Dyn* **229**, 465-74.

Perez-Pomares, J. M., Macias, D., Garcia-Garrido, L. and Munoz-Chapuli, R. (1997). Contribution of the primitive epicardium to the subepicardial mesenchyme in hamster and chick embryos. *Dev Dyn* **210**, 96-105.

Poelmann, R. E., Gittenberger-de Groot, A. C., Mentink, M. M., Bokenkamp, R. and Hogers, B. (1993). Development of the cardiac coronary vascular endothelium, studied with antiendothelial antibodies, in chicken-quail chimeras. *Circ Res* **73**, 559-68.

Que, J., Wilm, B., Hasegawa, H., Wang, F., Bader, D. and Hogan, B. L. (2008). Mesothelium contributes to vascular smooth muscle and mesenchyme during lung development. *Proc Natl Acad Sci U S A* **105**, 16626-30.

Red-Horse, K., Ueno, H., Weissman, I. L. and Krasnow, M. A. (2010). Coronary arteries form by developmental reprogramming of venous cells. *Nature* **464**, 549-53.

Riley, P. R. and Smart, N. (2011). Vascularizing the heart. *Cardiovasc Res* **91**, 260-8.

Schlueter, J., Manner, J. and Brand, T. (2006). BMP is an important regulator of proepicardial identity in the chick embryo. *Dev Biol* **295**, 546-58.

Schwarz, M. A., Caldwell, L., Cafasso, D. and Zheng, H. (2009). Emerging pulmonary vasculature lacks fate specification. *Am J Physiol Lung Cell Mol Physiol* **296**, L71-81.

Snider, P., Standley, K. N., Wang, J., Azhar, M., Doetschman, T. and Conway, S. J. (2009). Origin of cardiac fibroblasts and the role of periostin. *Circ Res* **105**, 934-47.

Stuckmann, I., Evans, S. and Lassar, A. B. (2003). Erythropoietin and retinoic acid, secreted from the epicardium, are required for cardiac myocyte proliferation. *Dev Biol* **255**, 334-49.

Sugi, Y. and Markwald, R. R. (1996). Formation and early morphogenesis of endocardial endothelial precursor cells and the role of endoderm. *Dev Biol* **175**, 66-83.

Sun, Y., Liang, X., Najafi, N., Cass, M., Lin, L., Cai, C. L., Chen, J. and Evans, S. M. (2007). Islet 1 is expressed in distinct cardiovascular lineages, including pacemaker and coronary vascular cells. *Dev Biol* **304**, 286-96.

Tevosian, S. G., Deconinck, A. E., Tanaka, M., Schinke, M., Litovsky, S. H., Izumo, S., Fujiwara, Y. and Orkin, S. H. (2000). FOG-2, a cofactor for GATA transcription factors, is essential for heart morphogenesis and development of coronary vessels from epicardium. *Cell* **101**, 729-39.

van Wijk, B., van den Berg, G., Abu-Issa, R., Barnett, P., van der Velden, S., Schmidt, M., Ruijter, J. M., Kirby, M. L., Moorman, A. F. and van den Hoff, M. J. (2009). Epicardium and myocardium separate from a common precursor pool by crosstalk between bone morphogenetic protein- and fibroblast growth factor-signaling pathways. *Circ Res* **105**, 431-41.

Vega-Hernandez, M., Kovacs, A., De Langhe, S. and Ornitz, D. M. (2011). FGF10/FGFR2b signaling is essential for cardiac fibroblast development and growth of the myocardium. *Development* **138**, 3331-40.

Viragh, S., Gittenberger-de Groot, A. C., Poelmann, R. E. and Kalman, F. (1993). Early development of quail heart epicardium and associated vascular and glandular structures. *Anat Embryol (Berl)* **188**, 381-93.

Vrancken Peeters, M. P., Gittenberger-de Groot, A. C., Mentink, M. M., Hungerford, J. E., Little, C. D. and Poelmann, R. E. (1997). The development of the coronary vessels and their differentiation into arteries and veins in the embryonic quail heart. *Dev Dyn* **208**, 338-48.

Weaver, M., Batts, L. and Hogan, B. L. (2003). Tissue interactions pattern the mesenchyme of the embryonic mouse lung. *Dev Biol* **258**, 169-84.

Wei, Y. and Mikawa, T. (2000). Fate diversity of primitive streak cells during heart field formation in ovo. *Dev Dyn* **219**, 505-13.

Wilm, B., Ipenberg, A., Hastie, N. D., Burch, J. B. and Bader, D. M. (2005). The serosal mesothelium is a major source of smooth muscle cells of the gut vasculature. *Development* **132**, 5317-28.

Yang, J. T., Rayburn, H. and Hynes, R. O. (1995). Cell adhesion events mediated by alpha 4 integrins are essential in placental and cardiac development. *Development* **121**, 549-60.

Yin, Y., Wang, F. and Ornitz, D. M. (2011). Mesothelial- and epithelial-derived FGF9 have distinct functions in the regulation of lung development. *Development* **138**, 3169-77.

Yung, S. and Chan, T. M. (2007a). Glycosaminoglycans and proteoglycans: overlooked entities? *Perit Dial Int* **27 Suppl 2**, S104-9.

Yung, S. and Chan, T. M. (2007b). Mesothelial cells. *Perit Dial Int* **27 Suppl 2**, S110-5.

Yung, S. and Chan, T. M. (2007c). Peritoneal proteoglycans: much more than ground substance. *Perit Dial Int* **27**, 375-90.

Yung, S., Coles, G. A., Williams, J. D. and Davies, M. (1994). The source and possible significance of hyaluronan in the peritoneal cavity. *Kidney Int* **46**, 527-33.

Yung, S., Thomas, G. J., Stylianou, E., Williams, J. D., Coles, G. A. and Davies, M. (1995). Source of peritoneal proteoglycans. Human peritoneal mesothelial cells synthesize and secrete mainly small dermatan sulfate proteoglycans. *Am J Pathol* **146**, 520-9.

Zhou, B., Ma, Q., Rajagopal, S., Wu, S. M., Domian, I., Rivera-Feliciano, J., Jiang, D., von Gise, A., Ikeda, S., Chien, K. R. et al. (2008a). Epicardial progenitors contribute to the cardiomyocyte lineage in the developing heart. *Nature* **454**, 109-13.

Zhou, B., von Gise, A., Ma, Q., Rivera-Feliciano, J. and Pu, W. T. (2008b). Nkx2-5- and Isl1-expressing cardiac progenitors contribute to proepicardium. *Biochem Biophys Res Commun* **375**, 450-3.

CHAPTER II

A COMPREHESIVE TIMELINE OF MESODERMAL DEVELOPMENT IN THE QUAIL SMALL INTESTINE

This chapter was submitted to Developmental Dynamics on June 28th, 2012 under the same title with the following authors:

Rebecca T. Thomason, David M. Bader, Nichelle I. Winters

Abstract

To generate the mature intestine, splanchnic mesoderm diversifies into six different tissue layers each with multiple cell types through concurrent and complex morphogenetic events. Hindering the progress of research in the field is the lack of a detailed description of the fundamental morphological changes that constitute development of the intestinal mesoderm. We utilized immunofluorescence and morphometric analyses of wild type and Tg(*tie1*:H2B-eYFP) quail embryos to establish a comprehensive timeline of mesodermal development in the avian intestine. The following landmark features were analyzed from appearance of the intestinal primordium through generation of the definitive structure: radial compartment formation, basement membrane dynamics, mesothelial differentiation, mesenchymal expansion and growth patterns, smooth muscle differentiation, and maturation of the vasculature. In this way, structural relationships between mesodermal components were identified over time. This integrated analysis presents a roadmap for investigators and clinicians to evaluate diverse experimental data obtained at individual stages of intestinal development within the longitudinal context of intestinal morphogenesis.

Introduction

Intestinal disorders affect a large number of individuals in both pediatric and adult settings. Many of these conditions including intestinal atresia, motility disorders, Hirschprung's disease, and gastrointestinal stromal tumors (GIST) have multiple and incompletely understood etiologies (Louw and Barnard, 1955; Mazur and Clark, 1983; Sanders, 1996; Hirota et al., 1998; Newgreen and Young, 2002; Heanue and Pachnis, 2007; Streutker et al., 2007; Appelman, 2011; Guzman et al., 2011). One of the difficulties in deciphering the mechanisms underlying these diseases is the lack of information available on the development of a major component of the gut tube—the intestinal mesoderm. Understanding development of the mesoderm is essential for a complete picture of the mechanisms leading to congenital as well as adult intestinal disorders. A description of the structure of the adult intestine reveals the complexity of the mesodermal tissues generated in the embryo.

The structure of the mature vertebrate intestine is remarkably conserved. The innermost layer, the mucosal epithelium, is comprised primarily of columnar epithelial cells resting on a basement membrane. Supporting the mucosal epithelium is a mesenchymal core called the lamina propria, which is composed of a capillary plexus, lymphatic vessels, nerves, myofibroblasts and fibroblasts. The lamina propria and mucosal epithelium are arranged into fingerlike projections, called villi, protruding into the lumen of the intestine. External to the mucosal epithelium, minor variations in structure are observed between the avian and mammalian intestine. The adult chick intestine lacks a submucosal connective tissue layer and muscularis mucosa. Instead, there are four concentric visceral smooth muscle cell layers that begin just subjacent to the lamina propria and are positioned outwardly in the following order: inner longitudinal, inner circular, outer circular and outer longitudinal (Gabella, 1985; Yamamoto, 1996). The inner longitudinal muscle layer of the avian is analogous to the mammalian

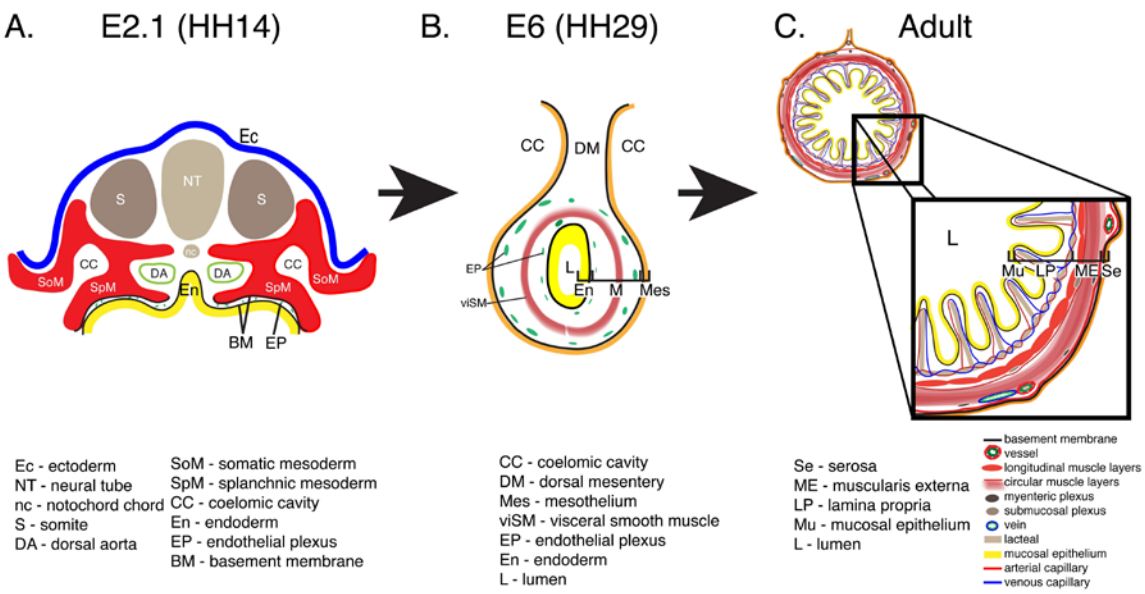

Figure 2.1 Schematic depicting the intestinal primordium, primitive intestinal tube, and adult intestine. A) Transverse section through an embryonic day (E) 2.1 quail embryo equivalent to Hamburger and Hamilton (HH) stage 14. At this stage, the intestinal primordium is open and comprised of splanchnic mesoderm (red; SpM), endoderm (yellow; En) and an intervening endothelial plexus (green, EP). **B)** At E6, the intestine is completely closed and composed of mesothelium (orange), a two layered endothelial plexus (green), a single visceral smooth muscle layer (red), and endoderm (yellow; En). **C)** In the adult intestine, villi are lined with a mucosal epithelium (yellow; Mu) and contain a lamina propria (LP) composed of capillaries, a lymphatic lacteal, and connective tissue. A four-layered muscularis externa (ME) surrounds the lamina propria. A serosal membrane (Se) lines the coelomic surface.

muscularis mucosa. The circular muscle layer of mammals including mice and humans can also be divided into two layers due to structural differences though is often referred to singularly (Eddinger, 2009). Thus, the most significant variation is the presence or absence of a submucosal connective tissue layer. The large blood vessels of the chick intestine reside within or just deep to the thin outer longitudinal visceral smooth muscle cell layer and extend circumferentially. Vascular branches dive deep into the intestinal layers to eventually supply the endothelial plexus of the villi (Jacobson and Noer, 1952). The enteric neuronal network is divided into two main regions: the first adjacent to the large blood vessels near the surface described above and the second between the inner circular and inner longitudinal smooth muscle layers (Gabella, 1985). Finally, at the coelomic surface is a serosal membrane composed of a flat sheet of epithelial cells called mesothelium with an underlying basement membrane and thin connective tissue layer (Figure 2.1).

On first examination, the embryonic intestinal primordium offers only hints of its eventual elaborate structure. After gastrulation in the avian embryo, the lateral plate mesoderm splits into splanchnic and somatic mesoderm bilaterally generating a right and left coelomic cavity between the two layers. The splanchnic mesoderm, underlying endoderm, and an intervening endothelial plexus compose the intestinal anlage and are initially organized as a flat sheet (Figure 2.1 A, (Meier, 1980; Pardanaud et al., 1989). This anlage folds laterally and from the anterior and posterior ends to meet at the ventral midline giving rise to a tube and uniting the right and left coelomic cavities into a common coelom (Figure 2.1 B, (Wells and Melton, 1999; Zorn and Wells, 2009). The epithelial endoderm gives rise to the mucosa that lines the villi and intestinal crypts (Mitjans et al., 1997; Madison et al., 2005; Dauça et al., 2007; Grosse et al., 2011). The splanchnic mesoderm diversifies to generate the connective tissue, vasculature, smooth muscle and serosal layers (McHugh, 1995; Hashimoto et al., 1999; Wilm et al., 2005;

Kim et al., 2007; Powell et al., 2011; Winters et al. 2012, in press). Migratory neural crest cells invade to form the enteric nervous system and the vascular system organizes from incompletely identified progenitors (Young and Newgreen, 2001; Young et al., 2004; Burns et al., 2009; Nagy et al., 2009). Throughout these processes, the intestine must undergo a dramatic increase in length and diameter herniating outside of the body cavity to accommodate its tremendous growth (Savin et al., 2011). Thus, cells of all three germ layers must coordinate invasion, migration, differentiation, growth, and tissue morphogenesis to generate the mature intestinal structure.

Despite comprising the majority of the adult intestine, development of the mesoderm is poorly described relative to the more extensively studied endodermal and neuronal components. Within the mesoderm, multiple cellular types and tissue layers develop in concert. Most studies are focused on the differentiation of a specific cell type during a narrow developmental window. Furthermore, studies utilize a variety of model organisms. Thus, assembling the available data distributed within the literature into a basic timeline of the major morphological changes that occur during intestinal development is extremely difficult. Knowledge of the temporal and spatial relationships of developmental events in the intestine is essential to design experiments and interpret data.

We sought to establish a comprehensive timeline of the major events in intestinal mesoderm development from the first appearance of the intestinal anlage to formation of the definitive structure in a single species. Quail embryos were selected due to their availability in large quantities, emerging transgenic models, and the ability to easily time their development with precision (Huss et al., 2008). Additionally, small intestine development has not been described in the quail (Grey, 1972; Gabella, 1985; Yamamoto, 1996; Hashimoto et al., 1999; Hiramatsu and Yasugi, 2004; Kim et al., 2007; Mao et al., 2010). Importantly, the major structural features of the avian intestine, with

the above noted variations, correspond with the mammalian intestine and thus the information obtained from studies of the avian embryo is widely applicable. We describe landmark features of intestinal mesoderm formation throughout embryogenesis that if analyzed at any single stage, provide an inclusive snapshot of the status of mesodermal development. Furthermore, through this integrated approach, we identified pivotal developmental time points at which key processes occur simultaneously. These data provide the field with the fundamental developmental and morphological guideposts in intestinal mesoderm development upon which variation in organogenesis caused by genetic, experimental and surgical intervention can be compared and further analyzed.

Materials and Methods

Embryos

Quail embryos (*Coturnix coturnix japonica*) were obtained from Ozark Egg Farm (Stover, Missouri). Tg(*tie1*:H2B-eYFP) quail embryos were a generous gift from Dr. Rusty Lansford (Caltech, Pasadena, CA). All eggs were incubated at 37°C in humidity and staged according to the Japanese quail and the Hamburger and Hamilton staging chart (Hamburger and Hamilton, 1992; Ainsworth et al., 2010). Adult intestines were isolated from mature four month old wild type quail.

Immunofluorescence

All embryos and tissues were fixed in 4% formaldehyde (Sigma F1635) in 1XPBS (pH 7.4) at room temperature or 4°C depending on tissue size. The samples were washed with 1XPBS (pH 7.4), cryoprotected in 30% sucrose, embedded in OCT (TissueTek 4583) and transverse sectioned (unless otherwise noted) at 5μm. Sections were rehydrated, washed with 1XPBS, and permeabilized with a 0.2% Triton-X 100 (Sigma

T9284) for 10 minutes, washed with 1XPBS, and blocked in 10% goat serum (Invitrogen 16210-072) + 1% BSA (Sigma A2153) in PBS. Samples were then treated with primary antibodies (see below) overnight at 4°C. Slides were then washed with 1XPBS and incubated with secondary antibodies (see below) for 60 minutes at room temperature. Slides were washed and mounted with ProLong Gold mounting agent (Invitrogen P36930).

Antibodies

Primary antibodies: laminin (Abcam ab11575; 1:200), cytokeratin (Abcam ab9377; 1:200), laminin (DSHB, 3H11 and 31 or 31-1; 1:25 (each)), anti-GFP (Invitrogen, A11122; 1:200), anti-αSMA Clone 1A4 (Sigma A2547; 1:200), αSMA (Abcam ab5694; 1:200), γSMA (MP Biomedicals 69133; 1:600). Secondaries: Alexa 488 and 568 (Invitrogen A11001, A11004; 1:500), TOPRO-3 (Invitrogen T3605; 1:1000), DAPI (Invitrogen D3571; 1:10,000).

Microscopy

Immunofluorescence was imaged using an Olympus Fluo-View1000 confocal microscope (Vanderbilt CISR Core). Images were taken in z-stack format and analyzed using FV-1000, Metamorph and Photoshop software. Brightness and contrast were adjusted for visual representation in Photoshop.

Morphometric Analysis

Small intestine sections were stained with laminin antibody and imaged on an EVOS microscope (Joe Roland, Goldenring Lab, Vanderbilt). ImageJ software was used to measure the distance between the outer and endodermal basement membranes of intestines aged E1.9 through E6 (eight to twenty samples analyzed at each stage). The

distances were averaged and the standard deviation and standard error of the mean were calculated in Excel. To determine the area of the mesenchymal space, six to ten samples were analyzed for each intestinal region (posterior, middle posterior, middle anterior, anterior) of each intestinal stage including: E8, E10, E12, E14, E16. Metamorph software (Vanderbilt CISR) was utilized to specify the mesenchymal region (area between outer and endodermal basement membrane). Average, standard deviation, and standard error of the mean were calculated in Excel. To determine the total length of the intestines, samples were dissected from quail embryos and the mesentery and vessels completely removed. Four to ten samples were measured for each stage including E6, E8, E10, E12, E14, E16. Averages, standard deviation, and standard error of the mean were calculated in Excel.

Results

Establishment and maturation of the major intestinal compartments

As described above, the adult avian intestine has seven concentric tissue layers, six of which are derived from the splanchnic mesoderm. However, there are only two continuous basement membranes within the intestine; one resides below the mucosal epithelium and the other is subjacent to the outer serosal mesothelium (Simon-Assmann et al., 1995; Lefebvre et al., 1999). These basement membranes divide the seven layers of the intestine into three compartments: the mucosa, the middle connective and muscular tissue (largest component), and the outer serosa. Notably, the intestinal primordium is composed of two epithelial sheets, endoderm and splanchnic mesoderm. Importantly, both epithelia have an underlying basement membrane. The epithelia enclose an intervening space that will eventually house the mesenchyme. Thus, similar to the adult structure, the intestinal primordium is divided by two basement membranes

into three compartments: endoderm (En), mesenchyme/mesenchymal space (M), splanchnic mesoderm (SpM)/outer epithelium (Mes) (Figure 2.1 A, black lines). While subsequent morphogenetic events will greatly increase the complexity of the cellular and tissue relationships, the arrangement of these basement membranes may represent one of the few histological similarities between the embryonic and adult intestine (Figure 2.1).

To determine whether this basic structural relationship is maintained throughout embryogenesis into adult life, we examined laminin staining throughout development of the intestine. Laminin is an integral component of basement membranes. At embryonic day 1.9 (E1.9, equivalent to HH12) in the quail embryo, two basement membranes with solid, uninterrupted laminin staining were identified below the endoderm and the splanchnic mesoderm, respectively (Figure 2.2 A-B, arrowheads). The basement membranes were distinctly separated along the majority of the medial-lateral axis though they did appear to contact one another at discrete points (Figure 2.2 B, arrows). The mesenchymal space was very narrow and sparsely populated with cells (Figure 2.2 B, asterisk). At E2.1 (HH14), laminin staining of the outer basement membrane appeared slightly fragmented (white arrowheads) and in limited, sporadic regions, the mesenchymal space contained a single layer of cells (Figure 2.2 C-D, asterisks). At E2.2 (HH16), the basement membrane underlying the outer epithelium was well dispersed evidenced by discontinuous laminin staining (Figure 2.2 E-F, white arrowheads). There were also multiple cell layers within the mesenchyme (Figure 2.2 F, asterisks). At E3.5 (HH21), the anterior and posterior portions of the intestine had folded into a tube while the middle portion remained open ventrally. In both the open and closed regions, the outer epithelial basement membrane had returned to an unbroken configuration (arrowheads) now enclosing a well-populated mesenchymal compartment (Figure 2.2 G-J,).

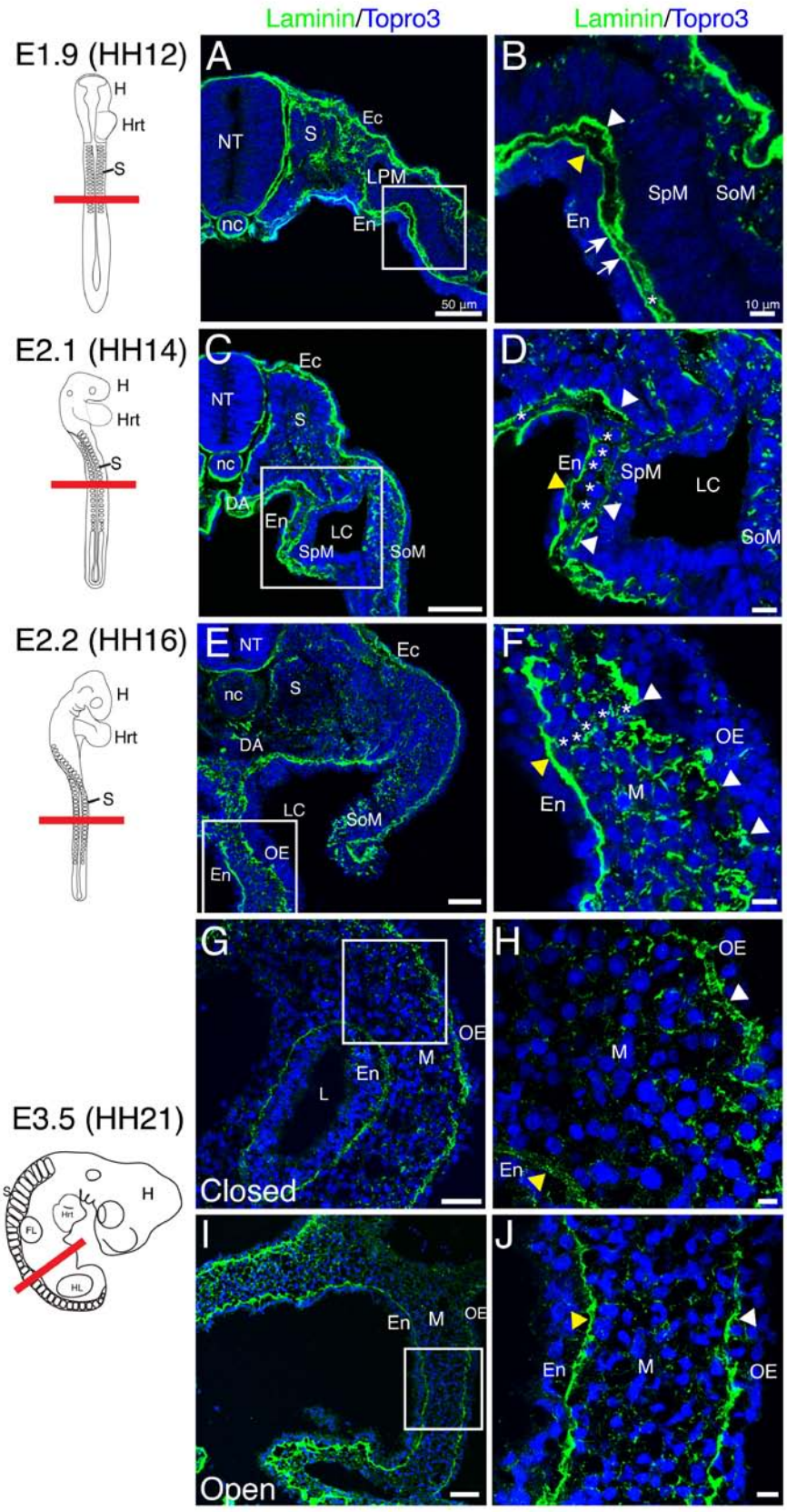
Laminin/Topro3
Laminin/Topro3
E1.9 (HH12)
H
Hrt
S
A
NT
S
Ec
LPM
nc
En
50 µm
B
SpM
SoM
En
10 µm
E2.1 (HH14)
H
Hrt
S
C
Ec
NT
S
nc
DA
En
LC
SpM
SoM
D
En
SpM
LC
SoM
E2.2 (HH16)
H
Hrt
S
E
NT
Ec
nc
S
DA
LC
SoM
OE
En
F
OE
M
En
E3.5 (HH21)
H
FL
HL
G
OE
M
En
L
Closed
H
OE
M
En
I
En
M
OE
Open
J
En
M
OE

Figure 2.2 Early basement membrane dynamics in generation of the mesenchymal compartment. Schematics in left column depict quail embryos at each stage and the red line denotes the plane of section. **A-B)** At E1.9, a continuous basement membrane lined the splanchnic mesoderm (white arrowhead) and endoderm (yellow arrowhead) with multiple apparent points of contact (arrows). Asterisk denotes a rare mesenchymal cell. **C-D**) The outer basement membrane began to break down at E2.1 (white arrowheads) and mesenchymal cells were more common (asterisks). The endodermal basement membrane remained solid (yellow arrowhead) **E-F)** At E2.2, there were multiple mesenchymal cell layers (asterisks) and the outer basement membrane was dispersed (white arrowheads). Yellow arrowhead denotes endodermal basement membrane. **G-J)** At E3.5, both the outer epithelial (white arrowhead) and endodermal (yellow arrowhead) basement membranes were continuous in the closed and open intestinal regions. Scale bars: 50μm (A, C, E, G, I) and 10μm (B, D, F, G, J). DA, dorsal aorta; Ec, ectoderm; En, endoderm; FL, forelimb; H, head; Hrt, heart; HL, hindlimb; L, lumen; LC, lateral cavity; LPM, lateral plate mesoderm; M, mesenchyme; nc, notochord; NT, neural tube; OE, outer epithelium; S, somites; SoM, somatic mesoderm; SpM, splanchnic mesoderm.

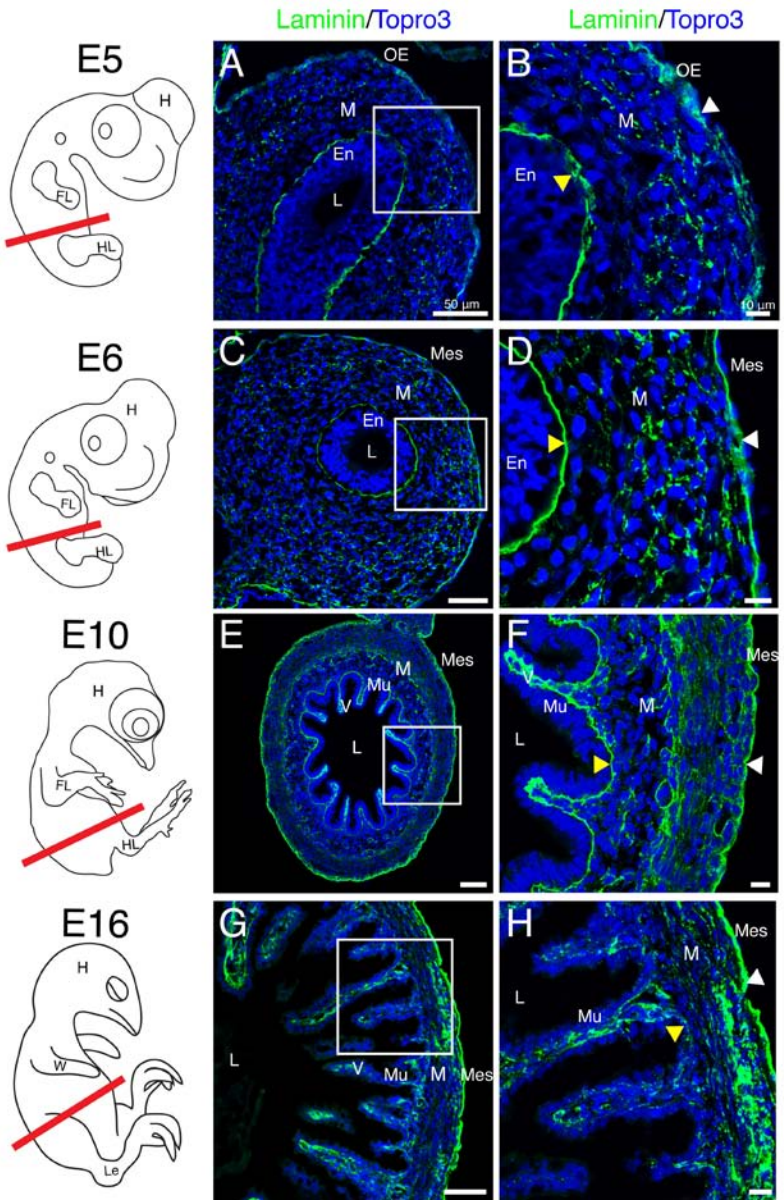

Figure 2.3 Basement membrane dynamics throughout gut tube closure and mesenchymal differentiation. Schematics in left column depict quail embryos at each stage and the red line denotes the plane of section. **A-B)** At E5, the outer epithelial basement membrane appeared dispersed (white arrowhead). Yellow arrowhead denotes endodermal basement membrane. **C-D)** At E6, both the outer (white arrowhead) and endodermal (yellow arrowhead) basement membranes were unbroken. **E-F)** At E10, villi (V) were present and both basement membranes were continuous (arrowheads). **G-H)** At E16, the mesenchyme was condensed (compare F and H). The outer basement membrane was robust and unbroken (white arrowhead) while the mucosal basement membrane weakly stained with laminin (yellow arrowhead). Scale bars: 50µm (A, C, E, G,) and 10µm (B, D, F, H). En, endoderm; FL, forelimb; H, head; HL, hindlimb; L, lumen; Le, leg; M, mesenchyme; Mes, mesothelium; Mu, mucosa; OE, outer epithelium; V, villi; W, wing.

Between E5 and E6, the gut tube completed ventral closure. At E5 (HH27), the outer epithelial basement membrane was again dispersed (Figure 2.3 A-B, white arrowhead) but quickly returned to a continuous configuration by E6 (HH29) (Figure 2.3 C-D, white arrowhead). Once solidified at E6, no further changes in the outer epithelial basement membrane were observed through E16. However, the mesenchymal layer underwent dynamic changes over these stages including contributing to villus formation at E10 (Figure 2.3 E-F) and mesenchymal compaction and differentiation (Figure 2.3 G-H). Additionally at E16, laminin staining in the endodermal basement membrane appeared diffuse (Figure 2.3 G-H, yellow arrowhead). Thus, though the outer basement membrane oscillates between discontinuous and continuous states, both basement membranes observed in the intestinal primordium were readily identified throughout development defining the three basic tissue compartments of the intestine.

Development of the outer epithelium

In the adult, the outer epithelium is a simple squamous cell layer, termed mesothelium, that is important for protection of coelomic organs and providing a non-adhesive surface for movement (Mutsaers, 2002; Mutsaers, 2004; Yung and Chan, 2007). We next sought to determine if the periodic dissociation of the outer basement membrane was correlated with differentiation of the outer epithelium into mesothelium. In the embryo and adult, the mesothelium expresses the intermediate filament protein cytokeratin and resides upon a continuous, laminin-enriched basement membrane. A recent lineage tracing study from our laboratory demonstrated that cells within the splanchnic mesoderm of the developing gut tube eventually give rise to the intestinal mesothelium (Winters et al., 2012, in press).

To investigate the development of the outer epithelium, we stained serial sections of the quail midgut with antibodies for the epithelial markers cytokeratin and

laminin. As described above, the outer epithelium and mesenchyme first appeared as distinct cellular layers at E2.1 (HH14). At this time, the outer epithelium was stratified and the underlying basement membrane was fragmented (see above, Figure 2.2 D). At E3.5 (HH21), the outer epithelium remained stratified and cytokeratin-negative. Laminin staining in the outer basement membrane (arrows) had returned to an unbroken configuration (Figure 2.4 A-C). Twelve hours later, at E4 (HH23), the outer epithelium was, for the first time, a single cell layer thick (arrowheads) though still cytokeratin-negative (Figure 2.4 D-F). At E5 (HH27), we observed weak cytokeratin staining (red) within the outer epithelium but dispersed laminin staining in the basement membrane (Figure 2.4 G-I, arrowheads). Finally, at E6 (HH29) a simple squamous epithelium with robust cytokeratin staining (red) and a continuous basement membrane (arrows) was present at the surface of the midgut characteristic of the adult structure (Figure 2.4 J-L). This mature configuration of the outer epithelium was observed throughout the remainder of development. Thus, the transition of the basement membrane to an unbroken conformation at E3.5 was associated with conversion of the outer epithelium from a stratified to simple layer. The subsequent breakdown and solidification of the outer basement membrane at E5-E6 was concurrent with differentiation of the outer cell layer into a mature, cytokeratin-positive mesothelium.

Expansion of the mesenchymal compartment

As described in Figure 2 and 3, the mesenchymal compartment underwent a dramatic expansion over these early stages of intestinal development. We next quantified the change in size of the mesenchymal compartment over time to determine if there was any correlation with basement membrane breakdown. We measured the distance between the endoderm and outer epithelial basement membranes at multiple medial-lateral positions to determine the average width of the mesenchymal

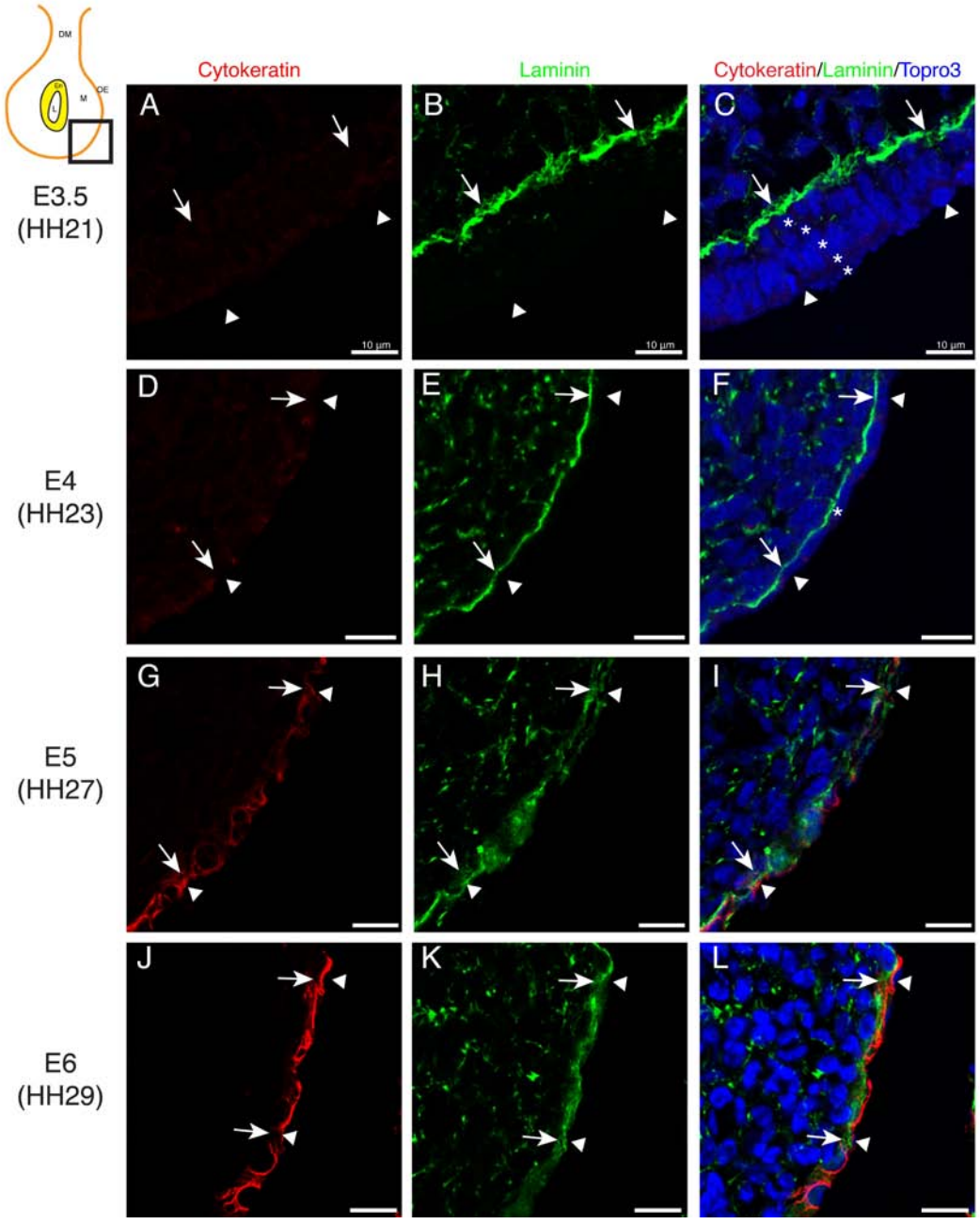

Figure 2.4 Mesothelial differentiation. Schematic in upper-left corner depicts the region of the gut tube that was imaged. **A-C)** At E3.5, the outer epithelium (arrowheads) was stratified (asterisks) and the basement membrane was continuous (arrows). No cytokeratin staining was evident at this time. **D-F)** At E4, the outer epithelium was a single cell layer thick (arrowheads) with a continuous basement membrane (arrows). Cytokeratin staining remained negative. **G-I)** At E5, laminin staining in the outer basement membrane was dispersed (arrows). Cytokeratin staining was present at low levels. **J-L)** At E6, laminin staining (arrows) was unbroken and cytokeratin staining was robust within the mesothelium (arrows). Scale bars: 10µm. DM, dorsal mesentery; En, endoderm; L, lumen; M, mesenchyme; OE, outer epithelium.

compartment at each stage. The mesenchymal space at E1.9 (HH12) was narrow averaging 7.5 μm in width. At E2.1 (HH14), despite the slight increase in the number of cells found in the mesenchymal space at this time, the overall average width was 6.4 μm. Between E2.1-E3.5 (HH14-HH21) the mesenchymal compartment expanded abruptly from 6.4 μm to 103 μm in width. This time period corresponded to the stages over which the outer basement membrane was broken down. Interestingly, after the basement membrane solidified again at E3.5, the distance between the two basement membranes decreased to 74 μm by E4. The second instance of outer basement membrane breakdown at E5 also correlated with a small increase in mesenchymal compartment width though generally the mesenchymal width trended downward between E3.5 and E6 (Figure 2.5 A).

Over subsequent stages, the outer basement membrane was solid and the intestinal tube was closed. We next examined mesenchymal cross-sectional area and intestinal length to determine if these variables changed proportionately over time. We quantified mesenchymal cross-sectional area by outlining both the inner and outer basement membranes and calculating the intervening pixels using Metamorph software. We divided the small intestine into quarters along the length of the tube, small intestine (SI) 1-4, and analyzed each region individually at each stage. We also measured the length of the small intestine over the same stages by dissecting away the mesentery and extending the intestine out in a straight line. The anterior regions of the small intestine had consistently larger mesenchymal areas than the posterior regions over all stages examined. Between E8 and E12, the mesenchymal area of each region remained surprisingly constant (Figure 2.5 B). However, there was a dramatic increase in small intestinal length (17.6 mm at E8 to 71.1 mm at E12) over the same time period. Indeed, between E6 and E12, the small intestine roughly doubled in length every two days elongating at an average rate of 11 mm/day (Figure 2.5 C).

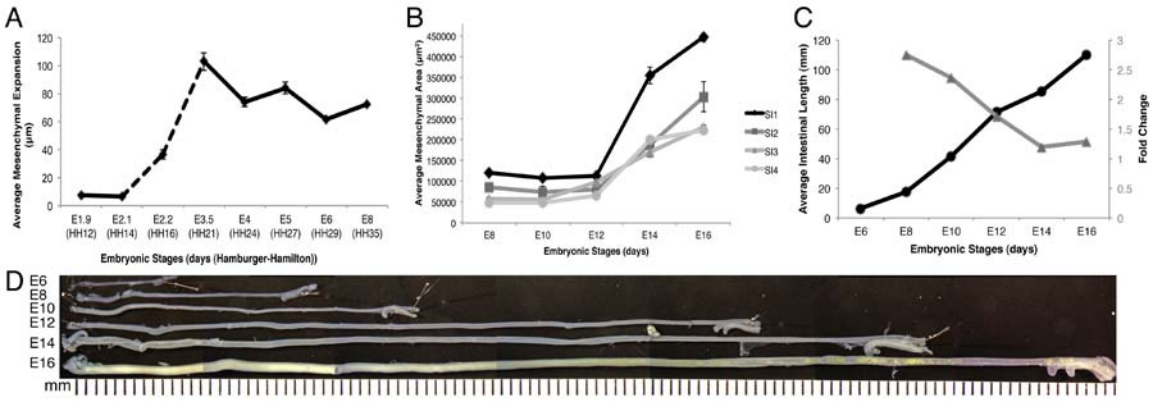

Figure 2.5 Quantification of mesenchymal expansion over time. A) Graph of the distance between the outer epithelial and endodermal basement membranes measured at key stages between E1.9 and E8. The dashed line represents the time period over which the outer basement membrane was dispersed. Solid lines indicate a continuous outer basement membrane was present. **B)** Four regions along the anterior-posterior axis of the small intestine (SI 1-4) were analyzed individually for mesenchymal cross-sectional area between E8 and E16. The cross-sectional area of each region was graphed independently. **C)** Small intestinal length measured between E6 and E16 (left axis, black circles). Fold change in intestinal length over the same time period (right axis, grey triangles). **D)** Photomontage of isolated small intestines with mesentery and blood vessels removed and pinned out to demonstrate their length.

Between E12 and E16, there was a notable increase in cross-sectional area throughout all four regions of the small intestine (Figure 2.5 B). There was also an increase in small intestinal length over these stages. The rate of intestinal lengthening between E6 and E16 was relatively steady averaging close to 10 mm/day (Figure 2.5 C, black line). However, this steady rate of growth represented a 4-fold increase in length between E8 and E12 and only a 1.5-fold increase between E12 and E16 (Figure 2.5 C, gray line). Thus, the rapid increase in mesenchymal cross-sectional area at E12 correlates with a decrease in the relative change in length.

Development of the muscularis layers and myofibroblasts

We next examined differentiation of the mesenchymal compartment. While initially uniform in appearance, the mature mesenchymal compartment is composed of varied tissue types including multiple layers of visceral smooth muscle that provide the force for peristaltic contractions. Other mesenchymal cells with limited contractile ability include the subepithelial myofibroblasts that closely surround the crypts and line the mucosa up into the villi. Using studies of the chicken as a reference, we expected four layers of visceral smooth muscle to develop in the quail small intestine: inner longitudinal, inner circular, outer circular, and outer longitudinal (Gabella, 1985; Gabella, 2002). These layers are largely distinguished based on morphological features; however, the outer circular layer of the adult chicken can also be identified molecularly as α-smooth muscle actin (α-SMA) expression is almost entirely replaced by γ-smooth muscle actin (γ-SMA) expression (Gabella, 1985; Yamamoto, 1996).

We utilized immunofluorescence for α- and γ-SMA to generate a comprehensive timeline of visceral smooth muscle and myofibroblast development in the quail small intestine. Faint staining for both α- and γ-SMA was first observed at E6 in a rudimentary circular layer (OC) within the mesenchyme (Figure 2.6 A-D). SMA-negative

mesenchymal cells were found on both the luminal and coelomic aspects (Figure 2.6 A-D, asterisks). At E10, an α-SMA-positive, γ-SMA-negative outer longitudinal (OL) layer was first observed within the submesothelial region (Figure 2.6 E-H). The inner circular (IC) layer was first distinguishable at E14 due to high levels of α-SMA and low levels of γ-SMA at the innermost aspect of the circular muscle layer (Figure 2.6 I-L). Also at E14, α-SMA-positive cells could occasionally be identified within the villi (data not shown). At E16, an α- and γ-SMA-positive inner longitudinal layer (IL) was visible and robust α-SMA-positive staining was present within the villi (arrowheads, Figure 2.6 M). The submucosal mesenchyme was concurrently reduced to a thin layer (asterisk) and the outer circular layer exhibited decreased staining for α-SMA (Figure 2.6 M-P). Finally, in the adult small intestine, γ-SMA was identified in all four layers of visceral smooth muscle but the outer circular layer did not stain for α-SMA at appreciable levels (Figure 2.6 Q-T). Additionally, the intestinal crypts were directly adjacent to the inner longitudinal visceral smooth muscle layer without any intervening submucosal mesenchyme (Figure 2.6 Q-T, arrows). Thus, the structure of the adult quail small intestine is similar to other avians, including the chicken (Gabella, 1985). The current study demonstrates that contractile cell differentiation in the quail intestine occurs in the following progression: outer circular layer at E6, outer longitudinal layer at E10, inner circular layer at E14, and inner longitudinal layer and subepithelial myofibroblasts at E16.

The organization of the endothelial plexus

Elaboration of the vasculature is critical for organ formation. The vasculature of the intestine is housed within the mesenchymal layer. The major arteries supplying the intestine (mesenteric arteries) branch from the aorta and reach the intestine by means of a mesentery (two mesothelial membranes closely apposed to one another). Once the mesenteric arteries reach the intestine, the large, muscularized branches stay near the

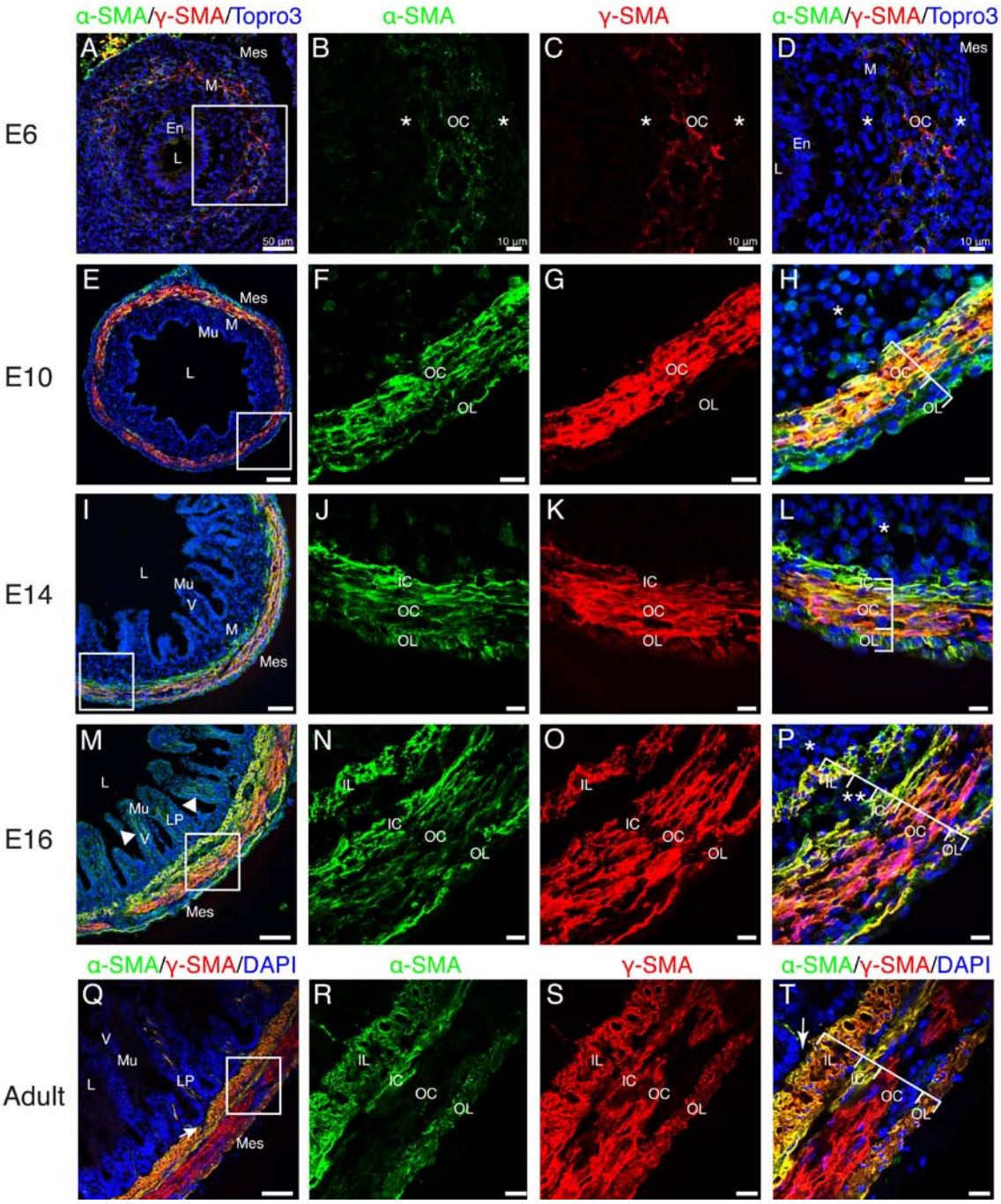
α-SMA/γ-SMA/Topro3
α-SMA
γ-SMA
α-SMA/γ-SMA/Topro3
E6
E10
E14
E16
Adult
α-SMA/γ-SMA/DAPI
α-SMA
γ-SMA
α-SMA/γ-SMA/DAPI
A
B
C
D
E
F
G
H
I
J
K
L
M
N
O
P
Q
R
S
T
Mes
M
En
L
Mu
V
LP
OC
OL
IC
IL
50 μm
10 μm

Figure 2.6 Differentiation of visceral smooth muscle. A-D) At E6, faint staining for α-SMA and γ-SMA defined the outer circular muscle layer. Asterisks represent SMA-negative mesenchymal cells bordering the outer circular muscle layer. **E-H)** Robust staining for α-SMA marked the outer circular and outer longitudinal muscle layers. γ-SMA was observed in the outer circular but not the outer longitudinal layer. SMA-negative submucosal mesenchyme was still present (asterisk). **I-L)** By E14, the inner circular layer (α-SMA-positive, weak γ-SMA) was evident. Asterisk denotes SMA-negative submucosal mesenchyme. **M-P)** At E16, four muscle layers were present including the inner longitudinal layer. All layers stained for both α-SMA and γ-SMA. Double asterisks denote submucosal neuronal plexus. Limited SMA-negative submucosal mesenchyme was present (asterisk). Arrowheads in M indicate SMA-positive staining within the villi. **Q-T)** In the adult intestine, the four visceral smooth muscle layers were directly subjacent to the lamina propria (arrow) with no intervening submucosal mesenchyme. The outer circular layer was α-SMA-negative. Scale Bars: 50μm (A, E, I, M, O) and 10μm (B-D, F-H, J-L, N-P, R-T). En, endoderm; IC, inner circular; IL, inner longitudinal; LP, lamina propria; L, lumen; M, mesenchyme; Mes, mesothelium; Mu, mucosa; OC, outer circular; OL, outer longitudinal; V, villi.

surface subjacent to the thin outer longitudinal layer of visceral smooth muscle. Other branches dive deep to supply a second tier of blood vessels that resides near the junction of the lamina propria and inner longitudinal smooth muscle layer. The third and most expansive tier is the extensive capillary network extending into the villi and localized just below the mucosal epithelium (Powell et al., 2011). The initial arrangement of the intestinal primordium with both basement membranes within microns of one another (Meier, 1980) allows a single, central endothelial plexus to contact both basement membranes and epithelia. The expansion of the mesenchyme necessitates growth and remodeling of the vascular plexus for this relationship to be maintained.

To understand how the vasculature of the intestine is remodeled from a single centrally located endothelial plexus into a multi-tiered vascular network, we utilized QH1 (early quail endothelial cell marker) staining and Tg(*tie1*:H2B-eYFP) quail embryos. These transgenic embryos express an H2B-eYFP fusion protein under control of the endothelial specific *Tie1* promoter (Poynter and Lansford, 2008; Sato et al., 2010). At E2.1 (HH14), endothelial cells were in close approximation to both the endoderm and splanchnic mesoderm (Figure 2.7 A-B, arrowheads). At E3 (HH18), YFP-positive endothelial cells were distributed along the medial-lateral axis of the intestinal primordium but remained within the middle of the mesenchymal layer thus losing close contact with both the endodermal and outer epithelial basement membranes (Figure 2.7 C-D, arrowheads). This configuration was maintained until E6 at which time the YFP-positive cells were organized into two layers one subjacent to the mesothelium and another layer juxtaposed to the developing submucosal layer (Figure 2.7 E-F, arrowheads). The two tiered endothelial network visible at E6 was also reported in Nagy et al. (2009).

At E10, the external endothelial layer was localized below the newly differentiated outer longitudinal visceral smooth muscle cell layer thus occupying the

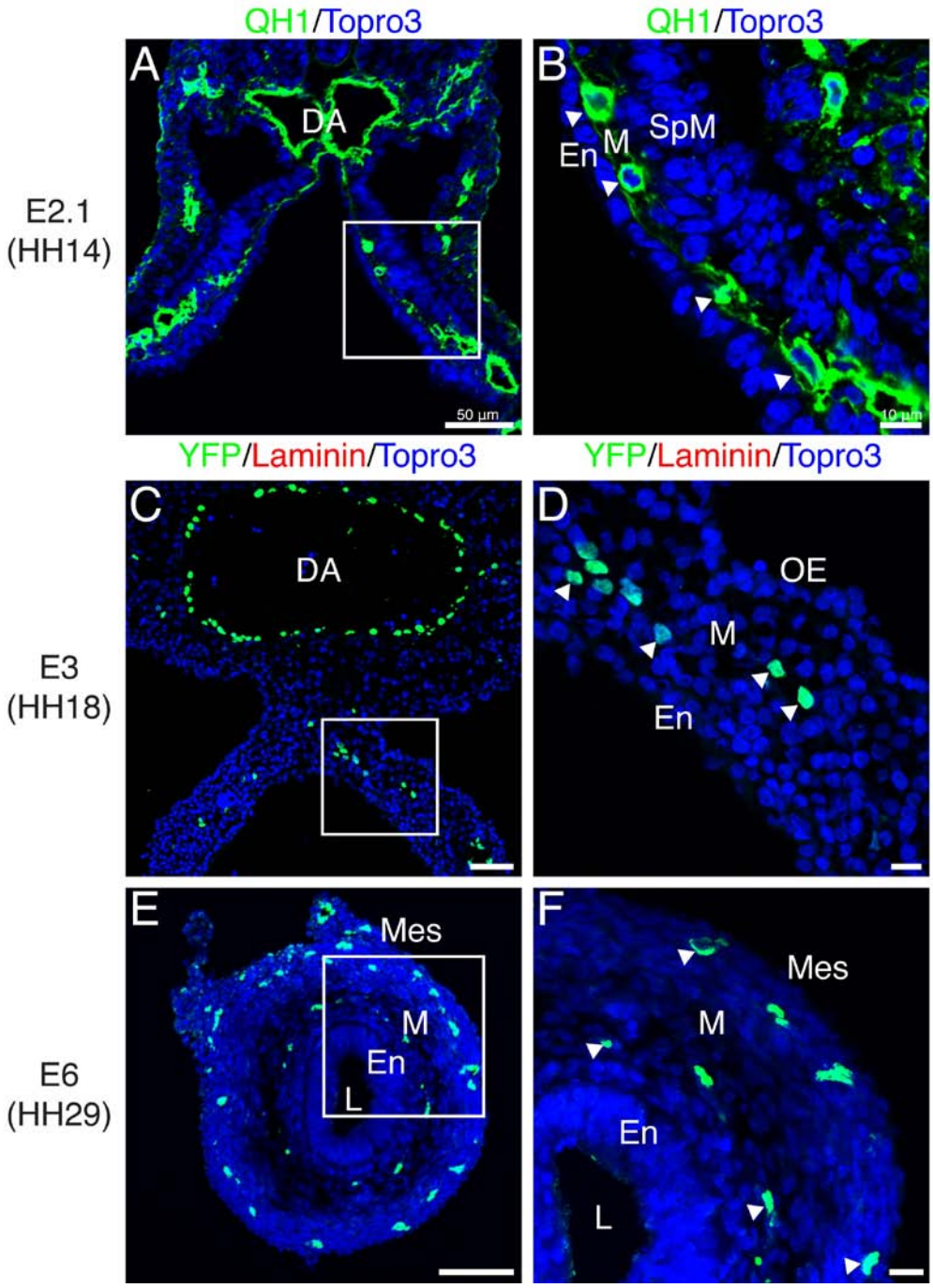

Figure 2.7 Generation of a two-tiered endothelial plexus. A-B) At E2.1, an endothelial plexus marked by QH1 (arrowheads) was present between the endoderm and splanchnic mesoderm. C-F: Sections through Tg(*tie1*:H2B-eYFP) quail intestinal primordia. **C-D)** At E3, the endothelial plexus (arrowheads) was detected in the middle of the multilayered mesenchyme. **E-F)** At E6, the endothelial plexus was organized into two concentric layers below the endoderm and mesothelium, respectively (arrowheads). Scale bars: 50µm (A, C, E) and 10µm (B, D, F). DA, dorsal aorta; En, endoderm; L, lumen; M, mesenchyme; Mes, mesothelium; OE, outer epithelium; SpM, splanchnic mesoderm.

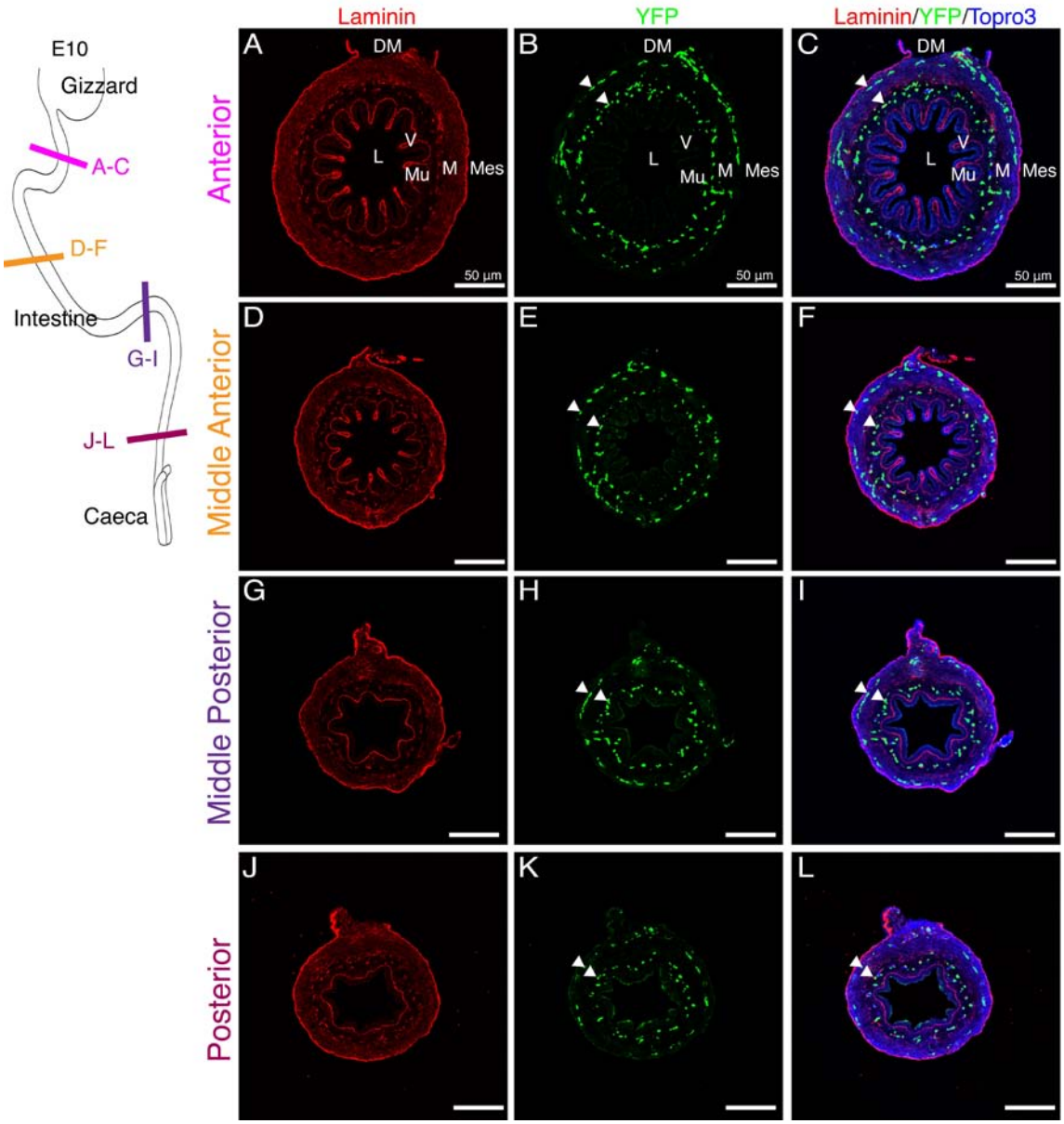

Figure 2.8 Endothelial plexus remodeling during villi formation. Schematic in upper-left corner depicts the regions of the intestine that were sectioned. E10 intestines were isolated from Tg(*tie1*:H2B-eYFP) embryos. **A-F)** Villi were present in the anterior region of the intestine. The endothelial plexus (YFP-positive) was organized in two concentric rings (arrowheads) but did not extend into the villi. **G-J)** In the posterior small intestine, ridges but no villi were identified. The endothelial plexus remained organized in two concentric rings (arrowheads). All images are to the same scale. Scale bars: 50µm (A-L). DM, dorsal mesentery; L, lumen; M, mesenchyme; Mes, mesothelium; Mu, mucosa, V, villi.

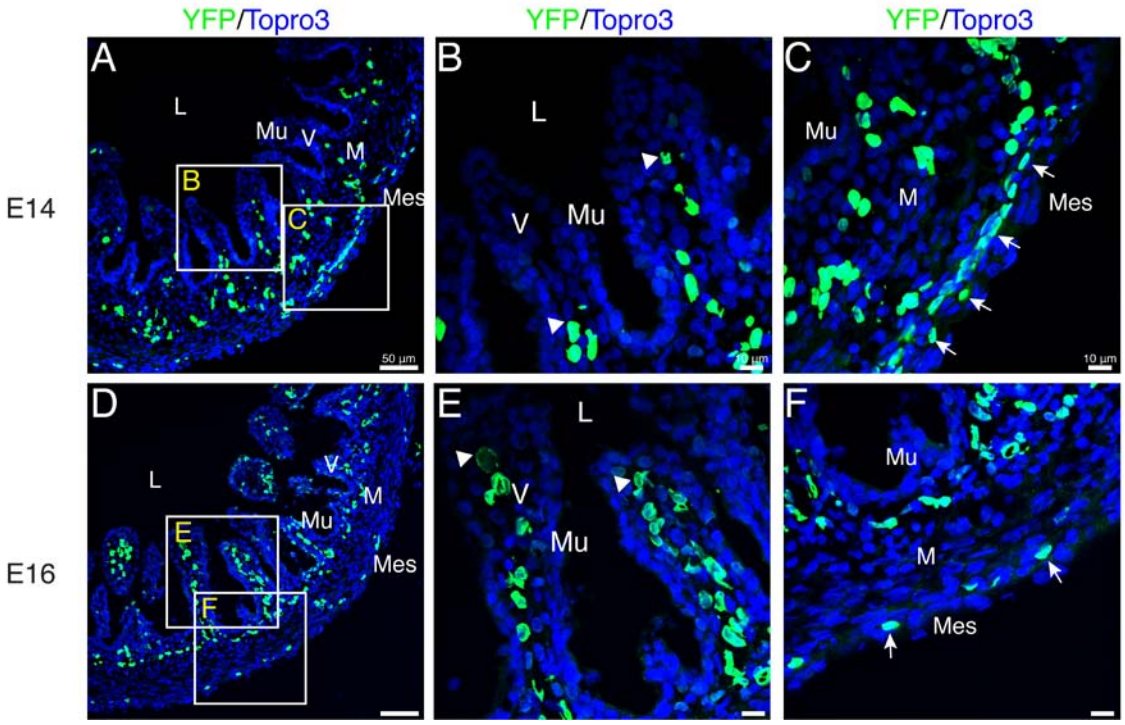

Figure 2.9 Extension of endothelial cells into the villi. Images are of sections through Tg(*tie1*:H2B-eYFP) quail. **A-B)** At E14, YFP-positive endothelial cells (arrowheads) were localized within the base of the villi in low numbers. **C)** The outer endothelial plexus was substantial at E14 (arrows). **D-E)** By E16, endothelial cells had reached the tip of the villi (arrowheads) and were present in high numbers. **F)** The outer endothelial plexus thinned by E16 (arrows). Scale bars: 50µm (A, D), 10µm (B-C, E-F). L, lumen; M, mesenchyme; Mes, mesothelium; Mu, mucosa; V, villi.

same space where the major vessels will be found in the adult. At this stage, villi were also first observed in the anterior region of the small intestine (Figure 2.8 A-F) though the posterior region only had small ridges protruding into the lumen (Figure 2.8 G-L). Notably, endothelial cells of the internal plexus (arrowheads) throughout both the anterior and posterior small intestine did not extend into the villi or ridges (Figure 2.8 A-L). We first observed endothelial cells within the villi at E14 in low numbers, four days after villi were apparent in the anterior portion of the gut tube (Figure 2.9 A-C, arrowheads). By E16, endothelial cells were found in abundance within the villi (Figure 2.9 D-F, arrowheads). Cells within the outer endothelial tier became fewer in number over time (Figure 2.9 C, F, arrows). Thus, development of the enteric endothelial network progresses through four phases. First, endothelial cells are scattered throughout the mesenchymal space. Second, they organize into two layers in the submesothelial region and submucosal mesenchyme, respectively. Third, differentiation of the outer longitudinal smooth muscle leads to localization of the external plexus below the muscle layer. Finally, endothelial cells penetrate the lamina propria of the villi.

Generation of muscularized surface blood vessels

While the vasculature of the villi remains as a capillary plexus, the vessels near the surface of the adult intestine are large caliber and muscularized. We next examined Tg(*tie1*:H2B-eYFP) intestines in whole mount to determine when large surface blood vessels were formed. At E6, the stage at which two distinct layers of endothelial cells were first apparent within the gut wall, there were not any major surface vessels (Figure 2.10 A, B). Instead, endothelial cells were uniformly distributed in a honeycomb-like pattern (Figure 2.10 B). By E10, mesenteric branches extending to the intestine were observed (arrows) though there were still no large vessels visible on the intestine proper (Figure 2.10 C, D). At E11, we first observed large blood vessels extending from the

dorsal mesentery over the gut tube proper (Figure 2.10 E, F, arrowheads). Throughout subsequent stages, the major vessels elongated to encompass a greater portion of the intestinal circumference (Figure 2.10 G-J, arrowheads).

A further mark of blood vessel maturity is recruitment and differentiation of vascular smooth muscle cells. We used immunofluorescence for α-SMA to determine when cells of the intestinal vasculature were muscularized. At E12, α-SMA staining was present within the outer longitudinal and outer circular smooth muscle layers but was not identified surrounding the YFP-positive endothelial cells (Figure 2.11 A-B). At E14, a single layer of α-SMA-positive cells surrounded the large blood vessels found near the surface of the intestine (Figure 2.11 C-D, arrowheads). At E16, rare blood vessels were observed containing multiple layers of vascular smooth muscle cells (Figure 2.11 E-F, arrowheads). In the adult intestine, large arteries with multiple layers of vascular smooth muscle were readily identified (Figure 2.11 G-H, arrowheads). Neighboring veins were large caliber though still poorly muscularized (Figure 2.11 G-H, arrows). Thus, the major blood vessels of the intestine are not muscularized until near hatching.

Discussion

Splanchnic mesoderm generates the bulk of the intestine and will diversify into serosa, connective tissue, musculature, and the enteric vasculature. However, relatively little is known about the development of the intestinal mesoderm. Our study provides a comprehensive examination of the major morphological changes that occur within the intestinal mesoderm starting with the establishment of the intestinal primordium and ending with the definitive structure. Through concurrent examination of multiple features we were able to identify temporal and spatial coordination between previously unlinked developmental events (Table 1). An examination of four critical time periods in intestinal mesoderm development is presented below highlighting novel correlations illustrated by

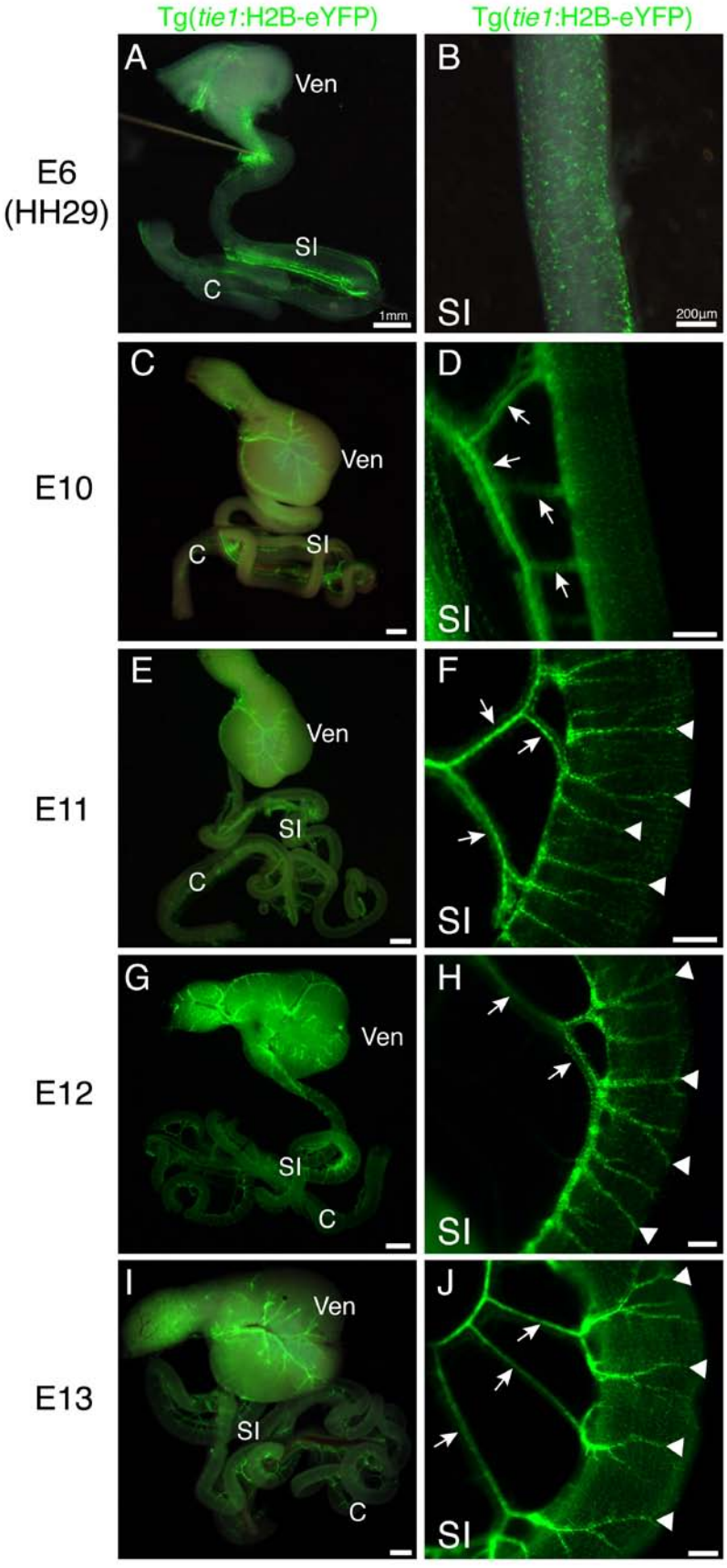
Tg(tie1:H2B-eYFP)
Tg(tie1:H2B-eYFP)
E6 (HH29)
E10
E11
E12
E13
A
B
C
D
E
F
G
H
I
J
Ven
SI
C
1mm
200μm

Figure 2.10 Development of large blood vessels of the small intestine. All panels are whole mount images of YFP fluorescence in isolated gut tubes from Tg(*tie1*:H2B-eYFP) quail. **A-B**: At E6, YFP-positive endothelial cells were evident in the wall of the small intestine in a honeycomb pattern. **C-D**: At E10, mesenteric vessels were visible (arrows) but large vessels on the small intestine proper were not observed. **E-F**: At E11, major vessels near the surface of the small intestine were present (arrowheads) Arrows denote mesenteric blood vessels. **G-J**: Major small intestinal vessels displayed further branching at E12 and E13 (arrowheads). Arrows denote mesenteric blood vessels. Scale bars: 1mm (A, C, E, G, I); 200μm (B, D, F, H, J). C, caeca; SI, small intestine; Ven; ventriculus.

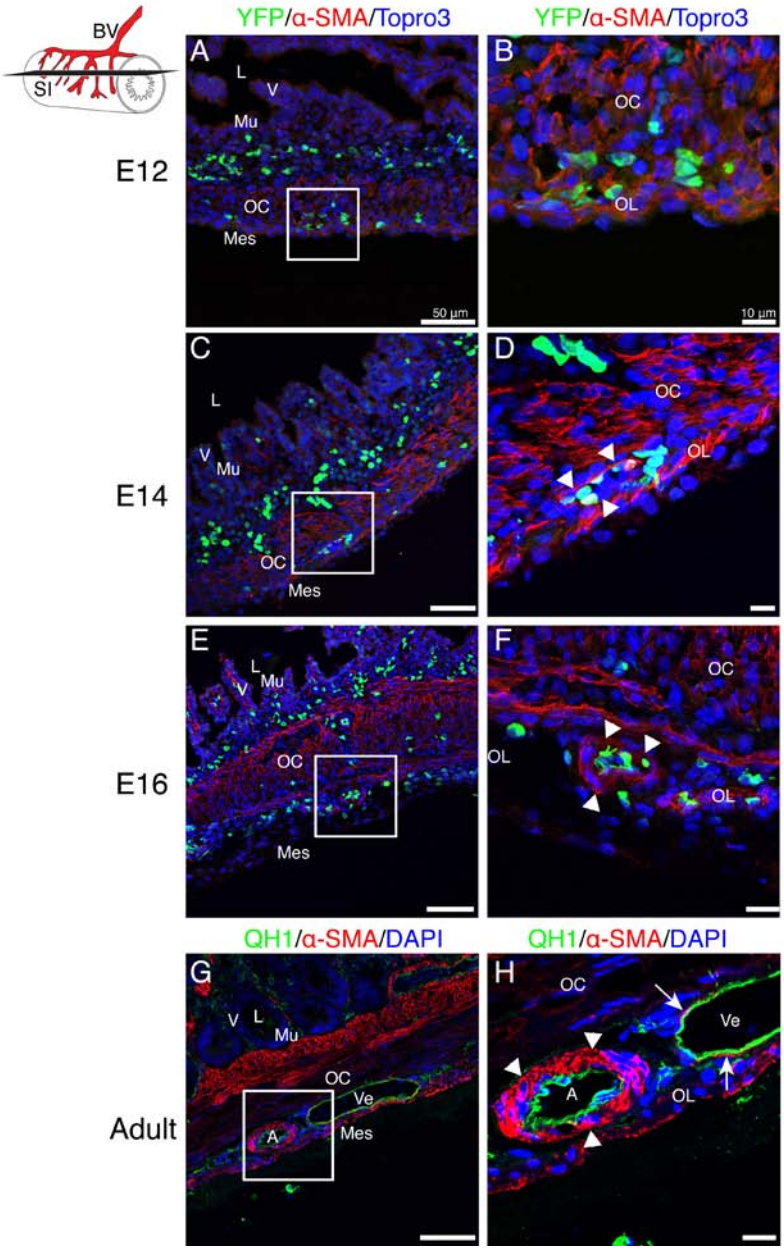

Figure 2.11 Muscularization of small intestinal blood vessels. Schematic in upper-left corner depicts the small intestine (SI), blood vessels (BV) and the orientation of sections (black slice). A-F: Sections from Tg(*tie1*:H2B-eYFP) intestines. **A-B**: At E12, YFP-positive endothelial cells subjacent to the coelomic surface were in close proximity to the visceral smooth muscle layers (OC, OL) but were not invested by vascular smooth muscle cells. **C-D**: At E14, vascular smooth muscle cells (α-SMA-positive, arrowheads) arranged in a single layer were identified surrounding YFP-positive endothelial cells localized near the coelomic surface of the small intestine. **E-F**: At E16, the vascular smooth muscle cells appeared more mature and were in multiple layers surrounding endothelial cells (arrowheads). **G-H**: QH1 staining of a wild type adult quail small intestine revealed mature vessels with multiple layers of vascular smooth muscle cells in large arteries (arrowheads) but only a single layer in veins (arrows). Scale bars: 50µm (A, C, E, G) and 10µm (B, D, F, H). A, artery; L, lumen; Mes, mesothelium; Mu, mucosa; OC, outer circular muscle layer; Ve, vein; V, villi.

Table 2.1 Stages at which key developmental events occur throughout the development of quail intestinal mesoderm.

E1.9	E2.2	E3.5	E4	E5	E6
• Continuous outer basement membrane • Narrow mesenchymal space • Single layered endothelial plexus • Open gut tube (GT)	• Dispersed outer basement membrane • Scattered mesenchymal cells • Single endothelial plexus • Open GT	• Continuous outer basement membrane • Multilayered mesenchyme • Peak in mesenchymal width • Stratified outer epithelium • Anterior and posterior closure of GT	• Continuous outer basement membrane • Contraction of mesenchymal width • Single layered outer epithelium	• Dispersed outer basement membrane • Increased mesenchymal width • Cytokeratin-positive outer epithelium	• Continuous outer basement membrane • Decreased mesenchymal width • Mesothelium • Completely closed GT • Endothelial plexus splits into two layers • Outer circular muscle layer • Length: 6mm
E10	**E11**	**E12**	**E14**	**E16**	
• Villi present • Outer Longitudinal muscle layer • Submesothelial layer of SMA-positive cells • Length: 42mm	• Large surface blood vessels	• Sharp increase in mesenchymal area • Length: 72mm	• Endothelial cells at base of villi • Myofibroblasts in lamina propria • Inner circular muscle layer • Single layer of vascular smooth muscle • Length: 85mm	• Endodermal basement membrane dispersed • Endothelial cells in tips of villi • Inner longitudinal muscle layer • Multilayered vascular media • Limited submucosal mesenchyme • Length: 110mm	

this study. These data provide developmental biologists and clinicians with a detailed baseline of normal development—the context with which perturbations of intestinal development generated by experimental manipulation and disease can be evaluated. Finally, this comprehensive analysis reveals heretofore unidentified cell and tissue relationships that generate numerous questions for future study.

Appearance of the intestinal anlage

Although not immediately apparent, the eventual architecture of the mature intestine is in fact represented in three features of the intestinal primordium. At the most fundamental level, the endoderm is localized ventrally and the mesoderm, dorsally in the flat intestinal anlage. Thus, when a tube is formed by folding the flat sheet ventrally, the endoderm will line the lumen and the mesoderm will form the coelomic surface reflecting their position in the adult structure. Second, the primordium is split into three compartments by two basement membranes, an arrangement maintained into maturity. Finally, from its earliest appearance, the vascular plexus is localized in the mesenchymal compartment juxtaposed to both basement membranes (Meier, 1980). These basic elements form the structural scaffold around which the flat sheet of the primordium folds to form a tube. Within this context, the mesenchymal space and its resident cells expand to generate the largest intestinal compartment, and the vasculature matures into a multi-tiered network.

Development of the mesenchymal compartment: E1.9-E5

Starting from this basic structure, the first significant change in intestinal mesoderm development is the generation of a multi-layered mesenchyme. Though forming the bulk of the intestine in the adult, this layer is essentially absent in the primordium—the endothelial plexus of the intestine is the only cell population to reside in

the mesenchymal compartment and contacts the basement membranes of both the endoderm and splanchnic mesoderm. The rapid cellular expansion of the mesenchymal compartment between E2.2 and E3.5 occurred concurrently with a breakdown of the outer basement membrane likely due to an ingress of cells from the outer epithelium into the mesenchyme. At E3.5, the mesenchymal compartment peaked in width and the outer epithelial basement membrane returned to an unbroken configuration. Throughout the subsequent stages in which a solid basement membrane was present the width of the mesenchymal compartment gradually decreased. A slight increase in mesenchymal width was observed at E5, which correlated with a second brief breakdown of the outer epithelial basement membrane. These features suggest the following sequence: inward migration of cells from the outer epithelium into the mesenchyme, cessation of migration and repair of the basement membrane, a second wave of inward migration, and final repair of the basement membrane. The potential of two temporally separated waves of migration into the mesenchymal space may indicate that specific mesenchymal lineages are added sequentially as suggested but not conclusively proven by cell lineage tracing studies (Wilm et al., 2005; Winters et al. 2012, in press).

Completion of intestinal tube formation: E5-E6

The next major change in intestinal development is the completion of tube formation that occurs at E6. At this stage, the mesothelium is fully differentiated, SMA is first observed in the outer circular visceral smooth muscle layer and the endothelial plexus splits into two layers. Each of these topics is considered below.

Mesothelial differentiation in the intestine has only recently been studied in any detail (Wilm et al., 2005; Kawaguchi et al., 2007; Winters et al, 2012, in press). In contrast, mesothelial development in the heart has been examined extensively. Cardiac mesothelium is derived from a localized, extrinsic progenitor pool that migrates to the

heart. Once at the surface of the heart, individual mesothelial cells undergo an epithelial-mesenchymal transition (EMT) to invade the underlying myocardium and give rise to vascular smooth muscle cells and intracardiac fibroblasts (Mikawa and Gourdie, 1996; Dettman et al., 1998; Männer, 1999; Pérez-Pomares et al., 2002; Guadix et al., 2006). Mesothelial cells of the intestine have a similar potential demonstrated by genetic lineage tracing in the mouse but are derived from a broadly distributed progenitor population intrinsic to the forming gut tube (Wilm et al., 2005; Winters et al., 2012 in press). The second brief breakdown of the outer basement membrane of the intestine occurred as the outer epithelium differentiated into a mesothelial layer. Thus, the second wave of inward migration into the mesenchyme may be specific to mesothelial cells or their progenitors providing cells of the future vascular or fibroblast lineage. The molecular regulation of EMT of the cardiac mesothelium has been investigated utilizing multiple murine genetic models (Wu et al., 2010; Baek and Tallquist, 2012). It may be of interest to examine these genetic models in the context of intestinal development to determine if a similar molecular network regulates EMT of mesothelia in the two organs.

In addition to contributing cells, mesothelium is also a signaling center during development (White, 2006; Olivey and Svensson, 2010; Svensson, 2010). The first visceral smooth muscle layer of the intestine differentiates in close proximity to the mesothelium with only a small layer of intervening SMA-negative cells. Endodermal Shh signals are known to be repressive to visceral smooth muscle differentiation in the chick thus positioning the initial smooth muscle cell layer at a distance from the mucosa (Sukegawa et al., 2000; Gabella, 2002). However, both *Shh* and *Ihh* knockouts in the mouse led to reduced visceral smooth muscle differentiation suggesting the role of Shh is not repressive alone (Ramalho-Santos et al., 2000; Mao et al., 2010). Intestinal mesothelial signaling has not been investigated though frequently developmental patterning is the result of integration of signals from two opposing sources (Irish et al.,

1989; Meinhardt, 2009). Precise positioning of the initial circular muscle layer and subsequent layers of smooth muscle may be the result of both endodermal and mesothelial signaling events though further investigation is required.

The endothelial plexus also divides into two layers at E6 (Nagy et al., 2009). Signals that pattern the intestinal vasculature are currently unknown. As cells are added to the mesenchyme, the endothelial plexus remains centrally located with increasing distance separating it from both basement membranes; thus, hypoxia might be proposed as a potential regulatory signal. However, quantification of the width of the mesenchymal compartment revealed there is actually a decrease in the distance separating the two basement membranes between E3.5 and E6. Thus, division of the endothelial plexus into two layers at this time may not be related simply to increased hypoxia due to mesenchymal growth. The division into two layers that reside near the mesothelial and mucosal surface, respectively, suggests chemotactic cues may originate from both epithelia to produce this pattern though further research is needed in this area.

Maturation of visceral smooth muscle and vascular components: E6-E16

The next major changes that occur within the mesenchymal compartment include differentiation of the remaining visceral smooth muscle cell layers, vascular remodeling and maturation, and extensive growth. It is unknown what directs the sequential differentiation of individual visceral smooth muscle cell layers though, as described above, roles for both the endoderm and mesothelium are possible. Interestingly, the appearance of the villi is temporally associated with generation of the outer circular and outer longitudinal visceral smooth muscle cell layers suggesting a potential mechanical relationship.

In studies of murine intestinal development, endothelial cells appear to play an important role in villus formation and remain in close association with the endoderm

throughout (Hashimoto et al., 1999; Kim et al., 2007). In the quail, villi form independent of a close morphological relationship with the vasculature. Indeed, endothelial cells do not invade the villi until days after they are formed. The cues leading to endothelial ingrowth into the villi are unknown. Also of potential interest, subepithelial myofibroblasts differentiate concurrent with endothelial migration into villi. Endothelial cells in endodermally-derived organs function in paracrine signaling independent of their function in supplying vascular flow to an area (Lammert et al., 2001; Matsumoto et al., 2001; Yoshitomi and Zaret, 2004; Jacquemin et al., 2006). Thus, regulation of villus maturation and myofibroblast differentiation may be related to signaling events from the nearby endothelial cells.

Finally, while the endothelial plexus of the intestinal primordium is known to be derived from the splanchnic mesoderm (Meier, 1980; Pardanaud et al., 1989), the origin of the large surface blood vessels is unclear. They are first visible in the mesentery and subsequently over the intestine suggesting they may grow via angiogenesis from the vitelline artery. Alternatively, they may be derived completely from remodeling of the existing endothelial plexus.

As detailed above, there remains much to be understood about intestinal development. Knowledge of the morphological underpinnings is vital if investigations of intestinal formation are to be placed into the larger context in which they occur. These studies provide a timeline of intestinal mesodermal development integrating information about multiple foundational features. With a broad view of intestinal development, potential interactions can be identified that range from the level of gene function, through cellular interactions, to tissue morphogenesis leading to the establishment of the definitive structure.

References

Ainsworth SJ, Stanley RL, Evans DJR. (2010). Developmental stages of the Japanese quail. *J Anat* **216**, 3-15.

Appelman HD. (2011). Morphology of gastrointestinal stromal tumors: Historical perspectives. *J Surg Oncol* **104**, 874-81.

Baek ST, Tallquist MD. (2012). Nf1 limits epicardial derivative expansion by regulating epithelial to mesenchymal transition and proliferation. *Development* **139**, 2040-49.

Burns AJ, Roberts RR, Bornstein JC, Young HM. (2009). Development of the enteric nervous system and its role in intestinal motility during fetal and early postnatal stages. *Semin Pediatr Surg* **18**, 196-205.

Dauça M, Bouziges F, Colin S, Kedinger M, Keller MK, Schilt J, Simon-Assmann P, Haffen K. (2007). Development of the vertebrate small intestine and mechanisms of cell differentiation. *Int J Dev Bio*l **34**, 205-18.

Dettman RW, Denetclaw W, Ordahl CP, Bristow J. (1998). Common epicardial origin of coronary vascular smooth muscle, perivascular fibroblasts, and intermyocardial fibroblasts in the avian heart. *Dev Biol* **193**, 169-181.

Eddinger TJ. (2009). Unique contractile and structural protein expression in dog ileal inner circular smooth muscle. *J Smooth Muscle Res* **45**, 217-30.

Gabella G. (1985). Structure of the musculature of the chicken small intestine. *Anat Embryol (Berl)* **171**,139-49.

Gabella G. (2002). Development of visceral smooth muscle. *Results Probl Cell Differ* **38**, 1-37.

Grey RD. (1972). Morphogenesis of intestinal villi. I. Scanning electron microscopy of the duodenal epithelium of the developing chick embryo. *J Morphol* **137**, 193-213.

Grosse AS, Pressprich MF, Curley LB, Hamilton KL, Margolis B, Hildebrand JD, Gumucio DL. (2011). Cell dynamics in fetal intestinal epithelium: implications for intestinal growth and morphogenesis. *Development* **138**, 4423-32.

Guadix JA, Carmona R, Muñoz-Chápuli R, Pérez-Pomares JM. (2006). In vivo and in vitro analysis of the vasculogenic potential of avian proepicardial and epicardial cells. *Dev Dyn* **235**, 1014-26.

Guzman MA, Prasad R, Duke DS, de Chadarévian J-P. (2011). Multiple intestinal atresias associated with angiodysplasia in a newborn. *J Pediatr Surg* **46**, 1445-48.

Hamburger, V. and Hamilton, H. L. (1992). A series of normal stages in the development of the chick embryo. 1951. *Dev. Dyn.* **195**, 231-72.

Hashimoto H, Ishikawa H, Kusakabe M. (1999). Development of vascular networks during the morphogenesis of intestinal villi in the fetal mouse. Kaibogaku zasshi. *J Anat* **74**, 567-76.

Heanue TA, Pachnis V. (2007). Enteric nervous system development and Hirschsprung disease: advances in genetic and stem cell studies. *Nat Rev Neurosci* **8**, 466-79.

Hiramatsu H, Yasugi S. (2004). Molecular analysis of the determination of developmental fate in the small intestinal epithelium in the chicken embryo. *Int J Dev Biol* **48,**1141-48.

Hirota S, Isozaki K, Y M, Hashimoto K, Nishida T, Ishiguro S, Kawano K, Hanada M, Kurata A, Takeda M, Muhammad Tunio G, Matsuzawa Y, Kanakura Y, Shinomura Y, Kitamura Y. (1998). Gain-of-function mutations of c-kit in human gastrointestinal stromal tumors. *Science* **279**, 577-80.

Huss D, Poynter G, Lansford R. (2008). Japanese quail (Coturnix japonica) as a laboratory animal model. *Lab Anim (NY)* **37**, 513-19.

Irish V, Lehmann R, Akam M. (1989). The Drosophila posterior-group gene nanos functions by repressing hunchback activity. *Nature* **338**, 646-48.

Jacobson LF, Noer RJ. (1952). The vascular pattern of the intestinal villi in various laboratory animals and man. *Anat Rec* **114**, 85-101.

Jacquemin P, Yoshitomi H, Kashima Y, Rousseau GG, Lemaigre FP, Zaret KS. (2006). An endothelial-mesenchymal relay pathway regulates early phases of pancreas development. *Dev Biol* **290**, 189-99.

Kawaguchi M, Bader DM, Wilm B. (2007). Serosal mesothelium retains vasculogenic potential. *Dev Dyn* **236**, 2973-79.

Kim KE, Sung H-K, Koh GY. (2007). Lymphatic development in mouse small intestine. *Dev Dyn* **236**, 2020-25.

Lammert E, Cleaver O, Melton D. (2001). Induction of pancreatic differentiation by signals from blood vessels. *Science* **294**, 564-67.

Lefebvre O, Sorokin L, Kedinger M, Simon-Assmann P. (1999). Developmental expression and cellular origin of the laminin alpha2, alpha4, and alpha5 chains in the intestine. *Dev Biol* **210**,135-50.

Louw JH, Barnard CN. (1955). Congenital intestinal atresia; observations on its origin. *Lancet* **269**, 1065-67.

Madison BB, Braunstein K, Kuizon E, Portman K, Qiao XT, Gumucio DL. (2005). Epithelial hedgehog signals pattern the intestinal crypt-villus axis. *Development* **132**, 279-89.

Männer J. (1999). Does the subepicardial mesenchyme contribute myocardioblasts to the myocardium of the chick embryo heart? A quail-chick chimera study tracing the fate of the epicardial primordium. *Anat Rec* **255**, 212-26.

Mao J, Kim B-M, Rajurkar M, Shivdasani RA, McMahon AP. (2010). Hedgehog signaling controls mesenchymal growth in the developing mammalian digestive tract. *Development* **137**, 1721-29.

Matsumoto K, Matsumoto K, Yoshitomi H, Rossant J, Zaret KS. (2001). Liver organogenesis promoted by endothelial cells prior to vascular function. *Science* **294**, 559-63.

Mazur MT, Clark HB. (1983). Gastric stromal tumors. Reappraisal of histogenesis. *Am J Surg Pathol* **7**, 507-19.

McHugh KM. (1995). Molecular analysis of smooth muscle development in the mouse. *Dev Dyn* **204,** 278-90.

Meier S. (1980). Development of the chick embryo mesoblast: pronephros, lateral plate, and early vasculature. *J Embryol Exp Morphol* **55**, 291-306.

Meinhardt H. (2009). Models for the generation and interpretation of gradients. *Cold Spring Harb Perspect Biol* **1**, a001362.

Mikawa T, Gourdie RG. (1996). Pericardial mesoderm generates a population of coronary smooth muscle cells migrating into the heart along with ingrowth of the epicardial organ. *Dev Biol* **174**, 221-32.

Mitjans M, Barniol G, Ferrer R. (1997). Mucosal surface area in chicken small intestine during development. *Cell Tissue Res* **290**, 71-8.

Mutsaers SE. (2002). Mesothelial cells: their structure, function and role in serosal repair. *Respirology* **7**, 171-91.

Mutsaers SE. (2004). The mesothelial cell. *Int J Biochem Cell Biol* **36**, 9-16.

Nagy N, Mwizerwa O, Yaniv K, Carmel L, Pieretti-Vanmarcke R, Weinstein BM, Goldstein AM. (2009). Endothelial cells promote migration and proliferation of enteric neural crest cells via beta1 integrin signaling. *Dev Biol* **330**, 263-72.

Newgreen D, Young HM. (2002). Enteric nervous system: Development and developmental disturbances--Part 1. *Pediatr Dev Pathol* **5**, 224-47.

Olivey HE, Svensson EC. (2010). Epicardial-myocardial signaling directing coronary vasculogenesis. *Circ Res* **106**, 818-32.

Pardanaud L, Yassine F, Dieterlen-Lievre F. (1989). Relationship between vasculogenesis, angiogenesis and haemopoiesis during avian ontogeny. *Development* **105**, 473-85.

Pérez-Pomares J-M, Carmona R, González-Iriarte M, Atencia G, Wessels A, Muñoz-Chápuli R. (2002). Origin of coronary endothelial cells from epicardial mesothelium in avian embryos. *Int J Dev Biol* **46**, 1005-13.

Powell DW, Pinchuk IV, Saada JI, Chen X, Mifflin RC. (2011). Mesenchymal cells of the intestinal lamina propria. *Annu Rev Physiol* **73**, 213-37.

Poynter G, Lansford R. (2008). Generating transgenic quail using lentiviruses. *Methods Cell Biol* **87**, 281-93.

Ramalho-Santos M, Melton DA, McMahon AP. (2000). Hedgehog signals regulate multiple aspects of gastrointestinal development. *Development* **127**, 2763-72.

Sanders KM. (1996). A case for interstitial cells of Cajal as pacemakers and mediators of neurotransmission in the gastrointestinal tract. *Gastroenterology* **111**, 492-515.

Sato Y, Poynter G, Huss D, Filla MB, Czirók A, Rongish BJ, Little CD, Fraser SE, Lansford R. (2010). Dynamic analysis of vascular morphogenesis using transgenic quail embryos. *PloS one* **5**, e12674.

Savin T, Kurpios NA, Shyer AE, Florescu P, Liang H, Mahadevan L, Tabin CJ. (2011). On the growth and form of the gut. *Nature* **476**, 57-62.

Simon-Assmann P, Kedinger M, De Arcangelis A, Rousseau V, Simo P. (1995). Extracellular matrix components in intestinal development. *Experientia* **51**, 883-900.

Streutker CJ, Huizinga JD, Driman DK, Riddell RH. (2007). Interstitial cells of Cajal in health and disease. Part I: normal ICC structure and function with associated motility disorders. *Histopathology* **50**,176-89.

Sukegawa A, Narita T, Kameda T, Saitoh K, Nohno T, Iba H, Yasugi S, Fukuda K. (2000). The concentric structure of the developing gut is regulated by Sonic hedgehog derived from endodermal epithelium. *Development* **127**,1971-80.

Svensson EC. (2010). Deciphering the signals specifying the proepicardium. *Circ Res* **106**,1789-90.

Wells JM, Melton DA. (1999). Vertebrate endoderm development. *Annu Rev Cell Dev Biol* **15**, 393-410.

White AC. (2006). FGF9 and SHH signaling coordinate lung growth and development through regulation of distinct mesenchymal domains. *Development* **133**,1507-17.

Wilm B, Ipenberg A, Hastie ND, Burch JBE, Bader DM. (2005). The serosal mesothelium is a major source of smooth muscle cells of the gut vasculature. *Development* **132**, 5317-28.

Wu M, Smith CL, Hall JA, Lee I, Luby-Phelps K, Tallquist MD. (2010). Epicardial spindle orientation controls cell entry into the myocardium. *Dev Cell 19*, 114-25.

Yamamoto Y, Kubota, T, Atoji, Y, Suzuki, Y. (1996). Distribution of alpha-vascular smooth muscle actin in the smooth muscle cells of the gastrointestinal tract of the chicken. *J Anat* **189**, 623-30.

Yoshitomi H, Zaret KS. (2004). Endothelial cell interactions initiate dorsal pancreas development by selectively inducing the transcription factor Ptf1a. *Development* **131**, 807-17.

Young H, Bergner A, Anderson R, Enomoto H, Milbrandt J, Newgreen D, Whitington P. (2004). Dynamics of neural crest-derived cell migration in the embryonic mouse gut. *Dev Biol* **270**, 455-73.

Young HM, Newgreen D. (2001). Enteric neural crest-derived cells: origin, identification, migration, and differentiation. *Anat Rec* **262**,1-15.

Yung S, Chan TM. (2007). Mesothelial cells. *Perit Dial Int* **27** Suppl 2, S110-15.

Zorn AM, Wells JM. (2009). Vertebrate endoderm development and organ formation. *Annu Rev Cell Dev Bio*l **25**, 221-51.

CHAPTER III

IDENTIFICATION OF A NOVEL DEVELOPMENTAL MECHANISM IN THE GENERATION OF MESOTHELIA

This chapter was accepted in *Development* on May 22, 2012 under the same title with the following authors:

Nichelle I. Winters, Rebecca T. Thomason, David M. Bader

Abstract

Mesothelium is the surface layer of all coelomic organs and critical for the generation of their vasculature. Still, our understanding of the genesis of this essential cell type is restricted to the heart where a localized, exogenous population of cells, the proepicardium, migrates to and envelops the myocardium supplying mesothelial, vascular, and stromal cell lineages. Currently it is unknown whether this pattern of development is specific to the heart or applies broadly to other coelomic organs. Using two independent long term lineage tracing studies, we demonstrate that mesothelial progenitors of the intestine are intrinsic to the gut tube anlage. Furthermore, a novel chick-quail chimera model of gut morphogenesis reveals these mesothelial progenitors are broadly distributed throughout the gut primordium and are not derived from a localized and exogenous proepicardium-like source of cells. These data demonstrate an intrinsic origin of mesothelial cells to a coelomic organ and provide a novel mechanism for the generation of mesothelial cells.

Introduction

The vertebrate coelom, or body cavity, and internal organs housed therein are all lined by a simple squamous epithelium called mesothelium. In the healthy adult,

mesothelia are relatively quiescent—their primary function is to form a non-adhesive surface for the movement of organs (Mutsaers and Wilkosz, 2007). However, mesothelia are also recognized as critical players in peritoneal sclerosis (Chegini, 2008; Yung and Chan, 2009), in the regulation of the injury microenvironment in myocardial infarction (Zhou et al., 2011) and for their ability to promote revascularization of diverse tissues including the heart (Takaba et al., 2006; Zhang et al., 1997). These functions of mesothelium in injury and repair reflect the dynamic behavior of mesothelia in embryonic development. While mesothelia are universally distributed in the pericardial, pleural and peritoneal cavities of all vertebrates, our understanding of mesothelial development is largely restricted to one organ, the heart.

Manasek (1969) and Ho and Shimada (1978) demonstrated that cardiac mesothelium (epicardium) originated from a discrete population of cells termed the proepicardium (PE) localized outside of the initial heart tube (Ho and Shimada, 1978; Manasek, 1969). Originating from the region of the sinus venosus, these cells migrate as an epithelium across the pericardial space to contact the naked myocardium (Ishii et al., 2010). Further dorsal-ventral migration of this epithelium over the heart tube leads to formation of the epicardium. Thus, epicardial precursors do not arise in situ but are recruited from a localized cell source exogenous to the splanchnic mesoderm of the developing organ.

Subsequent lineage tracing studies revealed that specific cells within the epicardium undergo epithelial-mesenchymal transition (Wu et al., 2010), invade the myocardium, and differentiate into fibroblasts, vascular smooth muscle, and endothelial cell populations (Dettman et al., 1998; Mikawa and Gourdie, 1996). Hepatic, pulmonary, and intestinal mesothelia have since been shown to provide vasculogenic and stromal populations to their respective organs (Asahina et al., 2011; Eralp et al., 2005; Morimoto et al., 2010; Perez-Pomares et al., 2004; Que et al., 2008; Wilm et al., 2005).

Wilm et al. demonstrated that the mesothelial marker *Wilms' tumor protein 1 (Wt1)* first appeared in the mesentery of the intestine and then later encompassed the gut tube in a dorsal-ventral direction. This expression pattern mirrored the dorsal-ventral migration of the epicardium seen in the heart and, from these data, our group hypothesized that "non-resident cells migrate to and over the gut to form the serosal mesothelium" (Wilm et al., 2005). These data in conjunction with the shared vasculogenic potential of mesothelia suggested the mechanism of mesothelial development and the function of this cell type in embryogenesis may be conserved in diverse coelomic cavities.

In contrast to the extensive analysis of epicardial development, careful examination of the primary literature reveals that little if anything is known about the origin of mesothelial cells in any coelomic organ other than the heart. Additionally, a change in terminology contributes to confusion in the literature regarding this cell type. The term "mesothelium" originally referred to the entire epithelial component of mesoderm as differentiated from the loose mesenchyme (Minot, 1890). The term did not refer to the specific simple squamous cell type we currently identify as mesothelium. Still, a review authored by Minot in 1890 using this original terminology appears to form the basis for the modern description on the origin of vertebrate coelomic mesothelia (Moore and Persaud, 1998; Mutsaers, 2002). An extensive review of the literature reveals no primary data addressing the origin of mesothelium. Taken together, it is clear that the program of proepicardial/epicardial development stands alone as a definitive model of development of this widely distributed cell type that is so critical for vertebrate organogenesis.

A question arises: Is there a common mechanism of mesothelial development? Fundamental to the resolution of this question is determining the origin of mesothelial precursors in diverse coelomic organs. Thus, we examined intestinal development to

determine whether mesothelium originated from an exogenous, localized source as seen in the heart or, conversely from a resident population of mesothelial progenitors within the gut itself. Using three independent experimental models, we demonstrate that the intestine derives its mesothelial layer from progenitor cells broadly resident within the splanchnic mesoderm and not from a PE-like structure extrinsic to the developing organ. These data provide new information concerning a fundamental process of intestinal development and reveal diversity in mechanisms regulating the generation of mesothelia.

Materials and Methods

In situ hybridization (ISH)

ISH was performed according to standard protocols (McGlinn and Mansfield, 2011). *Wt1* template (GenBank accession number AB033634.1) was kindly provided by Dr. Jorg Manner (Georg-August University of Gottingen, Germany) (Schulte et al., 2007).

Immunohistochemistry (IHC) and co-localization analysis

Immunohistochemical analysis of sectioned chick (Gallus gallus) or quail (Coturnix japonica) embryos was as published (Osler and Bader, 2004). All animal procedures were performed in accordance with institutional guidelines and IACUC approval. Chick embryos were staged according to Hamburger and Hamilton (Hamburger and Hamilton, 1992). The following primary antibodies were used: Anti-GFP (Invitrogen A11122, 1:200); Anti-laminin (Abcam Ab11575, 1:50); Anti-Laminin (DSHB 31 or 31-2 1:25); Anti-neurofilaments (DSHB RT97 1:50); Anti-smooth muscle actin (Sigma A2547 1:200), Anti-smooth muscle actin (Abcam Ab5694 1:200), QCPN (DSHB undiluted), 8F3 (DSHB 1:25), Anti-PGP9.5 (Zymed 38-1000, 1:200); Anti-cytokeratin (Abcam Ab9377, 1:100),

QH1 (DSHB, 1:200). The following secondary antibodies were used at a 1:500 dilution: Alexa fluor 488 or 568 Goat anti-rabbit (Invitrogen); Alexa fluor 488 or 568 Goat anti-mouse (Invitrogen). TOPRO-3 (Invitrogen T3605) at 1 µmol/L was applied for 20 min. Sections were imaged in Z-stacks using a LSM510 META Confocal with 0.4 µm optical slices. Each optical slice was analyzed for co-localization of the red and green channels using ImageJ followed by Z-projection for counting of cells. All IHC images presented in figures are Z-projections.

Microinjection

Windowed chick embryos (HH14-17) were lightly stained by placing a dried strip of neutral red (0.2 mg/mL) in 1% agar on top of the embryo. For contrast, 0.2 uL of 10% fast green solution (sterile filtered) was added to 5 µl viral or pCIG suspension (7 µg/µL) and then loaded into a pulled glass needle. The agar strip was removed and approximately 25-30 nanoliters were injected into both lateral cavities with aid of a micromanipulator and use of a Narishige IM300 microinjector with 2msec pulses at 38PSI.

Electroporation

pCIG-GFP in which GFP expression is driven by the chicken β-actin promoter was kindly provided by Dr. Michael Stark (Brigham Young University, Provo, UT, USA) (Lassiter et al., 2007). Chick eggs incubated 2.5 days were windowed by withdrawing 4 ml of albumin and cutting a hole in the top of the egg shell. The vitelline membrane over the posterior region of windowed HH14-HH17 embryos was removed with a tungsten needle. After pCIG-GFP microinjection, a small hole was made outside of the vascularized region through which the positive electrode was inserted below the embryo. The negative electrode was placed on top of the embryo and 5-7, 10 msec pulses at 15

V were delivered (ECM 830 electroporator; BTX Harvard Apparatus). After addition of Tyrode's salts solution with 1% pen/strep, the eggs were resealed with tape and incubated 8 days.

Production of pSNID retrovirus

The following plasmids were used: pSNID with both a GFP and βgal reporter a generous gift of Dr. Jeanette Hyer (UCSF, San Francisco, CA, USA) (Venters et al., 2008); pCI-VSVG (Addgene 1733); pCAGGS Gag/Pol (generous gift of Dr. Connie Cepko, Harvard University, Cambridge, MA, USA). Virus was produced in Phoenix-GP cells. Pheonix-GP cells (ATCC SD-3514) were grown to 70-80% confluence in DMEM supplemented with 10% FBS and split 1:3 onto four, 10 cm plates the night prior to transfection. Media was exchanged prior to transfection. For each plate, 4 ug DNA (2 ug pSNID, 1 ug VSV-G, 1 ug Gag/pol) was diluted in 100 uL serum free DMEM. To the DNA suspension, 24 uL PEI (1 mg/mL PEI, pH7; MW25K, Polysciences Inc 23966-2) was added, mixed by vortexing, incubated 15 min at room temperature, added to the cells overnight. Media was exchanged, media collected after 24 hrs, and stored at -80°C. 5 ml new media was added, media collected at 48 hrs, pooled with 24 hr collection, syringe filtered (45 um) and concentrated by ultracentrifugation (SW-28 rotor, 18000 RPM, 2 hours, 4°C). Supernatant was discarded and the ultracentrifuge tube drained by inverting for 60 sec. The viral pellet was resuspended in media that remained in the ultracentrifuge tube (~50-80 uL). Polybrene (Sigma H9268) was added to the viral suspension at final concentration of 100 ug/mL. After microinjection, infected cells were detected by GFP expression in whole mount using a fluorescence-detecting dissecting microscope or in section by staining with an anti-GFP antibody.

Titer assay

D17 cells were grown to 60% confluence in 6-well plates. Fresh media (DMEM + 7% FBS) with 10 µg/ml polybrene was added to the plates prior to infection. Concentrated viral suspension was serially diluted and added to the 6-well plates. At 48 hrs, cells were stained with Xgal to detect viral infection. The total number of positive clones in a well were counted to determine the total number of virions added. Viral titers reaching at least 10^7 virions/mL were aliquoted and stored at -80°C.

Generation of chick-quail chimeras

Splanchnopleure was dissected away from quail embryos staged 14-17. Dissection was carried out in sterile Tyrode's salt solution. Isolated splanchnopleure was bisected into anterior and posterior regions by cutting at the vitelline artery and then anterior and posterior splanchnopleure was further subdivided into 3-4 pieces. Chick embryos in windowed eggs were lightly stained with a strip of neutral red in agar. The vitelline membrane was removed with a tungsten needle and a small hole made through the somatopleure over the vitelline artery. The quail splanchnopleure graft was transferred into the chick egg and pushed through the hole with forceps and a tungsten needle into the right lateral cavity. Tyrode's salt solution with 1% penicillin/steptomycin was added to replace volume and eggs were then sealed with tape and incubated for 1-14 days. The number of graft and host derived mesothelial cells was determined by analyzing a subset of graft-derived gut tubes at multiple levels. The mesothelial layer was distinguished by morphology combined with cytokeratin or laminin staining. Nuclei within the mesothelial layer were manually identified and then subsequently identified as either QCPN or 8F3 positive.

Results

Trilaminar organization of the intestine is established prior to tube formation

The adult intestine is composed of three subdivisions or compartments: the inner mucosa with an underlying basement membrane, the middle “mesenchymal” layers harboring stromal and visceral smooth muscle cells, and the outer mesothelium with its own basement membrane. We used immunohistochemical staining for cytokeratin, an intermediate filament expressed by epithelia, and laminin, a component of basement membranes, to examine the intestine for establishment of these three compartments. By close examination of formation of these compartments, we sought to identify any potential mesothelial progenitor population within the gut tube either of a proepicardial-like morphology or any other tissue arrangement.

The splanchnopleure posterior to the heart tube of chick embyos was examined at early stages of intestinal morphogenesis, prior to gut tube closure. At the earliest stage examined, HH13, the splanchnopleure was bilaminar composed of endoderm and splanchnic mesoderm with almost no intervening mesenchymal cells (Figure 3.1 A-C, arrowhead). Each layer was individually underlain by a laminin-positive basement membrane that extended along the entire dorsal-ventral axis of the splanchnopleure (Figure 3.1 A-C, arrows).

At HH15, the splanchnopleure transitioned from having two major compartments to three. This was due to the establishment of a mesenchymal layer between the two basement membranes of the splanchnopleure (Figure 3.1 D-F). For ease of reference, we termed the three compartments endoderm, mesenchyme, and outer epithelium though at this time the outer epithelium does not express cytokeratin (Figure 3.1 F’). The transition to three compartments occurred evenly throughout the splanchnopleure, and no localized PE-like structure was observed throughout the entirety of the peritoneal

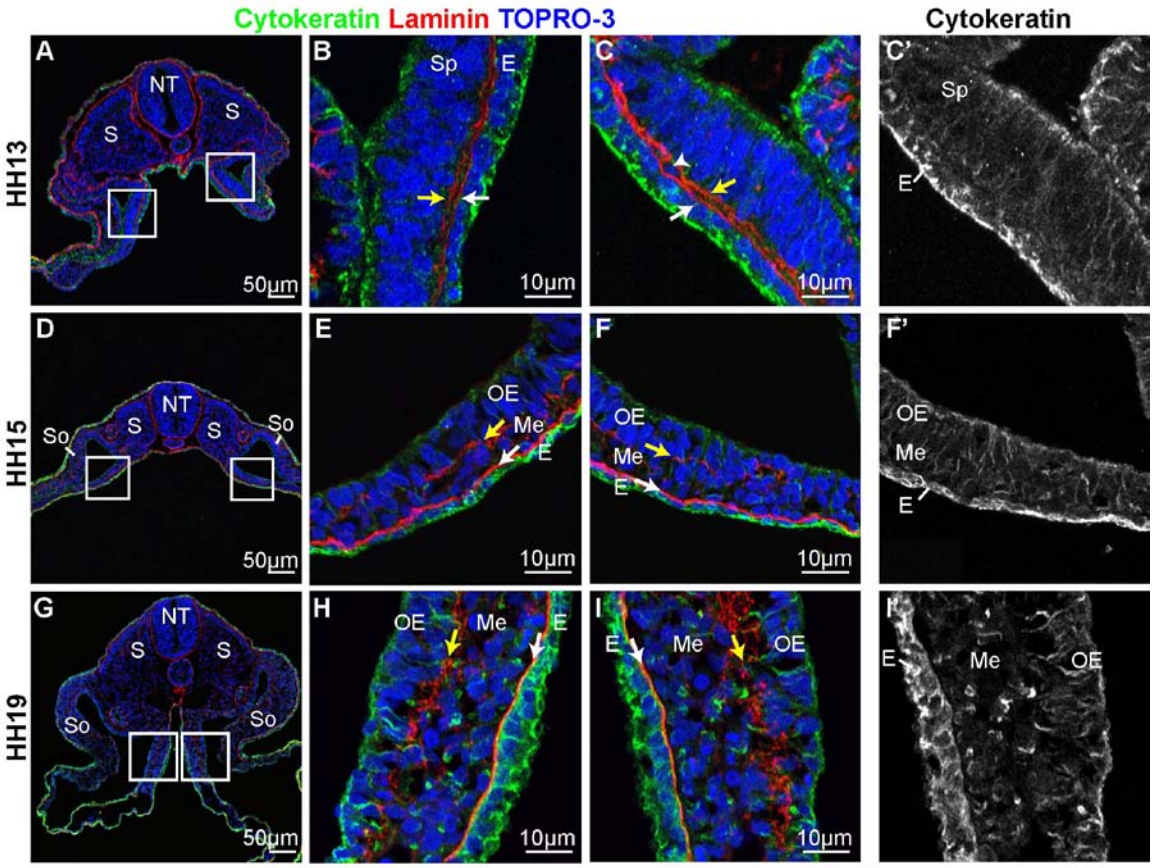

Figure 3.1 A trilaminar gut tube was generated by HH15. A) HH13 splanchnopleure was composed of two layers. **B-C)** Boxed regions shown in A). The splanchnic mesoderm appeared stratified and was underlain by a basement membrane (yellow arrow). The endoderm had its own basement membrane (white arrow). Arrowheads in C indicate a single mesenchymal cell. **C')** The endoderm but not the splanchnic mesoderm was cytokeratin positive at HH13. **D-F)** At HH15, a mesenchymal layer was observed residing between the aforementioned basement membranes (arrows). **F')** The outer epithelium was not cytokeratin positive at HH15. **G-I)** At HH19 the mesenchymal layer had expanded (space between two arrows) and the basement membrane of the outer epithelium had fragmented (outer arrow). **I')** The endoderm but not the outer epithelium was cytokeratin positive. E, endoderm; Me, mesenchyme; NT, neural tube; OE, outer epithelium; S, somite; So, somatic mesoderm; Sp, splanchnic mesoderm.

cavity. The outer epithelium remained stratified/pseudostratified, was underlain by a fragmented basement membrane (yellow arrow) and formed a uniform layer over the mesenchyme (Figure 3.1 D-F). With the appearance of the mesenchymal layer, the splanchnopleure was now in a trilaminar configuration which, as described above, is the basic organization of the adult intestine. The mesenchymal layer expanded through HH19 and the basement membrane of the outer epithelium remained fragmented (Figure 3.1 G-I, yellow arrow). The mesothelial marker *Wt1* was, however, not expressed specifically in the outer epithelium at these stages though *Wt1* staining was observed in the mesothelial component of the PE over the same period of time (Figure 3.2). Four days after the initial appearance of the outer epithelium (HH29, day 6) the layer attained the simple squamous morphology and robust cytokeratin expression of a definitive mesothelium (Figure 3.3 A-D). Thus, the three compartments of the intestine including a potential mesothelial progenitor layer, the outer epithelium, are established very early in development prior even to intestinal tube formation.

Mesothelial progenitors are resident to the splanchnic mesoderm

As a first step in identifying the origin of mesothelial progenitors, it was necessary to determine whether the outer epithelium was derived from resident cells of the splanchnic mesoderm layer or a migratory progenitor population undetected by the analyses described above. Thus, we devised a method to label and trace cells of the splanchnic mesoderm over time. A reporter plasmid expressing green fluorescent protein (GFP) from the chick β-actin promoter was injected into the lateral cavities of HH14 chick embryos, the stage prior to establishment of the mesenchymal layer (Figure 3.4 A). Microinjection was followed by electroporation with the electrodes oriented directly above and below the embryo to direct the DNA ventrally into the splanchnic mesoderm. Embryos were incubated for six hours post-electroporation to allow for GFP to

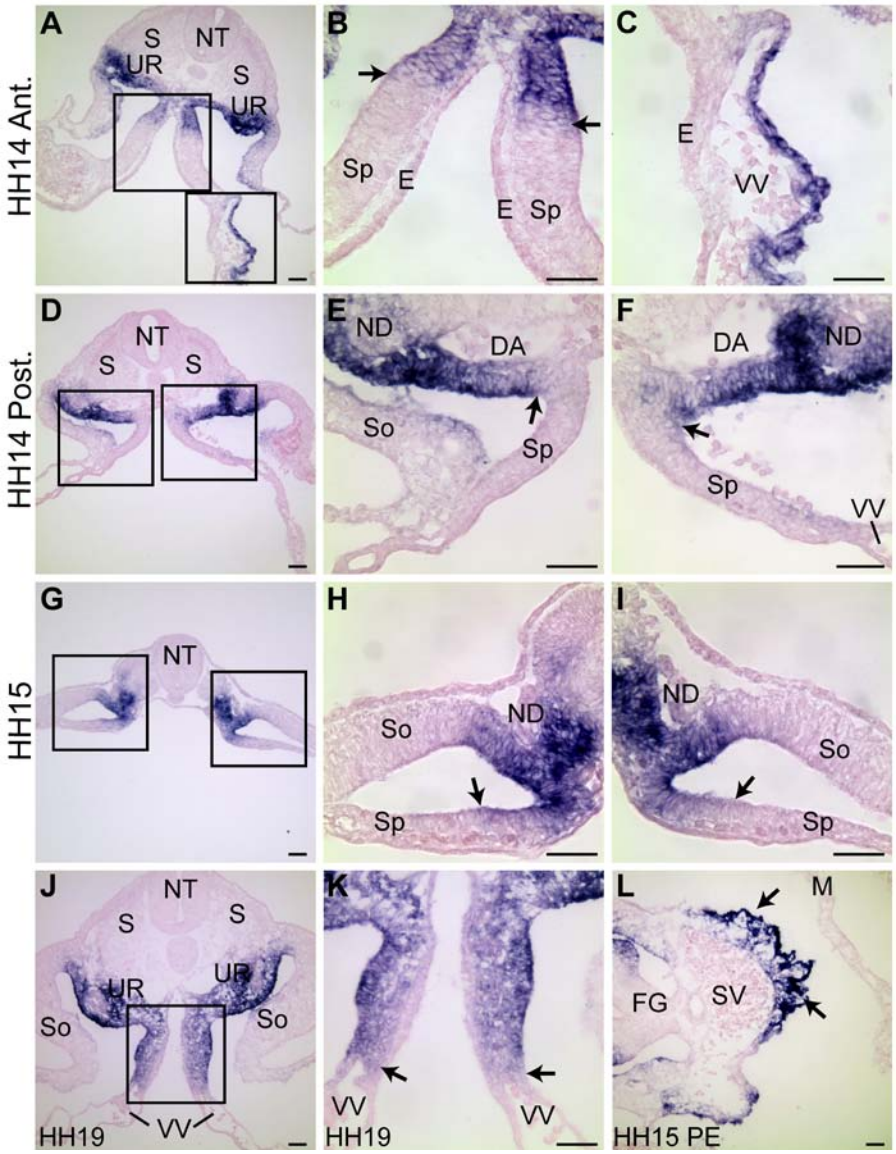

Figure 3.2 In situ hybridization for *Wt1*. Nephric precursors and the urogenital ridge expressed Wt1 at all stages examined (HH13-HH19). Arrows denote the ventral boundary of positive staining. **A-B)** At HH14, *Wt1* was not present within the anterior splanchnopleure except at the most dorsal aspect (arrows). **C)** The mesoderm over the vitelline vein (VV) also was *Wt1* positive anteriorly at HH14. **D-F)** In the posterior region of HH14 embryos, *Wt1* not identified in the splanchnopleure. **G-I)** At HH15, *Wt1* expression was variable along the A-P axis though expression did extend into the splanchnic mesoderm at some levels. Expression was not clearly restricted to the outer epithelium (arrows). **J-K)** At HH19, expression of *Wt1*, while still variable, was found extending throughout the entire splanchnic mesoderm up to the vitelline veins and including the mesenchymal layer (arrows). **L)** Representative image demonstrating *Wt1* expression in the PE (arrows). Note the lack of staining over the myocardium (M). DA, dorsal aorta; E; endoderm; FG, foregut; ND, nephric duct; NT, neural tube; S, somite; So, somatic mesoderm; Sp, splanchnic mesoderm; SV, sinus venosus; UR, urogenital ridge; VV, vitelline vein. Scale bar 40 µm.

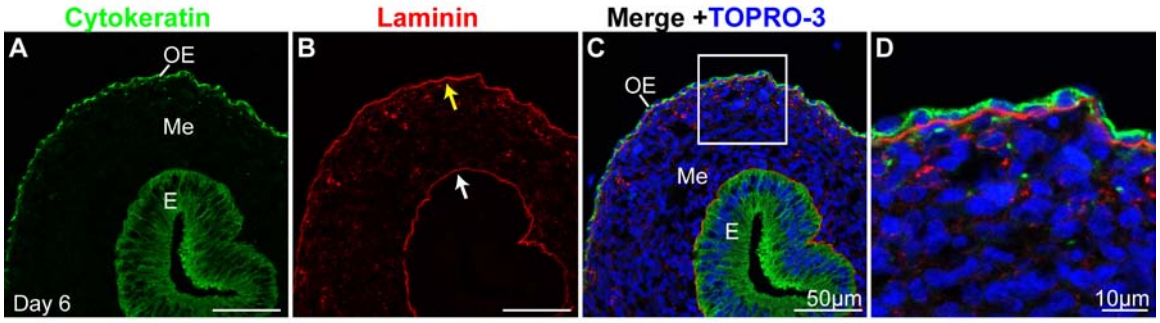

Figure 3.3 Definitive intestinal mesothelium is present at HH29 (Day 6). A) At day 6, a simple squamous, cytokeratin positive (green) meosthelium is present surrounding the intestine. **B)** A basement membrane underlies the mesothelium (red, yellow arrow). White arrow indicates the endodermal basement membrane. **C)** Merge. **D)** Higher magnification of boxed region shown in C). E, endoderm; Me, mesenchyme; OE, outer epithelium.

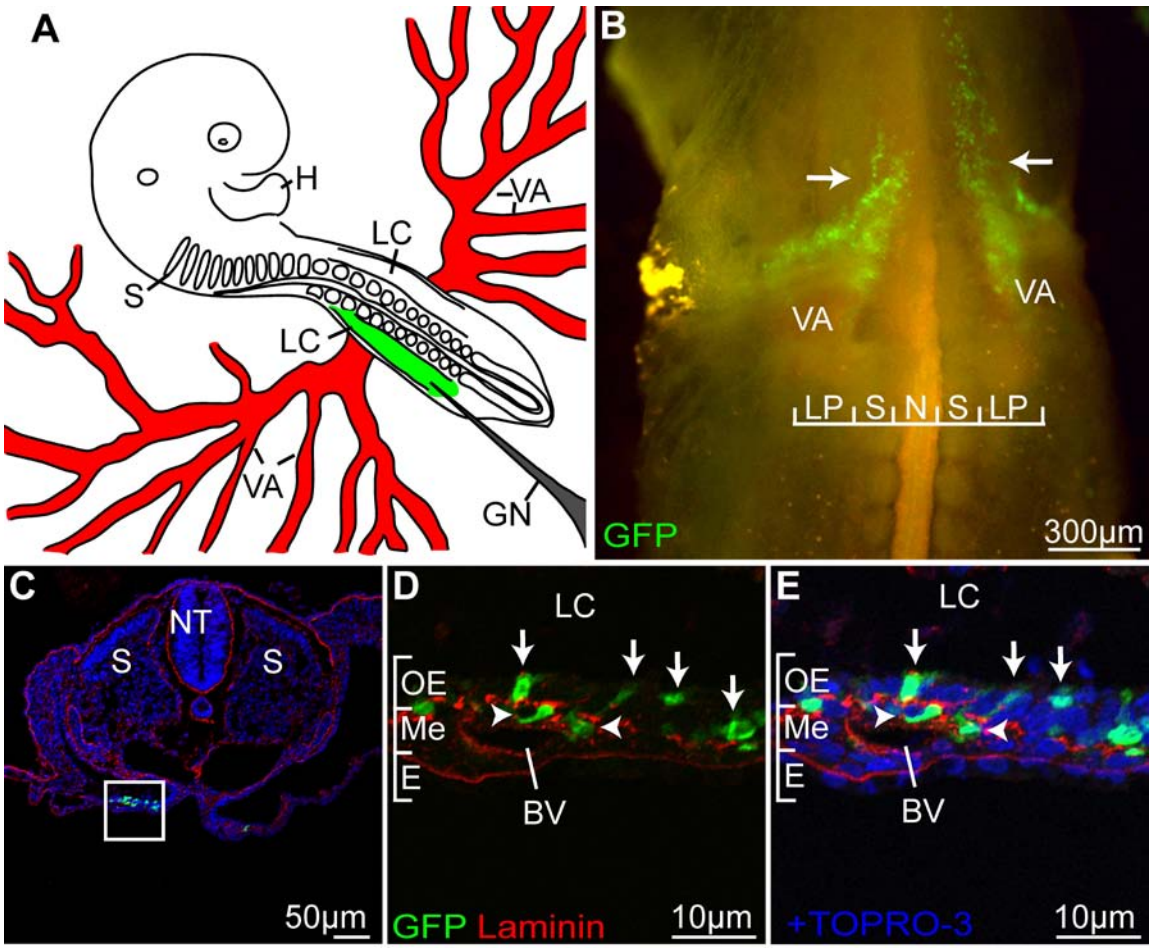

Figure 3.4 Electroporation of the splanchnic mesoderm at HH14 demonstrates labeling of the outer epithelium and mesenchyme. A) Schematic demonstrating injection of the GFP reporter plasmid into the right lateral cavity of an embryo in ovo. **B)** Wholemount image of the ventral surface of an embryo electroporated at HH14 and then incubated for 6 hours. Electrodes were placed near the vitelline artery. GFP was observed in the region near the vitelline artery and was restricted to the lateral plates (arrows). **C)** GFP-positive cells localized to the splanchnic mesoderm. **D)** Boxed area shown in C). GFP-positive cells were found primarily within the outer epithelium (arrows) with a few cells within the mesenchymal layer (arrowheads). No GFP-positive cells were identified in the endoderm. **E)** Merge of D with TOPRO-3. BV, blood vessel; GN, glass needle; H, heart; LC, lateral cavity; LP, lateral plate; Me, mesenchymal layer; N, notochord; NT, neural tube; OE, outer epithelium; S, somite, VA, vitelline artery.

accumulate to a detectable level and also encompass the time over which the splanchnopleure transitions from two to three layers. Whole mount imaging of electroporated embryos revealed bilateral GFP expression restricted to the region of the lateral plate near the vitelline arteries demonstrating the accuracy of the targeting method (Figure 3.4 B, arrows). Fluorescent imaging of sections through the targeted regions at six hours post-electroporation demonstrated that GFP-positive cells were present predominantly within the outer epithelium (71%; 454/640 total cells counted from four embryos, arrows) but also in the underlying mesenchyme (29%, 186/640 total cells counted, Figure 3.4 C-E, arrowheads). At no time was endoderm labeled with this method. Embryos electroporated between HH15-HH17 demonstrated similar labeling with 66% of GFP-positive cells within the outer epithelium (316/482 total cells counted, Figure 3.5). The presence of labeled cells in the outer epithelium and mesenchyme indicates the splanchnic mesoderm provides cells to both layers.

We next sought to determine if cells of the splanchnic mesoderm later gave rise to the mesothelium. For this experiment, embryos were electroporated between HH15-HH17 and incubated for eight days (the limit of GFP detection using this method) to day 10 of chick development. Examination of resulting small intestines revealed labeled cells were clearly resident within the mesothelial layer. These GFP-positive cells exhibited features typical of mesothelium including a close association with the basal lamina and a squamous morphology (Figure 3.6 A-D, arrows). In addition to the mesothelium, GFP-positive cells were identified throughout the gut tube including the muscularis externa (arrows) and penetrating as deep as the submucosa (arrowhead, Figure 3.6 E-H). Labeled cells were never observed in the endodermal mucosa. These data demonstrate that mesothelial precursors are resident to the splanchnic mesoderm and outer epithelial layer of the primitive intestine.

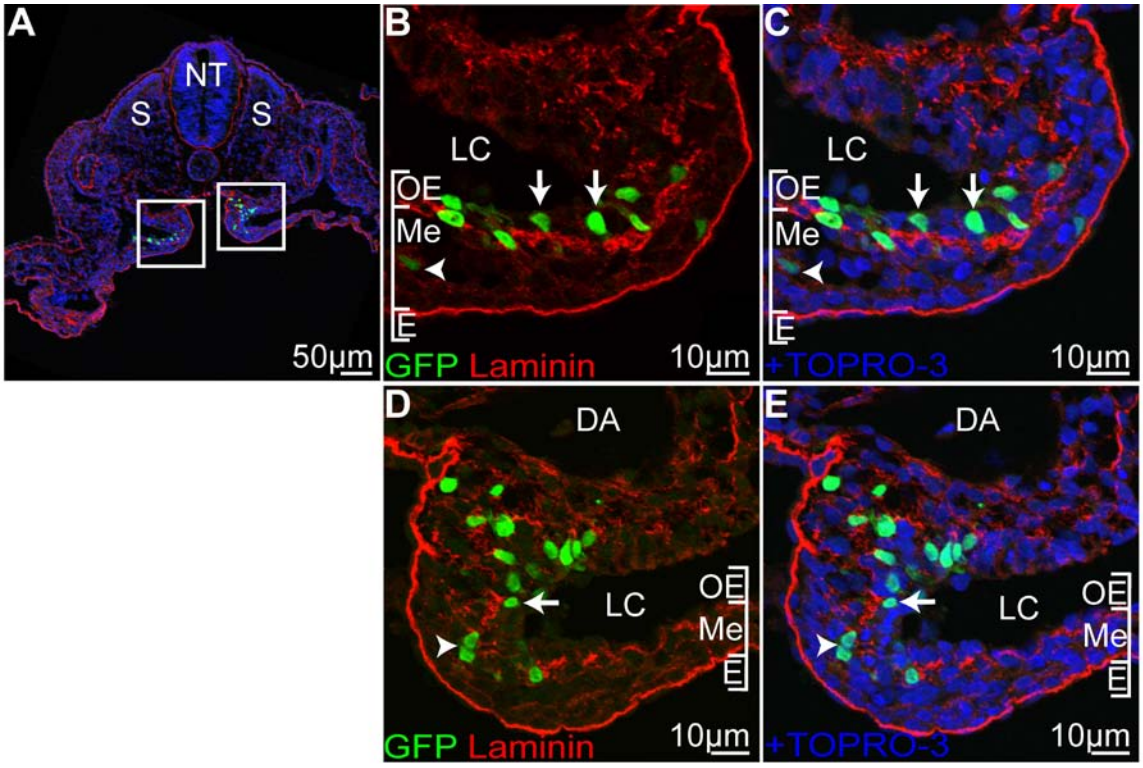

Figure 3.5. Electroporation of the splanchnic mesoderm at HH15. A) Section though an embryo 6 hours post-electroporation. Both right and left sides of the embryo were targeted (boxed areas) **B-E)** Higher power views of boxed areas. Cells within the outer epithelium (arrows) and mesenchyme (arrowheads) were GFP-positive. DA, dorsal aorta; E, endoderm; LC, lateral cavity; Me, mesenchymal layer; NT, neural tube; OE, outer epithelium; S, somite.

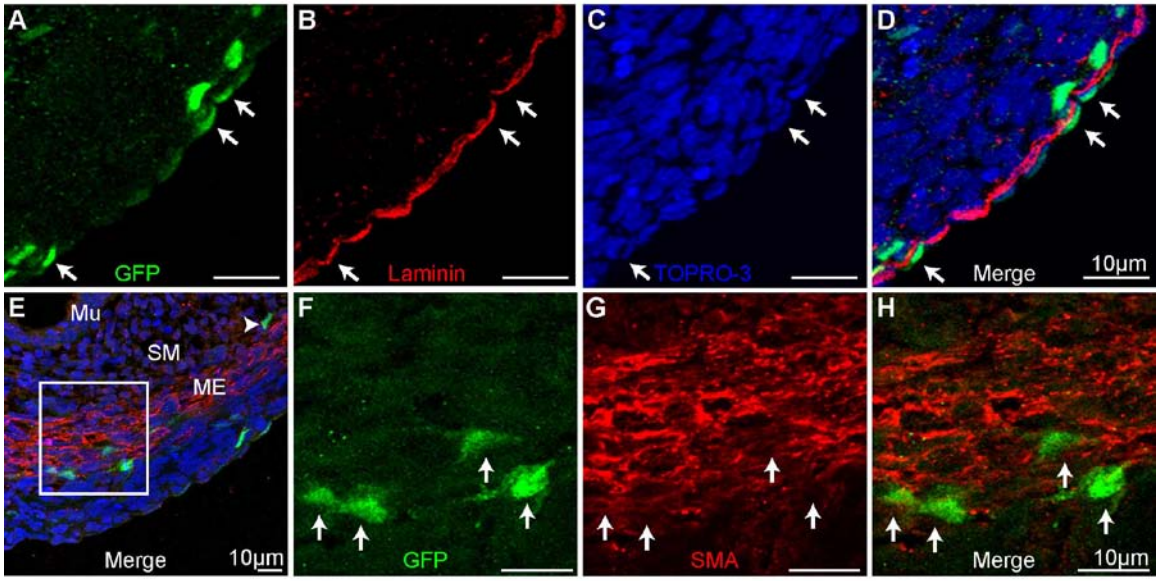

Figure 3.6 DNA electroporation demonstrates that splanchnic mesoderm harbors mesothelial progenitors. Sections through gut tubes of embryos electroporated at HH15-HH17 and incubated 8 days. **A-D)** GFP-positive cells (arrows) were identified within the squamous mesothelial layer of the intestine associated closely with the basement membrane (laminin, red). **E)** GFP-positive cells were also identified within the forming alpha-smooth muscle actin (SMA) positive muscularis externa (boxed region) and into the submucosa (arrowhead). **F-H)** Higher magnification of boxed region. GFP-positive cells within the muscularis externus were not SMA-positive (arrows). ME, muscularis externa; Mu, mucosa; SM, submucosa.

We utilized a second direct labeling approach to confirm and extend our findings. For these experiments, we used a replication incompetent retrovirus with broad tropism and a GFP reporter gene. Incorporation of the retroviral genome into infected cells allows for long term tracing without dilution of the label through cell division. High titer retrovirus was injected into the lateral cavities of HH14-17 embryos in the same manner as the electroporation plasmid to label the surface cells throughout the time points at which the splanchnopleure transitions between two to three compartments. Embryos were then incubated 14 days (to day 17 of development, hatching occurs at day 21) before the gut tubes were harvested.

Isolated gut tubes were first examined in whole mount for GFP expression. In embryos infected at HH14, a time prior to appearance of the middle mesenchymal layer, GFP-positive cells were present throughout the gut tube and mesentery and many appeared localized to the surface (Figure 3.7 A, arrows). GFP-positive cells also clearly associated with the vascular tree (Figure 3.7 B-B', arrows) and distributed in deep layers (Figure 3.7 C, arrows).Upon sectioning, surface GFP-positive mesothelial cells with a squamous morphology were clearly identified in close association with the external basal lamina (Figure 3.8 A-B, arrowhead). GFP-positive vascular smooth muscle cells were also present consistent with previously published data (Wilm et al., 2005). Other GFP-positive, SMA-negative cells were identified peripheral to the vascular media within the adventitia (Figure 3.8 C-D). We did not identify any GFP-positive endothelial cells. GFP-positive cells were also identified within the submucosa and muscularis externa but not within the mucosal epithelium (Figure 3.8E). Only 5% of GFP-positive cells localized within the muscularis externa were visceral smooth muscle cells (alpha-smooth muscle actin (SMA)-positive and spindle shaped) (Figure 3.8 F-H, arrowheads). The phenotype of the remaining cells could not be identified by morphology or by specific markers of smooth muscle, neurons, or epithelia and might best be characterized as

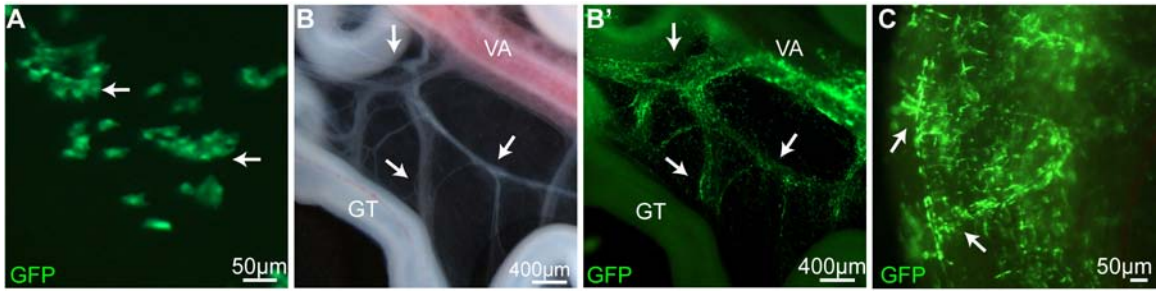

Figure 3.7 Long term retroviral lineage tracing of splanchnic mesoderm. Wholemount images of intestine from embryos infected with virus between HH14-HH17 and analyzed 14 days later. **A)** High magnification of intestinal surface demonstrated cells resembling mesothelium with prominent nuclei and broad cell processes (arrows). **B)** Brightfield image of gut tube demonstrating the vasculature (arrows). **B')** GFP fluorescence of gut tube pictured in B). GFP-positive cells surrounded the vasculature within the mesentery and intestine (arrows). **C)** GFP-positive cells were also found distributed deeply in the intestine (arrows). GT, gut tube; VA, vitelline artery.

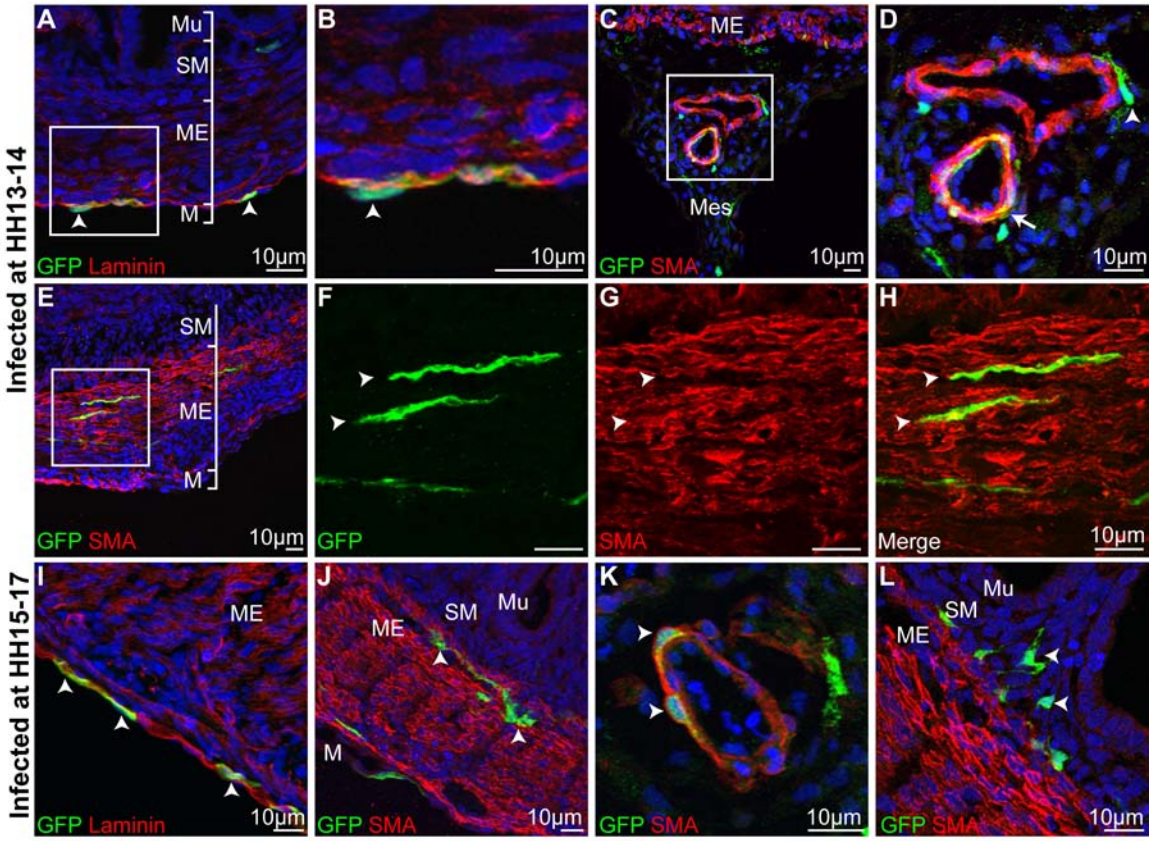

Figure 3.8 Lineage tracing of splanchnic mesoderm reveals mesothelial, perivascular, and mesenchymal derivatives. A-H) Sections of intestine from embryos infected between HH13-14 and isolated 14 days later. **A)** Squamous GFP-positive cells frequently populated the mesothelium (arrowheads) closely associating with the basement membrane (red, laminin). **B)** High magnification of boxed area in A). **C)** GFP-positive cells associated with large mesenteric blood vessels. **D)** High magnification of boxed area in C) demonstrates GFP-positive vascular smooth muscle cells (arrow) and perivascular cells (arrowhead). **E)** GFP-positive cells were identified within the muscularis externa. **F-H)** High magnification of boxed area shown in E). A rare population of GFP-positive cells found within the muscularis externus were spindle shaped and SMA-positive (arrowheads). **I-L)** Sections of intestine from embryos infected between HH15-17 and isolated 14 days later. **I)** Squamous GFP-positive cells populated the mesothelium (arrowheads) closely associating with the basement membrane (red, laminin). **J)** SMA-negative mesenchymal cells within the muscularis externa layer (arrowheads). **K)** GFP-positive vascular smooth muscle cells (arrowheads). **L)** Submucosal GFP-positive, SMA-negative cells. M, mesothelium; ME, muscularis externus; Mes, mesentery; Mu, mucosa, SM, submucosa.

stromal/mesenchymal by their location within the organ wall (Figure 3.8 J, L and data not shown). In embryos infected with the retrovirus between stages 15-17, after division of the splanchnic mesoderm into outer epithelium and mesenchyme, the same GFP-positive populations were identified at day 17 of development (Fig. 3.8 I-L). This independent assay confirmed that resident splanchnic mesoderm was the origin of mesothelium and that these cells are maintained within the definitive mesothelium.

Intestinal mesothelial progenitors are localized broadly throughout the splanchnic mesoderm

The current data establish that cells resident to the splanchnic mesoderm give rise to intestinal mesothelium. We next sought to determine if the majority of cells were derived from this resident population of progenitors and if the potential to generate mesothelium from resident cells was distributed broadly throughout the splanchnic mesoderm or restricted to subdivisions of the gut.

To address these questions, we developed a chick-quail chimera assay to analyze gut development. Bilateral splanchnopleure was isolated from HH13-17 quail embryos, divided into 6-7 pieces along the A-P axis, and then transplanted individually into the right lateral cavities (precursor to the coelomic cavity) of chick embryos staged between HH16-18 (Figure 3.9 A). The host chick embryos were incubated for 14 days post-transplantation (corresponding to day 16.5 of quail development) and then harvested to identify where the transplanted tissue incorporated and whether mesothelial differentiation transpired. Strikingly, the transplanted splanchnopleure did not incorporate into the host gut tube but rather formed an independent “gut tube” within the coelomic cavity connected to the host only through a mesentery (Figure 3.9 B). At 14 days post-transplantation, graft-derived gut tubes were similar to a normally developing small intestine with an elongated tubular shape and a single dorsal mesentery (Figure 3.9 C,

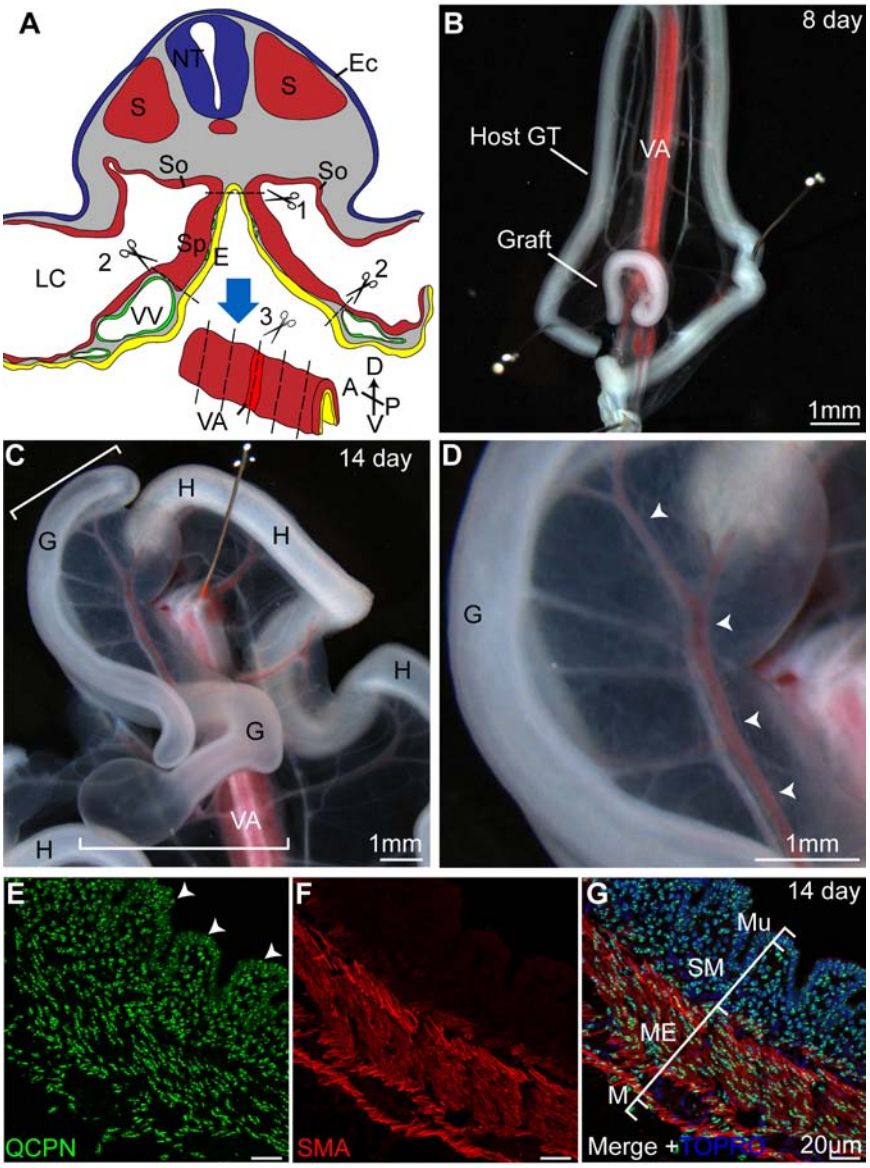

Figure 3.9 Transplanted splanchnopleure forms a highly structured gut tube. A) Transplants were generated by cutting along the dorsal aspect of the splanchnopleure (1) and the ventral edges near the vitelline veins (2). The splanchnopleure was then cut along the A-P axis (3) to generate 6-7 pieces for transplantation. **B)** A representative graft-derived gut tube 8 days after transplantation. The graft had generated a tube and attached to the mesentery of the host gut tube. **C)** A representative graft-derived gut tube 14 days after transplantation (G, bracketed). The graft-derived gut tube was attached to the host (H) via a mesentery. **D)** The mesentery of the graft-derived gut tube contained a regular arrangement of blood vessels (arrowheads). **E-G)** Sections through the graft-derived gut tube demonstrated normal morphogenesis with villi (arrowheads), submucosa (SM), and a SMA-positive muscularis externus layer. All layers were derived from quail cells (QCPN-positive, green). E, endoderm; Ec, ectoderm; G, graft-derived gut tube; H, host gut tube; LC, lateral cavity; M, mesothelium; ME, muscularis externa; Mu, mucosa; NT, neural tube; S, somite; So, somatic mesoderm; Sp, splanchnic mesoderm; SM, submucosa; VA, vitelline artery; VV, vitelline vein.

brackets) housing a well organized vasculature (Figure 3.9 D, arrowheads; observed in 16 chick-quail chimeras). Transverse sections through graft-derived gut tubes demonstrated a remarkable intestinal organization with an inner mucosa with villus folds (arrowheads), a submucosa, and a muscularis externa with smooth muscle differentiation (Figure 3.9 E-G). Staining for quail specific QCPN demonstrated all layers of the graft were quail derived (Figure 3.9 E-G). Specific regions in the graft did not stain with QCPN but were positive for a pan-neuronal marker, PGP9.5 (Figure 3.10 A-E asterisks). Co-staining for a marker of chick cells (8F3) and PGP9.5 confirmed these cells originated from host neural crest cells (Figure 3.10 F-J). Interestingly, the host-derived neural crest cells that invaded the graft organized into typical submucosal and myenteric plexuses (Figure 3.10). Transplanted splanchnopleure isolated both prior to (HH13-HH14) and after (HH15-17) establishment of a trilaminar configuration produced identical results (Figure 3.11).

Co-staining for QCPN with cytokeratin revealed that mesothelium covering the graft-derived gut tube and within the mesentery originated from transplanted quail splanchnopleure (Figure 3.11 A-F, arrowheads). We quantified the number of mesothelial cells in graft-derived gut tubes that were QCPN-positive and found that on average 85% of mesothelial cells were quail derived. Furthermore, 94% of mesothelial cells in graft-derived gut tubes were negative for a marker specific to chick cells (8F3) (Figure 3.11 G-I). The difference between the two percentages is likely due to the variation in staining patterns; QCPN is a perinuclear antigen often with distinct puncta of staining while 8F3 is cytoplasmic and more easily visualized (Figure 3.11 J-L). Both figures denote the great majority of graft-derived mesothelial cells were derived from transplanted tissue.

Tissue morphogenesis was identical between both anterior and posterior derived grafts and, critical to the current studies, the mesothelium was always quail-derived

regardless of whether the graft was obtained from an anterior or posterior location in the source splanchnopleure (100% of cases examined, Figure 3.11 A-F). Taken together, these data demonstrate that mesothelial progenitors are broadly distributed along the A-P axis of the intestine and there is not a localized or restricted PE-like source of mesothelial cells.

Discussion

Mesothelia are essential for the generation of diverse cell types within all coelomic organs investigated thus far (Asahina et al., 2011; Eralp et al., 2005; Mikawa and Gourdie, 1996; Perez-Pomares et al., 2004; Que et al., 2008; Wilm et al., 2005). Despite the importance of this cell type in organogenesis, the origin of mesothelium had only been established in the heart where mesothelium is derived from a localized, extrinsic cell population, the PE. Identification of the origin of mesothelial cells is essential for studies of the molecular regulation of mesothelial differentiation, vascular formation, and mesothelial-dependent signaling in intestinal development and organogenesis in general. Here, using three independent methods, we demonstrate that intestinal mesothelium is derived from a resident population of cells broadly distributed within the splanchnic mesoderm. Thus, gut mesothelium does not arise in the same manner as described in the heart and reveals a novel paradigm for the generation of this essential cell type. Discovery of the origin of gut mesothelium is critical for further analysis of regulatory mechanisms governing mesothelial development, repair in the adult, and origin of disease

Previously, we demonstrated through a genetic lineage tracing study in mouse that vascular smooth muscle cells of the intestine were derived from mesothelium. Furthermore, expression of *Wt1* was first observed in the mesentery and then progressively encompassed the intestinal tube suggesting a migratory mesothelial

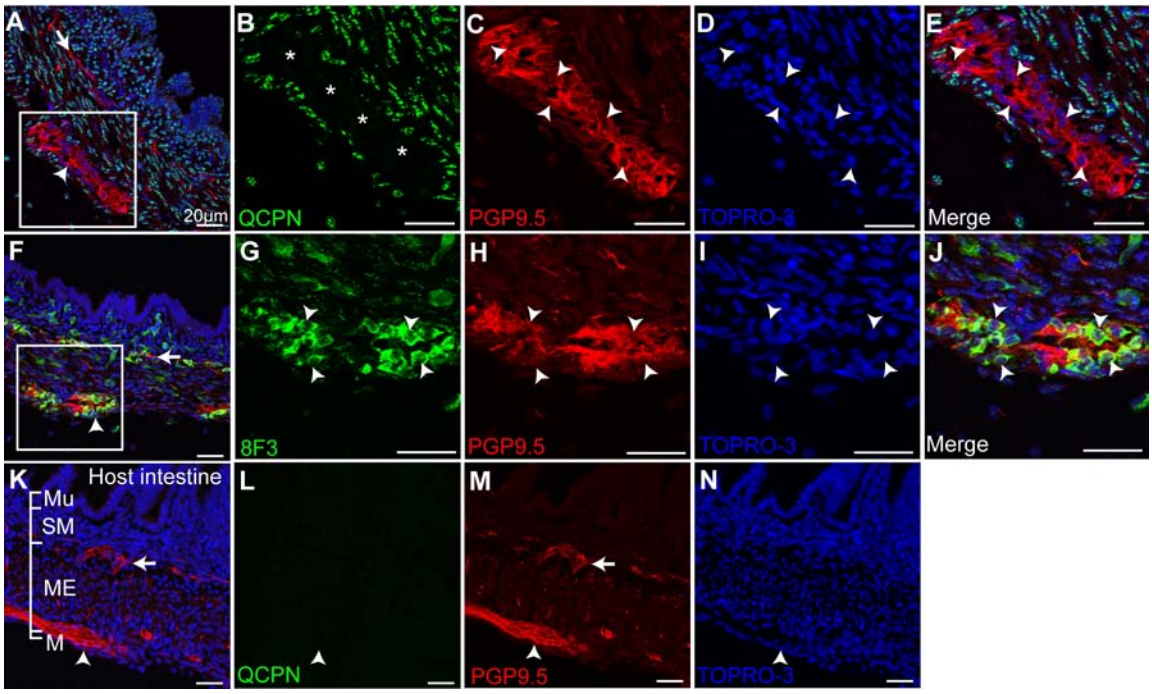

Figure 3.10 Invasion of graft-derived gut tube by chick neural crest. A) Neuronal cells identified by PGP9.5 staining were found throughout the graft-derived gut tube organized into submucosal (arrow) and myenteric plexuses (arrowhead). **B-E)** Higher magnification of boxed area in A). QCPN-negative cells within the graft (asterisks) were PGP9.5-positive (arrowheads). **F-J)** Staining for the chick cell marker 8F3 co-localized with PGP9.5 staining (arrowheads). **K-N)** Immunostaining for QCPN and PGP9.5 in a host gut tube demonstrating the typical organization into submucosal (arrow) and myenteric (arrowhead) plexuses. **L)** QCPN-positive cells were not found within the host gut tube. M, mesothelium; ME, muscularis externa; Mu, mucosa; SM, submucosa.

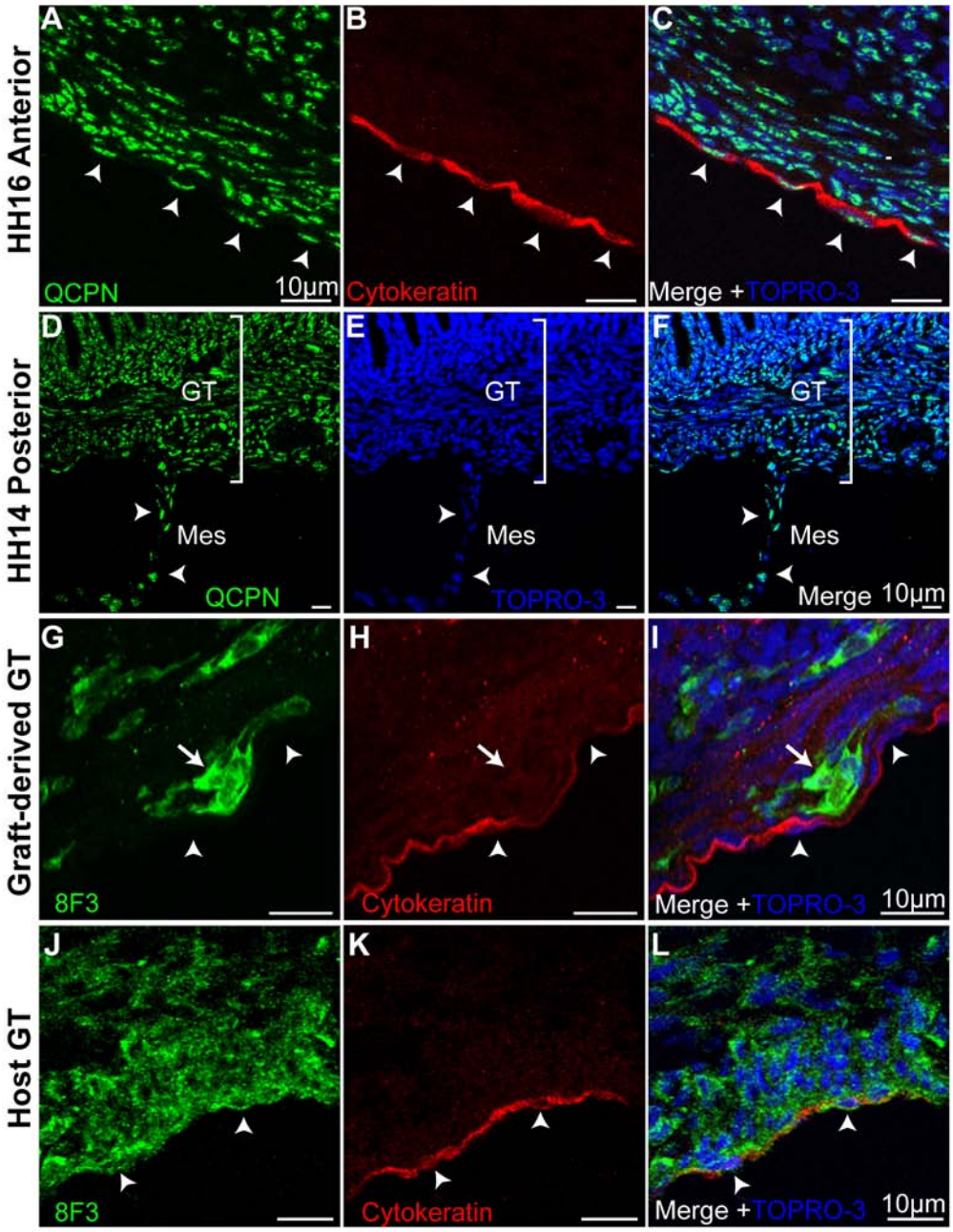

Figure 3.11 Graft mesothelium is quail derived. A-C) Section of graft-derived gut tube generated from tissue isolated from the anterior splanchnopleure of a HH16 quail donor. Co-staining for QCPN and cytokeratin demonstrated that the mesothelial cells lining the graft were quail derived (arrowheads). **D-F)** Section of a graft-derived gut tube generated from the posterior splanchnopleure of a HH14 quail donor. QCPN staining demonstrates the mesenteric mesothelium is quail derived (arrowheads). **G-I)** Host-derived cells (8F3-positive) were also identified within the graft (arrows). However, 8F3-positive chick cells were only rarely (6%) identified within the mesothelial layer (arrowheads) of the graft-derived gut tube. **J-L)** Staining of a chick (host) gut tube reveals mesothelial cells (arrowheads) robustly label with the chick marker 8F3. GT, gut tube; Mes, mesentery.

population may exist as observed in the heart (Wilm et al., 2005). However, a PE-like structure or clear evidence of a migratory population was not identified. Furthermore, *Wt1* is not a marker specific only to mesothelium (Zhou et al., 2011). Here, through the use of direct labeling and transplantation studies in the avian embryo, we have demonstrated that mesothelial progenitors of the intestine are broadly resident to the splanchnic mesoderm and not derived from an exogenous migratory source. This progenitor population is present prior to tube formation but does not specifically express *Wt1*. While there may be variation between species in intestinal mesothelial origin and *Wt1* expression patterns, it is possible that murine mesothelial progenitors are also resident broadly in the intestine and *Wt1* is expressed in a dorsal-ventral direction as mesothelial differentiation proceeds. Still, further experimentation is needed to resolve this issue amongst different species.

The intestines, lungs, liver, and pancreas are all gut tube derivatives formed from endoderm or endodermal buds that are surrounded by splanchnic mesoderm. In contrast, the heart wall is not a gut tube derivative but rather is derived solely from splanchnic mesoderm excluding endoderm dorsally. The splanchnic mesoderm, which makes up the majority of the heart wall, is not thought to contain mesothelial progenitors (Gittenberger-de Groot et al., 2000.; Manner et al., 2005). In contrast, the present study demonstrates that mesothelial precursors are resident broadly to the surface of the developing gut splanchnic mesoderm prior to endodermal budding and mucosal differentiation. Considering the unique features of cardiac development and the early specialization of the cardiac splanchnic mesoderm (i.e. it is a contractile tube before PE-derived mesothelium contacts the organ), we postulate mesothelial development in the lungs, liver and pancreas as gut tube derivatives will be found to more closely resemble the intestinal rather than the cardiac model of mesothelial development.

The molecular foundation for the variation in proepicardial and intestinal mesothelial development is currently unknown. However, Ishii et al. report that the liver bud is at least partially responsible for induction of markers of the PE including *Wt1*, *Tbx18* and *capsulin.* Liver bud transplanted ectopically into the lateral embryo distal to the heart induced *Wt1* in the closely adjoining tissue. Interestingly, the lung bud and stomach did not have similar inductive capabilities in that system (Ishii et al., 2007). For the majority of the mesothelium not in contact with the liver bud, alternative inductive tissues and signals must be involved. Other studies have uncovered potential roles for BMP in villous protrusion of the PE (Ishii et al., 2010), a behavior observed in cardiac but not intestinal mesothelial development (from the current study), and for both BMP and FGF signals in the lineage specification of epicardial cells (Kruithof et al., 2006; Schlueter et al., 2006). With identification of the fundamental mechanism of intestinal mesothelial formation, studies on the molecular regulation of behaviors unique to either the intestinal or cardiac mesothelium can proceed.

While the origin of mesothelial cells in the intestine and heart are clearly divergent, there do exist conserved features of mesothelial development and differentiation. The presence of a small number of host mesothelial cells in graft-derived gut tubes suggests that intestinal mesothelium can be migratory as previously observed with epicardial mesothelium. Whether this is a normally occurring event in gut development or simply a “blending” of cells in this particular experimental model, it is evident that mesothelial progenitors of the gut and/or definitive gut mesothelium are capable of movement or active migration. Mesothelial cells in the heart, lungs, intestines, and liver all give rise to stromal cells including vascular smooth muscle, endothelium, fibroblasts, and other “mesenchymal” cells (Asahina et al., 2011; Dettman et al., 1998; Eralp et al., 2005; Mikawa and Gourdie, 1996; Perez-Pomares et al., 2004; Que et al., 2008; Wilm et al., 2005). Both cardiac and peritoneal mesothelia of the adult retain the

ability to generate stromal progeny. When stimulated, adult omental mesothelial cells differentiate into vascular smooth muscle cells and can directly contribute cells to an injured blood vessel (Kawaguchi et al., 2007; Shelton et al., 2012). Fibroblast and vascular smooth muscle cell differentiation from previously quiescent mesothelium has also been observed following myocardial infarction (Zhou and Pu, 2011). Thus, while the mechanism generating intestinal mesothelial cells is different from that of the heart, once established, these two progenitor populations appear to have similar differentiative potentials.

Other disease processes involving mesothelia reflect the developmental potential of this cell type. For example, peritoneal sclerosis, a fibrotic thickening of the abdominal serosal membranes, is frequently observed following peritoneal dialysis (Devuyst et al., 2010). Mesothelial cells have recently been recognized both as a source of fibrotic cells and a signaling center for aberrant vasculogenesis (Aroeira et al., 2005; Braun et al., 2011; Yanez-Mo et al., 2003; Yung and Chan, 2009). In another example, pulmonary fibrosis is first observed as a fibrotic thickening just below the pulmonary mesothelium that progressively moves inward (King et al., 2011). The role of mesothelium in this disease has also recently been the focus of studies and reviews as a signaling center or source of fibrotic cells (Acencio et al., 2007; Decologne et al., 2007; Mutsaers et al., 2004). These pathologies have a direct root in the developmental potential of mesothelium to give rise to fibroblasts and vascular smooth muscle. Thus, investigation of the diversity of mesothelial populations is critical to understanding their behavior in these various organs systems and disease processes.

Following discovery of the proepicardium, studies on development of cardiac mesothelium were able to rapidly progress. Currently, our understanding of epicardial biology encompasses the detailed cell lineage, mechanisms of molecular differentiation during development, and pathological behavior. We are now poised to move forward

with similar studies of non-cardiac mesothelial populations. Mesothelial cells of diverse organs and body cavities have been considered a uniform population due to their ultrastructural similarity and apparent shared developmental potential. Our data demonstrate that at least cardiac and intestinal mesothelia are heterogeneous populations with varied developmental histories that must be considered independently. Understanding the developmental origin of diverse mesothelia is essential for understanding the role mesothelial, vascular, and stromal cells may play in the development and homeostasis of these organs in the adult.

References

Acencio, M. M., Vargas, F. S., Marchi, E., Carnevale, G. G., Teixeira, L. R., Antonangelo, L. and Broaddus, V. C. (2007). Pleural mesothelial cells mediate inflammatory and profibrotic responses in talc-induced pleurodesis. *Lung* **185**, 343-8.

Aroeira, L. S., Aguilera, A., Selgas, R., Ramirez-Huesca, M., Perez-Lozano, M. L., Cirugeda, A., Bajo, M. A., del Peso, G., Sanchez-Tomero, J. A., Jimenez-Heffernan, J. A. et al. (2005). Mesenchymal conversion of mesothelial cells as a mechanism responsible for high solute transport rate in peritoneal dialysis: role of vascular endothelial growth factor. *Am J Kidney Dis* **46**, 938-48.

Asahina, K., Zhou, B., Pu, W. T. and Tsukamoto, H. (2011). Septum transversum-derived mesothelium gives rise to hepatic stellate cells and perivascular mesenchymal cells in developing mouse liver. *Hepatology* **53**, 983-95.

Braun, N., Alscher, D. M., Fritz, P., Edenhofer, I., Kimmel, M., Gaspert, A., Reimold, F., Bode-Lesniewska, B., Ziegler, U., Biegger, D. et al. (2011). Podoplanin-positive cells are a hallmark of encapsulating peritoneal sclerosis. *Nephrol Dial Transplant* **26**, 1033-41.

Chegini, N. (2008). TGF-beta system: the principal profibrotic mediator of peritoneal adhesion formation. *Semin Reprod Med* **26**, 298-312.

Decologne, N., Kolb, M., Margetts, P. J., Menetrier, F., Artur, Y., Garrido, C., Gauldie, J., Camus, P. and Bonniaud, P. (2007). TGF-beta1 induces progressive pleural scarring and subpleural fibrosis. *J Immunol* **179**, 6043-51.

Dettman, R. W., Denetclaw, W., Jr., Ordahl, C. P. and Bristow, J. (1998). Common epicardial origin of coronary vascular smooth muscle, perivascular fibroblasts, and intermyocardial fibroblasts in the avian heart. *Dev Biol* **193**, 169-81.

Devuyst, O., Margetts, P. J. and Topley, N. (2010). The pathophysiology of the peritoneal membrane. *J Am Soc Nephrol* **21**, 1077-85.

Eralp, I., Lie-Venema, H., DeRuiter, M. C., van den Akker, N. M., Bogers, A. J., Mentink, M. M., Poelmann, R. E. and Gittenberger-de Groot, A. C. (2005). Coronary artery and orifice development is associated with proper timing of epicardial outgrowth and correlated Fas-ligand-associated apoptosis patterns. *Circ Res* **96**, 526-34.

Gittenberger-de Groot, A. C., Vrancken Peeters, M. P., Bergwerff, M., Mentink, M. M. and Poelmann, R. E. (2000). Epicardial outgrowth inhibition leads to compensatory mesothelial outflow tract collar and abnormal cardiac septation and coronary formation. *Circ Res* **87**, 969-71.

Hamburger, V. and Hamilton, H. L. (1992). A series of normal stages in the development of the chick embryo. 1951. *Dev. Dyn.* **195**, 231-272.

Ho, E. and Shimada, Y. (1978). Formation of the epicardium studied with the scanning electron microscope. *Dev Biol* **66**, 579-85.

Ishii, Y., Langberg, J. D., Hurtado, R., Lee, S. and Mikawa, T. (2007). Induction of proepicardial marker gene expression by the liver bud. *Development* **134**, 3627-37.

Ishii, Y., Garriock, R. J., Navetta, A. M., Coughlin, L. E. and Mikawa, T. (2010). BMP signals promote proepicardial protrusion necessary for recruitment of coronary vessel and epicardial progenitors to the heart. *Dev Cell* **19**, 307-16.

Kawaguchi, M., Bader, D. M. and Wilm, B. (2007). Serosal mesothelium retains vasculogenic potential. *Dev Dyn* **236**, 2973-9.

King, T. E., Jr., Pardo, A. and Selman, M. (2011). Idiopathic pulmonary fibrosis. *Lancet* **378**, 1949-61.

Kruithof, B. P., van Wijk, B., Somi, S., Kruithof-de Julio, M., Perez Pomares, J. M., Weesie, F., Wessels, A., Moorman, A. F. and van den Hoff, M. J. (2006). BMP and FGF regulate the differentiation of multipotential pericardial mesoderm into the myocardial or epicardial lineage. *Dev Biol* **295**, 507-22.

Lassiter, R. N., Dude, C. M., Reynolds, S. B., Winters, N. I., Baker, C. V. and Stark, M. R. (2007). Canonical Wnt signaling is required for ophthalmic trigeminal placode cell fate determination and maintenance. *Dev Biol* **308**, 392-406.

Manasek, F. J. (1969). Embryonic development of the heart. II. Formation of the epicardium. *J Embryol Exp Morphol* **22**, 333-48.

Manner, J., Schlueter, J. and Brand, T. (2005). Experimental analyses of the function of the proepicardium using a new microsurgical procedure to induce loss-of-proepicardial-function in chick embryos. *Dev Dyn* **233**, 1454-63.

McGlinn, E. and Mansfield, J. H. (2011). Detection of gene expression in mouse embryos and tissue sections. *Methods Mol Biol* **770**, 259-92.

Mikawa, T. and Gourdie, R. G. (1996). Pericardial mesoderm generates a population of coronary smooth muscle cells migrating into the heart along with ingrowth of the epicardial organ. *Dev Biol* **174**, 221-32.

Minot, C.-S. (1890). The mesoderm and the coelom of vertebrates. *The American Naturalist* **24**, 877-898.

Moore, K. L. and Persaud, T. V. N. (1998). The developing human : clinically oriented embryology. Philadelphia: Saunders.

Morimoto, M., Liu, Z., Cheng, H. T., Winters, N., Bader, D. and Kopan, R. (2010). Canonical Notch signaling in the developing lung is required for determination of arterial smooth muscle cells and selection of Clara versus ciliated cell fate. *J Cell Sci* **123**, 213-24.

Mutsaers, S. E. (2002). Mesothelial cells: their structure, function and role in serosal repair. *Respirology* **7**, 171-91.

Mutsaers, S. E., Prele, C. M., Brody, A. R. and Idell, S. (2004). Pathogenesis of pleural fibrosis. *Respirology* **9**, 428-40.

Mutsaers, S. E. and Wilkosz, S. (2007). Structure and function of mesothelial cells. *Cancer Treat Res* **134**, 1-19.

Osler, M. E. and Bader, D. M. (2004). Bves expression during avian embryogenesis. *Dev Dyn* **229**, 658-67.

Perez-Pomares, J. M., Carmona, R., Gonzalez-Iriarte, M., Macias, D., Guadix, J. A. and Munoz-Chapuli, R. (2004). Contribution of mesothelium-derived cells to liver sinusoids in avian embryos. *Dev Dyn* **229**, 465-74.

Que, J., Wilm, B., Hasegawa, H., Wang, F., Bader, D. and Hogan, B. L. (2008). Mesothelium contributes to vascular smooth muscle and mesenchyme during lung development. *Proc Natl Acad Sci U S A* **105**, 16626-30.

Schlueter, J., Manner, J. and Brand, T. (2006). BMP is an important regulator of proepicardial identity in the chick embryo. *Dev Biol* **295**, 546-58.

Schulte, I., Schlueter, J., Abu-Issa, R., Brand, T. and Manner, J. (2007). Morphological and molecular left-right asymmetries in the development of the proepicardium: a comparative analysis on mouse and chick embryos. *Dev Dyn* **236**, 684-95.

Shelton, E., Poole, S., Reese, J. and Bader, D. (2012). Omental grafting:a cell-based therapy for blood vessel repair. *J Tissue Eng Regen Med*, doi: 10.1002/term.528.

Takaba, K., Jiang, C., Nemoto, S., Saji, Y., Ikeda, T., Urayama, S., Azuma, T., Hokugo, A., Tsutsumi, S., Tabata, Y. et al. (2006). A combination of omental flap and growth factor therapy induces arteriogenesis and increases myocardial perfusion in chronic myocardial ischemia: evolving concept of biologic coronary artery bypass grafting. *J Thorac Cardiovasc Surg* **132**, 891-99.

Venters, S. J., Dias da Silva, M. R. and Hyer, J. (2008). Murine retroviruses re-engineered for lineage tracing and expression of toxic genes in the developing chick embryo. *Dev Dyn* **237**, 3260-9.

Wilm, B., Ipenberg, A., Hastie, N. D., Burch, J. B. and Bader, D. M. (2005). The serosal mesothelium is a major source of smooth muscle cells of the gut vasculature. *Development* **132**, 5317-28.

Wu, M., Smith, C. L., Hall, J. A., Lee, I., Luby-Phelps, K. and Tallquist, M. D. (2010). Epicardial spindle orientation controls cell entry into the myocardium. *Dev Cell* **19**, 114-25.

Yanez-Mo, M., Lara-Pezzi, E., Selgas, R., Ramirez-Huesca, M., Dominguez-Jimenez, C., Jimenez-Heffernan, J. A., Aguilera, A., Sanchez-Tomero, J. A., Bajo, M. A., Alvarez, V. et al. (2003). Peritoneal dialysis and epithelial-to-mesenchymal transition of mesothelial cells. *N Engl J Med* **348**, 403-13.

Yung, S. and Chan, T. M. (2009). Intrinsic cells: mesothelial cells -- central players in regulating inflammation and resolution. *Perit Dial Int* **29** Suppl 2, S21-7.

Zhang, Q. X., Magovern, C. J., Mack, C. A., Budenbender, K. T., Ko, W. and Rosengart, T. K. (1997). Vascular endothelial growth factor is the major angiogenic factor in omentum: mechanism of the omentum-mediated angiogenesis. *J Surg Res* **67**, 147-54.

Zhou, B., Honor, L. B., He, H., Ma, Q., Oh, J. H., Butterfield, C., Lin, R. Z., Melero-Martin, J. M., Dolmatova, E., Duffy, H. S. et al. (2011). Adult mouse epicardium modulates myocardial injury by secreting paracrine factors. *J Clin Invest* **121**, 1894-904.

Zhou, B. and Pu, W. T. (2011). Epicardial epithelial-to-mesenchymal transition in injured heart. *J Cell Mol Med* **15**, 2781-3.

CHAPTER IV

CHICK-TRANSGENIC QUAIL CHIMERAS IN STUDIES OF EMBRYONIC DEVELOPMENT

Abstract

The first chick-quail chimera was generated over 40 years ago to study embryonic development; however, the technique is used relatively infrequently today. The generation of transgenic quail offers a powerful tool to use in conjunction with classical chimera-based experimentation. We utilized transgenic quail that express a fluorescent protein in endothelial cells as donors to generate chick-quail chimeras to examine in detail the origin and development of the intestinal and limb vasculature. The combination of these methodologies provides developmental biologists with a novel approach to answer long standing questions in embryology.

Introduction

Chick-quail chimeras have long been used as a lineage tracing method in studies of embryology (Le Douarin, 1973). Their unique utility lies in the ability to reliably distinguish quail from chick cells thus providing an inheritable and irreversible mark (Le Douarin, 1973; Le Douarin et al., 2008). Furthermore, avian embryos are easily accessed within the egg and tolerate surgical procedures well. Japanese quail offer the additional advantage of small size and rapid sexual maturation (Huss et al., 2008). The major disadvantage of avian embryos has been the lack of methods to generate transgenic animals. However, through the use of retroviral transduction, both transgenic chick and quail have been generated (McGrew et al., 2008; Sato et al., 2010) and other non-retroviral based methods are under research (Mizushima et al., 2010; Park and Han, 2012).

Vascular development is an area of particular interest to scientists and physicians of many fields ranging from developmental biology to oncology. Endothelial networks vary greatly between coelomic organs not only in their basic architecture but also in their molecular profile (Atkins et al., 2011). Furthermore, disease is often specific to an individual vascular bed or even to a region of a single vascular bed (Davies et al., 2010). It is not known if there is an embryological basis for the endothelial variation observed in the adult or in disease. Indeed, the embryological origins of endothelial cells are still not entirely known. Coelomic organs are thought to derive their vasculature from remodeling of an intrinsic vascular plexus rather than recruiting a vascular network from elsewhere as has been demonstrated to occur in the limbs (Pardanaud et al., 1989). However, in the heart, the coronary blood vessels must be recruited to the myocardial wall presenting an exception to this general rule of coelomic vasculogenesis (Dettman et al., 1998; Mikawa and Gourdie, 1996). Multiple origins of coronary endothelial cells have been proposed including the proepicardium, sinus venosus, and endocardium (Ishii et al., 2009; Katz et al.; Red-Horse et al., 2010).Thus, despite the many studies focused on endothelial development, much remains to be discovered.

Through use of transgenic quail generated by Dr. Rusty Lansford (Cal Tech; (Sato et al., 2010)), we generated chick-quail chimeras in which the vasculature of the graft could be viewed by fluorescence in whole mount. A segment of transplanted quail splanchnopleure formed a morphologically mature intestinal tube within the chick host coelomic cavity. The graft-derived gut tube demonstrated remarkable remodeling of the endothelial plexus. Both arterial and venous endothelial cells were derived from grafted tissue as were vascular smooth muscle cells. Transplantation of somatopleure revealed novel vascular contributions to the limb. Taken together, this study demonstrates the combination of transgenics with the classical embryological technique of chimera generation can be of great utility in experimental developmental biology.

Materials and Methods

Preparation of host chick embryos

Eggs were incubated for approximately 60 hours to stage HH15-17, windowed and stained with Neutral Red as described in Chapter 3.

Generation of splanchnopleure chimera

Tg(*tie1*:H2B-eYFP) transgenic quail were incubated for approximately 56 hours to HH15-17. Splanchnopleure was isolated and transplanted as described in Chapter 3.

Generation of somatopleure chimera

Tg(*tie1*:H2B-eYFP) quail were incubated for approximately 56 hrs. Embryos were dissected in sterile Tyrode's solution + 1% penicillin/streptomycin. The somatopleure was isolated by cutting transversely through the embryo just posterior to the heart, separating the splanchnopleure and somatopleure with a tungsten needle, and then cutting adjacent to the somites/segmental plate on both the right and left sides. Special care was taken to exclude somitic tissue. The isolates were transferred into a tissue culture dish containing DMEM with high glucose. The isolate from each side was then cut into four pieces along the anterior posterior axis. The neutral red agar strip was removed from a host chicken embryo and the vitelline membrane removed with a tungsten needle. A hole was then made through the somatopleure of the host embryo near the vitelline artery. An individual donor somatopleure segment was transferred with forceps into the host chicken egg. The transplant was then pushed into the coelomic cavity with a tungsten needle and forceps. Syringe filtered Tyrode's solution + 1% penicillin/streptomycin was added to the egg to replace volume. The chick eggs were sealed with two layers of transparent tape and placed into a humidified incubator.

Imaging

After 7 to 14 days incubation, host chick embryos were isolated and a midline incision was made from the region of the yolk sac through the thoracic cavity. Host embryos with attached grafts were then submerged in PBS in a culture dish with a layer of Sylgard at the bottom. Insect pins were used to hold the body wall of the host embryos open. A Zeiss M165FC fluorescent dissecting microscope with a Retiga EXi Fast1394 camera was used to image the eYFP fluorescence in whole mount.

Fixation and sectioning

After imaging, grafts were isolated in combination with the directly adherent chick tissue and fixed overnight in 4% formaldehyde. Tissue was washed 3X5 min in PBS rolling at room temperature and placed in 30% sucrose in PBS overnight. Tissue was transferred to an embedding mold and excess sucrose was removed with a transfer pipette. The tissue was covered with OCT and incubated at room temperature for 30 min to 1 hour depending on the tissue size to allow the OCT to infiltrate around the tissue. The molds were then placed in ethanol cooled with dry ice to freeze. Blocks were stored at -20°C. Sections were cut at 6µm on a Leica CM3050 cryostat and stored at -20°C.

Immunohistochemistry and confocal imaging

As described in Chapter 3.

Results

Generation of chick-transgenic quail splanchnopleure chimeras

An endothelial plexus is present between the splanchnopleure and endoderm as early as the 4 somite stage (HH8) in the quail embryo [DeRuiter et al., 1993] (Figure 4.1

A-B). We isolated donor tissue from Tg(*tie1*:H2B-eYFP) quail that express an eYFP-H2B fusion protein under control of the *Tie-1* promoter. The gene *Tie-1* encodes a receptor tyrosine kinase expressed specifically in endothelial cells. The entire splanchnopleure posterior to the heart of a donor quail embryo was isolated and divided into six equal segments. At the time of isolation, an endothelial plexus was present within the splanchnopleure between the splanchnic mesoderm and endoderm (Figure 4.1 A-B, arrows). An individual segment of splanchnopleure was transplanted into the coelomic cavity near the vitelline artery of a HH15-HH17 host chick embryo. After transplantation, the host embryos were incubated for at least 24 hours and up to two weeks. Remarkably, at 24 hours post-transplantation, the earliest time point examined, the donor splanchnopleure segments had already formed a vascular attachment to the host. The grafts were typically attached to the host via a single vessel (Figure 4.1 C-D, arrow). At this time point, while endothelial cells were clearly present in abundance within the graft, no obvious organization of the vasculature was observed other than the attachment to the host (Figure 4.1 D).

We isolated two week post-transplantation grafts to determine how the graft vascular network was remodeled over time. At 14 days, the grafted splanchnopleure segments had generated a well-formed intestinal tube with a mesentery (Figure 4.2 A). The grafts were typically supplied by a single major blood vessel of quail origin (eYFP-positive) connected directly to the host vitelline artery (inset, arrow) that then ramified within the graft mesentery (Figure 4.2 B-C). Both arteries (arrow) and veins (arrowhead) contained eYFP-positive endothelial cells (Figure 4.2 D). Cross-sections through a representative graft revealed the vasculature was organized into a three-tiered plexus: external layer near the surface of the intestine, an internal layer near the base of the villi, and a capillary network extending into the lamina propria of the villi (Figure 4.2 E-F). The blood vessels were in close approximation to HNK-1-positive enteric neural crest cells.

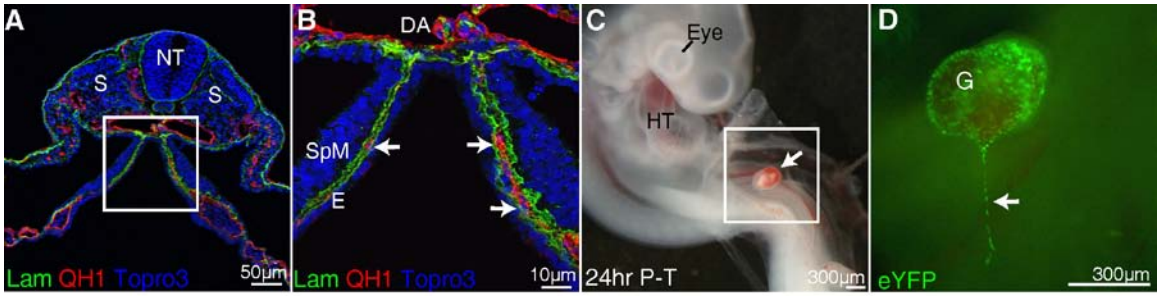

Figure 4.1 Splanchnopleure plexus and host attachment. A) Transverse section of a HH14 quail embryo. **B)** Boxed region show in A). QH1-positive endothelial cells (arrows) reside between the basement membranes (laminin, green) of the splanchnic mesoderm (SpM) and endoderm (E). **C)** Twenty-four hours post-transplantation the splanchnopleure graft has formed a ball (arrow) within the coelomic cavity of the host chick embryo. **D)** Wholemount eYFP fluorescence of the graft (G) within the coelomic cavity. A quail derived blood vessel (arrow) attached the graft to the host chick body wall. DA, dorsal aorta; E, endoderm; G, graft; HT, heart tube; lam, laminin; NT, neural tube; P-T, post-transplantation; S, somite; SpM, splanchnic mesoderm.

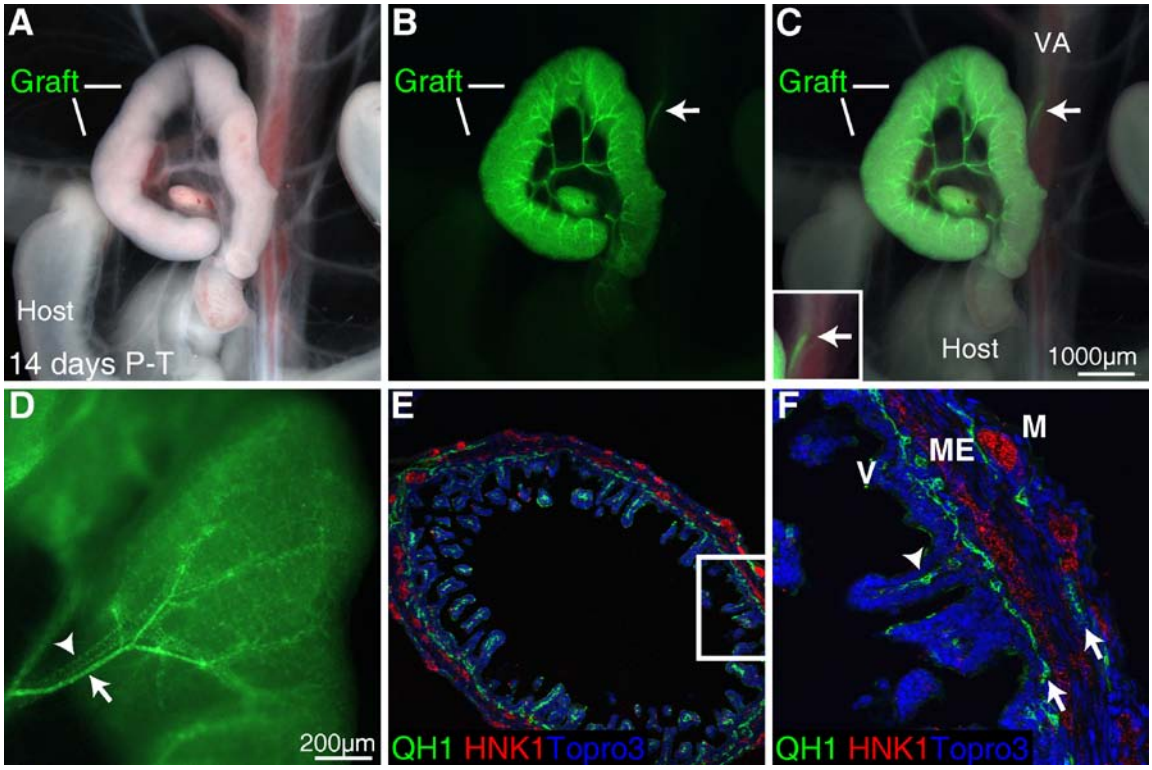

Figure 4.2 Two week post-transplantation graft-derived gut tube. A) Bright field of 14 day post-transplantation graft attached to host mesentery and vitelline artery. **B)** eYFP-positive quail-derived endothelial cells were found in a well organized vascular network within the graft. **C)** A single quail-derived vessel (arrows, inset) attached to the host vitelline artery (VA). **D)** Both veins (arrowhead) and arteries (arrow) were eYFP-positive. **E)** Cross-section through 14 day post-transplantation graft. **F)** Boxed region in E. QH1-positive endothelial cells were organized into an outer and inner endothelial layer (arrows) and extended into the villi (arrowheads). The two outer endothelial layers closely associated with HNK-1-positive neural crest cells (red) of the submucosal and myenteric plexuses. M, mesothelium; ME, muscularis externa; P-T, post-transplantation; V, villi; VA, vitelline artery

Thus, the vasculature of the graft was organized in the same manner as a normally developing quail intestine (Thomason et al, submitted; Nagy et al., 2012)

In a chimera sectioned through the host vitelline artery, the fusion of the quail vessel and chick vitelline artery was observed directly. Staining for eYFP and QCPN revealed that quail endothelial cells formed the complete lining of a large blood vessel that penetrated the host vitelline artery forming a contiguous lumen (Figure 4.3 A-B). Blood cells were present within the lumens of both the chick and quail vessel indicating flow between the two likely occurred (Figure 4.3 B, blue). Interestingly, the smooth muscle layers surrounding the quail vessel were derived from the chick near the point of fusion (Figure 4.3 A-B). Very few non-endothelial quail cells (arrowhead) were found within the host mesentery housing the vitelline artery indicating the endothelial cells of the graft were the major invasive cell type (Figure 4.3 A). Cross sections through graft-derived gut tubes revealed both endothelial (arrowheads) and vascular smooth muscle cells (arrows, identified by their morphology and close association with endothelial cells) were QCPN positive indicating their quail origin (Figure 4.3 C, arrows). These data indicate vascularization of the graft including generation of both veins and arteries largely occurs by the differentiation or remodeling of endothelial cells intrinsic to the intestinal splanchnopleure. The vascular smooth muscle of the graft is also generated from resident progenitor cells.

Generation of chick-transgenic quail somatopleure chimeras

Somatopleure, composed of ectoderm and somatic mesoderm, gives rise to the body wall and limb buds. We isolated somatopleure from HH14 Tg(*tie1*:H2B-eYFP) quail embryos prior to limb bud formation and divided it along the anterior-posterior axis into small segments for transplantation into the coelom of a host chicken embryo (Winters, 2012 In press). After 7 days incubation, host embryos were sacrificed to visualize

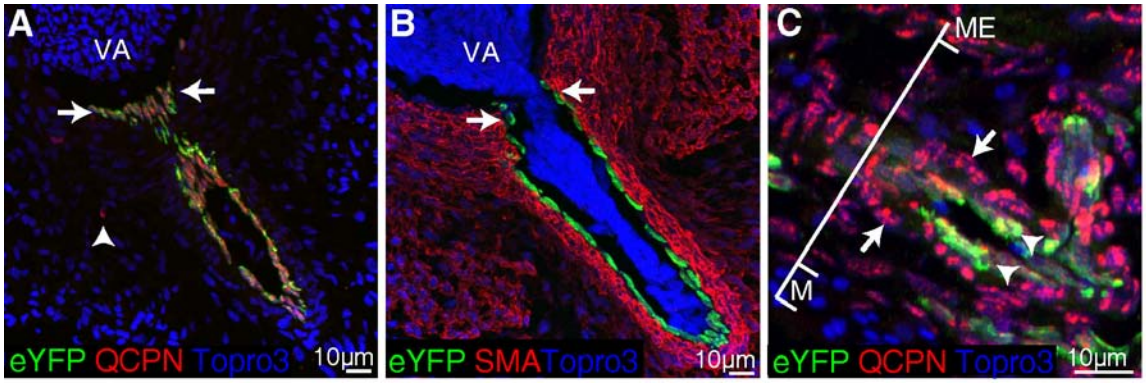

Figure 4.3 Vascular smooth muscle cells of the graft. A) A quail-derived vessel penetrated the host vitelline artery (arrows). Quail endothelial cells were eYFP-positive. QCPN-positive cells near the host were almost entirely endothelial. Rare eYFP-negative QCPN-positive quail cells (arrowhead) were identified near the host vitelline artery. **B)** Vascular smooth muscle cells near the host vessel were chick derived. The lumens of the two vessels were contiguous (arrows) with blood flowing between (blue). **C)** Within the graft, QCPN-positive vascular smooth muscle cells surrounded the eYFP-positive endothelial cells (arrowhead). M, mesothelium; ME, muscularis externa; VA, vitelline artery.

maturation of the grafts. Some degree of limb formation was observed in 6/10 embryos (Figure 4.4 A). Interestingly, in all cases, the grafts attached to the body wall near the apex of the thoracic cavity—the internal aspect of where the host wing emerged. Additionally, the grafts were firmly embedded in the host body wall (Figure 4.4 A). This is in contrast to the grafted splanchnopleure which connected to the host via only a mesentery in almost all cases (Figure 4.2).

Examination of the somatopleure grafts for eYFP fluorescence in whole mount revealed a subset of vessels derived from the transplanted tissue (Figure 4.4 B). The graft derived vessels ran along the medial and lateral aspects of the limb digits reflecting the typical vascular organization of a normally developing limb (Figure 4.4 C-D). Interestingly, only arteries (arrows) appeared to be quail-derived with adjacent veins (containing pooled blood) negative for eYFP (Figure 4.4 D, arrowhead). A large, quail-derived major supply vessel that directly contacted the host could be observed in some cases (Figure 4.4 E-F, arrow). However, more often, the vasculature extending between the graft and host was host derived (Figure 4.4 E-F, arrowheads). Overall, the somatopleure grafts had much fewer quail-derived vessels than the splanchnopleure grafts consistent with prior data (Pardanaud, et al., 1989).

Discussion

Our study demonstrates the utilization of transgenic quail tissue in the generation of a chimera. Previous studies demonstrated the broad potential of splanchnic mesoderm to generate endothelial cells (Pardanaud et al., 1989). However, it was unknown if transplanted tissue underwent typical vascular remodeling including differentiation into veins and arteries. With the use of transgenic quail tissue, the overall architecture of the vascular network could be observed. Transplanted splanchnic mesoderm generated a complete vascular network including vascular smooth muscle

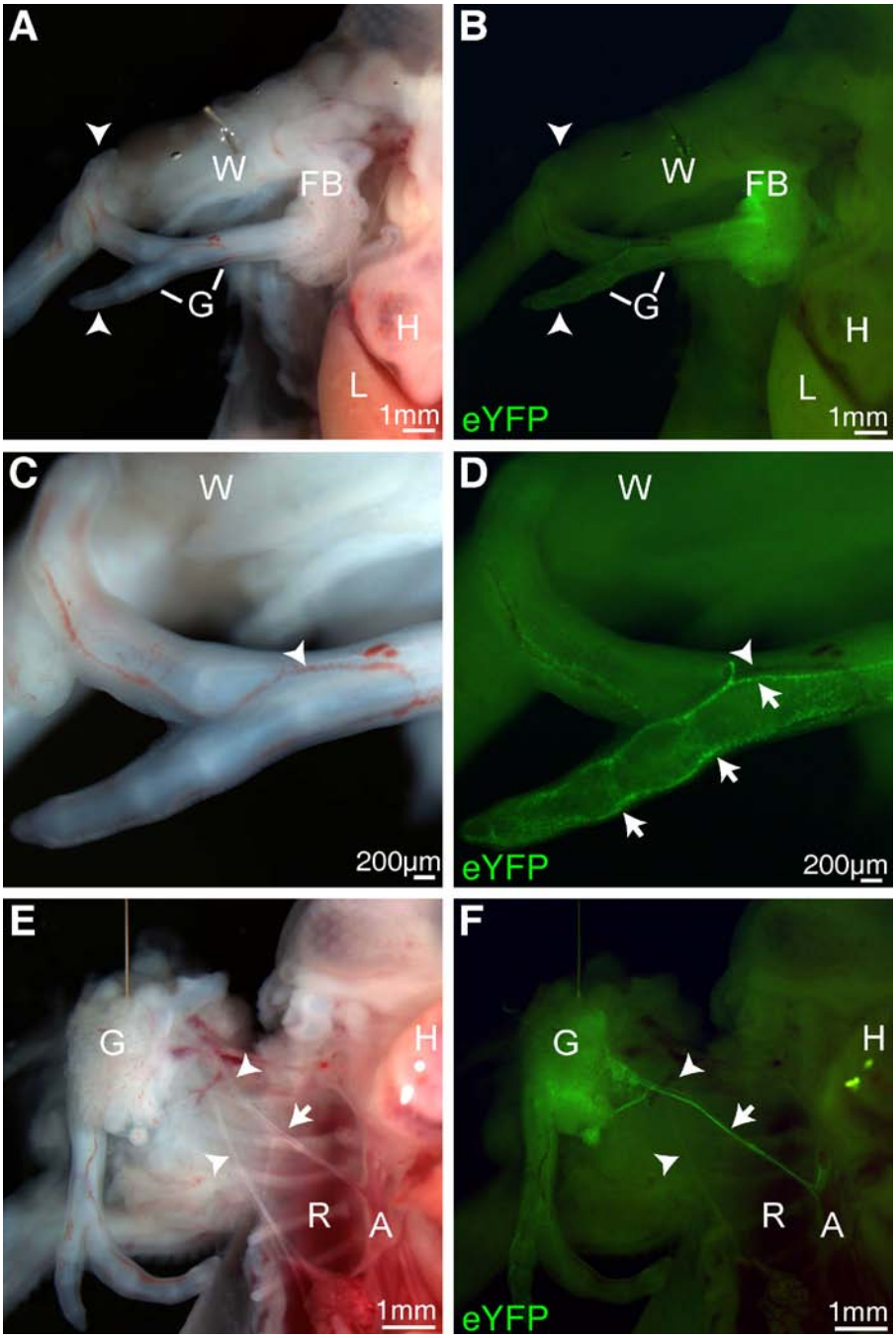

Figure 4.4 Somatopleure graft 7 days post-transplantation. A-B) A somatopleure graft (G) attached to host body wall within the apex of the thoracic cavity. The graft exhibited features of the hind limb including two toes (arrowheads) and feather buds (FB). **C-D)** A small number of blood vessels of the graft were derived from the quail (arrows, eYFP-positive). Adjacent blood vessels were eYFP-negative (arrowhead). **E-F)** The major supply vessel to the graft branched from the aorta (A) and was partly composed of quail endothelial cells (arrow). Other vascular segments of the supply vessel were eYFP-negative (arrowheads). A, aorta; G, graft; H, heart; L, liver; R, ribs; W, wing.

from mesenteric vessels to the capillary plexus of the villi. Both veins and arteries were generated by quail tissue. This demonstrates intestinal splanchnopleure contains all of the necessary progenitor cells to generate a complete vasculature. The somatic mesoderm displayed a marked reduction in vasculogenic potential compared to splanchnic mesoderm, as expected (Pardanaud et al., 1989). However, a significant vascular contribution from grafted tissue was observed. Interestingly, the vasculature that differentiated from somatic mesoderm appeared to be arterial and not venous suggesting an early specification of endothelial progenitor cells may occur within the vascular progenitors contained within the somatopleure. Future studies with this methodology will focus on other coelomic organs including the heart which has a potentially unique method of vasculogenesis.

The objective of developmental biologists is often to isolate a particular gene or cell type for study. Transgenic techniques have allowed considerable control over certain variables, such as gene expression, and correspondingly advanced experimental designs. The combination of transgenics with surgical manipulations allows an additional layer of control and isolation from confounding variables. For example, knockout of a particular gene often affects multiple cell types and can lead to embryonic lethality even though the organ of interest is not essential for embryonic survival (Moore et al., 1999; Phoon et al., 2004; Saito et al., 2012). Isolation of the organ and *in vitro* culture is effective in some situations though is constrained by the lack of a vascular supply (Burke et al., 2010). Transplantation of the same organ into a host embryo provides a vascular supply and allows strikingly normal development to proceed. Additionally, tissues of interest can be recombined or treated with a retrovirus or small molecule before transplantation. Mouse-chick chimeras can also be generated (Fontaine-Perus et al., 1997; Pudliszewski and Pardanaud, 2005).

Coelomic transplantation in particular offers several unique advantages. The technique is simple to perform and does not require replacement of the host tissue. As demonstrated here, grafted tissue may attach to regions near the natural environment and undergo remarkably normal morphogenesis. The host can be grown until hatching (or beyond) to allow long term growth and differentiation of the graft. Thus, transplantation of transgenic quail tissue into the chick coelom, an old trick with a new twist, has wide applicability for answering questions of developmental biology.

References

Atkins, G. B., Jain, M. K. and Hamik, A. (2011). Endothelial differentiation: molecular mechanisms of specification and heterogeneity. *Arterioscler Thromb Vasc Biol* **31**, 1476-84.

Burke, Z. D., Li, W. C., Slack, J. M. and Tosh, D. (2010). Isolation and culture of embryonic pancreas and liver. *Methods Mol Biol* **633**, 91-9.

Davies, P. F., Civelek, M., Fang, Y., Guerraty, M. A. and Passerini, A. G. (2010). Endothelial heterogeneity associated with regional athero-susceptibility and adaptation to disturbed blood flow in vivo. *Semin Thromb Hemost* **36**, 265-75.

DeRuiter, M. C., Gittenberger-de Groot, A. C., Poelmann, R. E., VanIperen, L. and Mentink, M. M. (1993). Development of the pharyngeal arch system related to the pulmonary and bronchial vessels in the avian embryo. With a concept on systemic-pulmonary collateral artery formation. *Circulation* **87**, 1306-19.

Dettman, R. W., Denetclaw, W., Jr., Ordahl, C. P. and Bristow, J. (1998). Common epicardial origin of coronary vascular smooth muscle, perivascular fibroblasts, and intermyocardial fibroblasts in the avian heart. *Dev Biol* **193**, 169-81.

Fontaine-Perus, J., Halgand, P., Cheraud, Y., Rouaud, T., Velasco, M. E., Cifuentes Diaz, C. and Rieger, F. (1997). Mouse-chick chimera: a developmental model of murine neurogenic cells. *Development* **124**, 3025-36.

Huss, D., Poynter, G. and Lansford, R. (2008). Japanese quail (Coturnix japonica) as a laboratory animal model. *Lab Anim (NY)* **37**, 513-9.

Ishii, Y., Langberg, J., Rosborough, K. and Mikawa, T. (2009). Endothelial cell lineages of the heart. *Cell Tissue Res* **335**, 67-73.

Katz, T. C., Singh, M. K., Degenhardt, K., Rivera-Feliciano, J., Johnson, R. L., Epstein, J. A. and Tabin, C. J. (2012). Distinct compartments of the proepicardial organ give rise to coronary vascular endothelial cells. *Dev Cell* **22**, 639-50.

Le Douarin, N. (1973). A biological cell labeling technique and its use in expermental embryology. *Dev Biol* **30**, 217-22.

Le Douarin, N., Dieterlen-Lievre, F., Creuzet, S. and Teillet, M. A. (2008). Quail-chick transplantations. *Methods Cell Biol* 87, 19-58.

McGrew, M. J., Sherman, A., Lillico, S. G., Ellard, F. M., Radcliffe, P. A., Gilhooley, H. J., Mitrophanous, K. A., Cambray, N., Wilson, V. and Sang, H. (2008). Localised axial progenitor cell populations in the avian tail bud are not committed to a posterior Hox identity. *Development* **135**, 2289-99.

Mikawa, T. and Gourdie, R. G. (1996). Pericardial mesoderm generates a population of coronary smooth muscle cells migrating into the heart along with ingrowth of the epicardial organ. *Dev Biol* **174**, 221-32.

Mizushima, S., Takagi, S., Ono, T., Atsumi, Y., Tsukada, A., Saito, N., Sasanami, T., Okabe, M. and Shimada, K. (2010). Novel method of gene transfer in birds: intracytoplasmic sperm injection for green fluorescent protein expression in quail blastoderms. *Biol Reprod* **83**, 965-9.

Moore, A. W., McInnes, L., Kreidberg, J., Hastie, N. D. and Schedl, A. (1999). YAC complementation shows a requirement for Wt1 in the development of epicardium, adrenal gland and throughout nephrogenesis. *Development* **126**, 1845-57.

Nagy, N., Burns, A. J. and Goldstein, A. M. (2012). Immunophenotypic characterization of enteric neural crest cells in the developing avian colorectum. *Dev Dyn* **241**, 842-51.

Pardanaud, L., Yassine, F. and Dieterlen-Lievre, F. (1989). Relationship between vasculogenesis, angiogenesis and haemopoiesis during avian ontogeny. *Development* **105**, 473-85.

Park, T. S. and Han, J. Y. (2012). piggyBac transposition into primordial germ cells is an efficient tool for transgenesis in chickens. *Proc Natl Acad Sci U S A* **109**, 9337-41.

Phoon, C. K., Ji, R. P., Aristizabal, O., Worrad, D. M., Zhou, B., Baldwin, H. S. and Turnbull, D. H. (2004). Embryonic heart failure in NFATc1-/- mice: novel mechanistic insights from in utero ultrasound biomicroscopy. *Circ Res* **95**, 92-9.

Pudliszewski, M. and Pardanaud, L. (2005). Vasculogenesis and angiogenesis in the mouse embryo studied using quail/mouse chimeras. *Int J Dev Biol* **49**, 355-61.

Red-Horse, K., Ueno, H., Weissman, I. L. and Krasnow, M. A. (2010). Coronary arteries form by developmental reprogramming of venous cells. *Nature* **464**, 549-53.

Saito, Y., Kojima, T. and Takahashi, N. (2012). Mab21l2 is essential for embryonic heart and liver development. *PLoS One* **7**, e32991.

Sato, Y., Poynter, G., Huss, D., Filla, M. B., Czirok, A., Rongish, B. J., Little, C. D., Fraser, S. E. and Lansford, R. (2010). Dynamic analysis of vascular morphogenesis using transgenic quail embryos. *PLoS One* **5**, e12674.

CHAPTER V

CONCLUSIONS AND FUTURE DIRECTIONS

The studies presented here provide a detailed analysis of both vascular and mesothelial formation in the developing intestine. Summating the three studies, we propose the following model of intestinal development. The intestine begins as a flat sheet including splanchnic mesoderm and endoderm. The future mucosal and mesothelial basement membranes of the adult intestine are already present within the intestinal primordium subjacent to the endoderm and splanchnic mesoderm, respectively (Figure 2.2, 2.3). Cells within the stratified splanchnic mesoderm layer are specified to a mesothelial, fibroblast, or visceral smooth muscle cell fate. These progenitors are organized with the mesothelial precursors near the surface and the visceral smooth muscle cell progenitors deep, adjacent to the inner basement membrane (Ch. III—absence of visceral smooth muscle cell progeny identified by labeling surface cells). The mesenchymal layer of the intestine is established by migration of fibroblast and visceral smooth muscle cell progenitors through the outer basement membrane. This migration is concurrent with breakdown of the outer basement membrane (Figure 2.2, 2.5, 3.4). The migratory fibroblast and visceral smooth muscle cell progenitors join the endothelial plexus that resides between the splanchnic mesoderm and endoderm (Figure 2.7). Throughout this process, the mesothelial progenitors remain on the surface of the intestine external to the outer basement membrane. A second wave of migration through the outer basement membrane occurs as mesothelial cells delaminate and migrate into the mesenchyme providing vascular smooth muscle cell progenitors (Figure 2.4, 3.8). The mesenchyme at this time consists of endothelial, stromal, visceral smooth muscle and vascular smooth muscle cell progenitors. The endothelial network of the adult

intestine is formed by remodeling and expansion of the primordial endothelial network (Figure 4.2). Vascular smooth muscle cells differentiate late in development though the progenitors are present throughout the intestinal primordium (Figure 2.11, 4.3). The model is summarized in Figure 5.1.

This model of intestinal development departs from what is known about cardiac development in two fundamental ways. First, at least the majority of cardiogenic splanchnic mesoderm does not retain the potential to differentiate into mesothelium, fibroblasts, or vascular smooth muscle. Thus, the splanchnic mesoderm layer of the heart gives rise to a relatively homogenous population including cardiomyocytes and related cells of the cardiac conduction system (Laugwitz et al., 2008). Within a limited area at the inflow tract of the heart, the splanchnic mesoderm may contain a mixed pool of progenitors able to give rise both to the PE and cardiomyocytes (van Wijk et al., 2009). This is in contrast to the splanchnic mesoderm of the intestine which contains throughout its anterior-posterior axis the progenitors for visceral and vascular smooth muscle, mesothelium, and fibroblasts. Second, the primordial endothelial plexus of the embryo contained within the cardiogenic region does not give rise to the blood vessels supplying the myocardium but rather contributes only to the endocardium. This is in contrast to all other coelomic organs that have been investigated to date in which the primordial endothelial plexus expands and remodels to generate the mature vascular network of the adult (DeRuiter et al., 1993; Gouysse et al., 2002; le Noble et al., 2004; Pardanaud et al., 1989).

The remaining coelomic organs are all gut tube derivatives developing from endodermal buds that grow into the surrounding splanchnic mesoderm. Thus, these organs may be expected to more closely resemble the intestine in their generation of mesothelium than the heart. Future studies will investigate mesothelial formation in the lung, liver, pancreas and spleen through the same methodology applied in determining

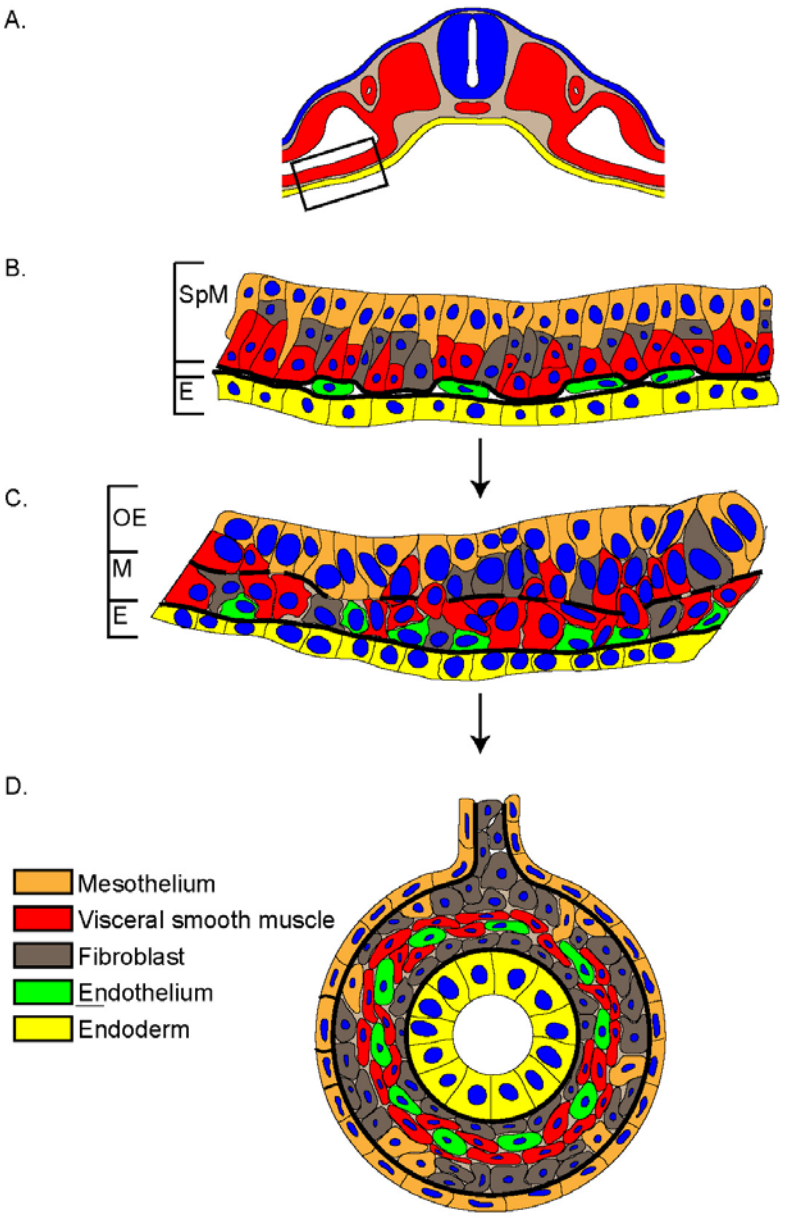

Figure 5.1 Model of intestinal development.

A) Schematic of a transverse section through an early avian embryo depicting the region of the splanchnopleure that will generate the intestine (boxed). **B)** The intestinal anlage is composed of splanchnic mesoderm (SpM) and endoderm (E) with two basement membranes (thick black lines). The splanchnic mesoderm contains mesothelial (orange), visceral smooth muscle cell (red) and fibroblast (gray) progenitors. The mesothelial progenitors are localized at the surface with other progenitors localized deep. An endothelial plexus (green) resides within the mesenchymal space (between the two basement membranes). **C**) Visceral smooth muscle and fibroblast progenitors migrate through the dispersed outer basement membrane to establish the mesenchyme (M) leaving mesothelial progenitors on the surface**. D)** A second wave of migration occurs when mesothelial progenitors invade the mesenchyme to give rise to vascular smooth muscle cell progenitors.

the origins of intestinal mesothelium described in Chapter III including electroporation, retroviral labeling and chick-quail chimera generation. These proposed studies will determine if the heart is unique or represents just one of multiple mechanisms of mesotheliogenesis

The mechanism underlying the variation in mesothelial formation between the heart and intestine is unknown. However, several observations point at the exclusion of endoderm in the heart tube as an essential discrepancy. The splanchnic mesoderm of the intestine maintains a close morphological relationship with the endoderm throughout development and crosstalk between the endoderm and mesoderm is well documented (Noah et al., 2011). We demonstrate here that mesothelial progenitors are resident throughout the intestinal primordium. In contrast, in the heart, the splanchnic mesoderm is in contact with the endoderm for only a short period. However, the PE develops in close approximation to the liver bud, an endodermal outgrowth, at the caudal end of the heart tube. At the rostral end of the heart tube where it again comes into close approximation to the endoderm, an additional minor source of mesothelial progenitors is present. This mesothelial population normally lines the great vessels of the heart but can migrate over a portion of the myocardium when proepicardial development is inhibited (Gittenberger-de Groot et al., 2000). Thus, the majority of the heart tube splanchnic mesoderm is removed from the endoderm and does not generate mesothelial cells. However, mesothelial progenitors are present at both the rostral and caudal ends of the heart tube at the points at which the splanchnic mesoderm is brought back into close association with the endoderm. These observations suggest endoderm may be a source of inductive cues leading to mesothelial development.

To determine if the endoderm is required for mesothelial specification, *in vitro* culture and chick-quail chimera experiments will be employed. The endoderm and mesoderm can easily be isolated from one another with a brief enzymatic treatment.

Thus, intestinal mesoderm can be isolated and cultured with or without endoderm to determine if mesothelial differentiation occurs as determined by expression of mesothelial markers including *Wt1* and *Tbx18*. Furthermore, isolated splanchnic mesoderm transplanted into the coelomic cavity does not form an independent structure but rather attaches to and merges with the body wall (data not shown). Thus, this provides an *in vivo* model to determine whether mesothelial differentiation from the splanchnic mesoderm occurs when it develops at a distance from the endoderm. Finally, intestinal splanchnopleure or mesoderm alone will be transplanted into the region of the cardiac crescent to determine if the transplanted mesoderm can incorporate into the heart tube and generate mesothelium within the cardiac environment.

The precise inductive signals leading to mesothelial formation are still largely unknown even in the extensively studied PE. In the intestine, the mesothelial lineage appears to diverge from the visceral smooth muscle lineage and localize to the surface of the mesoderm soon after formation of the intestinal anlage. Thus, the cues leading to mesothelial differentiation in the intestine must be present before this time. Maintenance signals may also be required to retain mesothelial specification. Future studies will focus on identifying candidate genes that may be involved in the induction of mesothelium in the intestine.

Other tissues may offer further insight into the inductive tissue interactions and signals involved in mesothelial development. Mesothelium lines the entire coelom including the body wall which is derived from somatopleure. Additionally, the spleen is generated entirely by mesodermal derivatives and does not include endoderm. The origin of mesothelium for both the body wall and the spleen is unknown but is of particular interest in determining the potential role of endoderm in mesothelial development and identifying mechanisms of mesothelial formation. Chick-quail chimeras in which a region of the chick somatopleure is replaced with quail tissue will address the

origin of body wall mesothelium. Development of splenic mesothelium will be investigated as described above. These proposed experiments will explore in depth the mechanisms of mesotheliogenesis throughout the coelomic cavity.

The heart also appears to be an exception to the general mechanism of vascular formation among coelomic organs. The resident endothelial plexus of the heart has a relatively limited potential for remodeling. It generates the endocardium but does not contribute to the vasculature supplying the organ. Thus, the myocardial wall must recruit a vascular supply from other sources. All other coelomic organs have an intrinsic capacity to generate blood vessels (Gouysse et al., 2002; Pardanaud et al., 1989). However, the origin of coronary endothelium may still have roots in the primary endothelial plexus established in the embryo. The PE serves, at least in part, as a conduit for hepatic and sinus venosus endothelium to vascularize the myocardium. Both the sinus venosus and hepatic endothelium are derived from remodeling of the primary endothelial network that resides between the splanchnic mesoderm and endoderm (DeRuiter et al., 1993; Gouysse et al., 2002). The limited endothelial plasticity within the heart may be related to a functional restriction (i.e. the intact endocardium is required for cardiac function) and/or a lack of inductive signals promoting remodeling and angiogenesis.

The endoderm has been demonstrated to be critical for vasculogenesis (Pardanaud et al., 1989). Recombining somatic mesoderm, which normally has a very limited vasculogenic potential, with endoderm prior to transplantation into the coelom of a host embryo led to increased vasculogenesis from the somatic mesoderm and additionally supported invasion of the host by transplant-derived vessels (Pardanaud and Dieterlen-Lievre, 1999). Thus, endoderm appears to promote vasculogenesis from mesodermal tissue and angiogenesis from existing endothelial networks. The absence of endoderm within the heart may promote the stability of the endocardium. To

determine if the endoderm can promote angiogenesis from the endocardium into the myocardium, quail heart tubes isolated prior to epicardial formation will be placed in culture with or without a segment of endoderm placed within the lumen. The presence of endothelial cells within the myocardium will be determined by staining for QH1. Cardiogenic mesoderm with the underlying endoderm will also be isolated prior to tube formation for transplantation into the coelom of a host embryo or for explant culture to determine if cardiac endothelial behavior is altered by the presence of endoderm.

The studies presented herein offer many novel insights into intestinal and mesothelial development and impact broadly our consideration of coelomic organogenesis and vasculogenesis. Ongoing studies will further elucidate the mechanisms leading to mesothelial differentiation throughout the coelomic cavity and the unique method of vascular formation in the heart.

References

DeRuiter, M. C., Gittenberger-de Groot, A. C., Poelmann, R. E., VanIperen, L. and Mentink, M. M. (1993). Development of the pharyngeal arch system related to the pulmonary and bronchial vessels in the avian embryo. With a concept on systemic-pulmonary collateral artery formation. *Circulation* **87**, 1306-19.

Gittenberger-de Groot, A. C., Vrancken Peeters, M. P., Bergwerff, M., Mentink, M. M. and Poelmann, R. E. (2000). Epicardial outgrowth inhibition leads to compensatory mesothelial outflow tract collar and abnormal cardiac septation and coronary formation. *Circ Res* **87**, 969-71.

Gouysse, G., Couvelard, A., Frachon, S., Bouvier, R., Nejjari, M., Dauge, M. C., Feldmann, G., Henin, D. and Scoazec, J. Y. (2002). Relationship between vascular development and vascular differentiation during liver organogenesis in humans. *J Hepatol* **37**, 730-40.

Laugwitz, K. L., Moretti, A., Caron, L., Nakano, A. and Chien, K. R. (2008). Islet1 cardiovascular progenitors: a single source for heart lineages? *Development* **135**, 193-205.

le Noble, F., Moyon, D., Pardanaud, L., Yuan, L., Djonov, V., Matthijsen, R., Breant, C.,

Fleury, V. and Eichmann, A. (2004). Flow regulates arterial-venous differentiation in the chick embryo yolk sac. *Development* **131**, 361-75.

Noah, T. K., Donahue, B. and Shroyer, N. F. (2011). Intestinal development and differentiation. *Exp Cell Res* **317**, 2702-10.

Pardanaud, L. and Dieterlen-Lievre, F. (1999). Manipulation of the angiopoietic/hemangiopoietic commitment in the avian embryo. *Development* **126**, 617-27.

Pardanaud, L., Yassine, F. and Dieterlen-Lievre, F. (1989). Relationship between vasculogenesis, angiogenesis and haemopoiesis during avian ontogeny. *Development* **105**, 473-85.

van Wijk, B., van den Berg, G., Abu-Issa, R., Barnett, P., van der Velden, S., Schmidt, M., Ruijter, J. M., Kirby, M. L., Moorman, A. F. and van den Hoff, M. J. (2009). Epicardium and myocardium separate from a common precursor pool by crosstalk between bone morphogenetic protein- and fibroblast growth factor-signaling pathways. *Circ Res* **105**, 431-41.